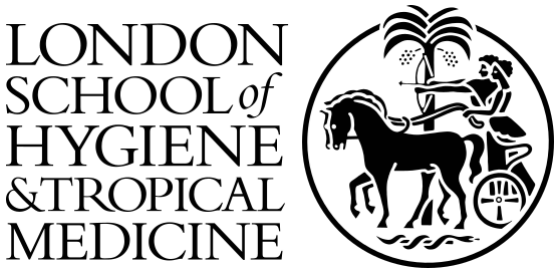

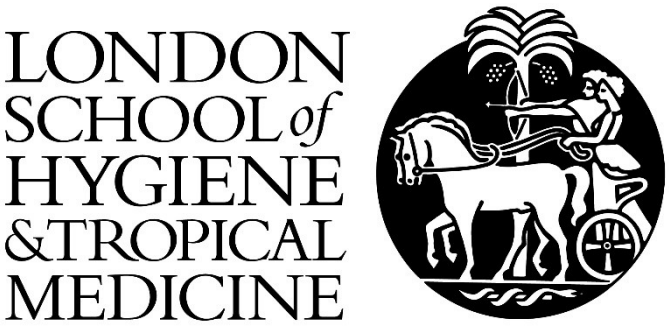

Understanding T cell and antibody-mediated immune mechanisms against malaria infection

Samuel Guy Thorburn

Thesis submitted in 2017 in accordance with the requirements for the degree of Doctor of Philosophy

University of London

Faculty of Infectious and Tropical Diseases
Department of Immunology and Infection
London School of Hygiene and Tropical Medicine

Supervisor: Dr Julius Hafalla
Co-supervisor: Professor Eleanor Riley
Funding by: Medical Research Council

Declaration

I, **Samuel G. Thorburn**, confirm that the work presented in this thesis is my own. Where information has been derived from other sources I confirm that this has been indicated in the thesis.

Acknowledgments

I would like to take this opportunity to first thank my supervisor Dr Julius Hafalla for allowing me to join the Hafalla group. You have always made time for discussion and your insight and experience have been invaluable in the development of my projects. Your encouragement to work with other groups has led to several unique experiences working in Berlin, Paris, Copenhagen, Belo-Horizonte and also in Manila, where I spent a fantastic 3 month placement as part of my MRC studentship. Being in such a collaborative environment has allowed me to work on projects with groups within LSHTM and with groups internationally, leading to exposure to a broad range of techniques and research I would otherwise have not experienced.

I would also like to thank Professor Eleanor Riley, who has provided regular support and advice and has always made available her extensive knowledge of immunology, which has been extremely useful throughout my PhD. The individual members of the Riley and Hafalla groups have been a constant support, particularly Matt Gibbins, who did an incredible job with our mosquito colony as well as always being available to help with experiments (particularly when an extra pair of hands were needed for animal injections) or discuss ideas. Martin Goodier, Matt White, Jason Mooney, Carolyn Nielsen and Asia-Sophia Wolf in the Riley group always patiently listened to lab meeting presentations throughout my PhD and, even though some of my projects were particularly uninteresting to them, always offered insightful advice or comment. In addition, I worked with MSc students during their projects, who contributed to my chapters. For his contribution to chapter 2 I would like to thank Saif-U-Rehman Khan and for their contribution to the project presented in chapter 5 I would like to thank Athena Li and Marta Campillo Poveda.

I cannot thank Carolynne Stanley or Liz King enough for their tireless work towards running lab 234 so well and also for Liz's seemingly limitless knowledge of flow cytometry. Additionally, Holly Burrell-Saward and Liz McCarthy have been fantastic with their training and help with all things microscopy at LSHTM. For my animal experiments, all the staff in the Biological Services Facility at LSHTM were a great help. Their management of the facility, care for all of the animals and availability to answer all questions made my research infinitely easier.

Several of my experiments would not have been possible without the help of Dr Katja Müller and Professor Kai Matuschewski at the Max Planck Institute, Berlin. I would like to thank them for their experiments immunising mice and sending over serum as well as sending over mosquitoes when needed. The microarray work presented in chapter 5 would not have been possible without the work of Claus Schafer-Nielsen who synthesised the peptides and Morten Nielsen has been a fantastic source of experience with the analysis of the incredible amount of data that was produced.

Finally I must thank my friends and family for their love and support throughout my PhD. My fiancée Kathryn has been incredible for the past few years, not only putting up with me moving down to London for a PhD but even moving down herself for an entire year, I couldn't have done this without you. My brother Will and sisters Nancy and Polly, their spouses Chloë, Kieron and Caspian and my parents have been fantastic throughout, always available to talk, always ready with words of encouragement and regularly keeping me up to date on the latest malaria breakthrough via forwarding me news articles. Dheraj, Alistair, James and John have been great friends and flatmates during the past 4 years, always on-call for a trip to the pub. I hope you all know how important you have been throughout this part of my life.

Abstract

CD8$^+$ T cells have been implicated in protective immune responses in pre-erythrocytic malaria and pathogenic responses in blood stage malaria, making them an important factor in determining the outcome of infection. Natural exposure to pre-erythrocytic malaria infection does not elicit sterile protection in humans, whereas multiple immunisations with large numbers of radiation attenuated sporozoites can. This protection is largely due to parasite-specific CD8$^+$ T cells; however, antibody responses have also been shown to be functional in pre-erythrocytic infection. Unfortunately, there is a paucity in known antigens other than the immunodominant protein circumsporozoite protein (CSP) that are recognised by antibodies in the pre-erythrocytic stages. With regard to blood stage infection, there are a variety of outcomes ranging from non-clinical patent infection to cerebral malaria due to immune-mediated pathology. Indeed, there are several different mouse models of malaria that each produce different outcomes, suggesting there may be subtle differences in immune regulation, which has previously been investigated by our group but is not fully understood.

The research presented here attempts to address three hypotheses. First, I hypothesised that the requirement for high doses of antigen at multiple intervals for sterilising protection is at least in part due to inhibition of CD8$^+$ T cell activation via regulatory pathways that are stimulated during exposure to attenuated sporozoites. Secondly, I hypothesised that T cell regulation during blood stage infection through the interleukin 10 receptor (IL-10R) confers resistance in a BALB/c model of *Pb* ANKA infection, which is normally refractory to experimental cerebral malaria (ECM). Finally, I hypothesise that protective immunisation of C57BL/6 and BALB/c with attenuated *Pb* ANKA sporozoites leads to the production of non-CSP antibodies that may be viable candidates for further vaccine research.

In order to test my first hypothesis I investigated co-inhibitory molecules cytotoxic T lymphocyte antigen 4 (CTLA-4), programmed death ligand 1 (PD-L1) and PD-L2 and regulatory cytokines IL-27 and IL-10. Using mouse models, I gave a single non-protective immunisation of γ-radiation attenuated *Pb* ANKA sporozoites and investigated the CD8$^+$ T cell immune response in the absence of each regulatory pathway. Antibody-mediated blockade of CTLA-4 concurrently with a normally non-

protective radiation attenuated *Pb* ANKA sporozoite immunisation in C57BL/6 mice led to a significant increase in sporozoite antigen-specific interferon gamma (IFNγ) producing $CD8^+$ T cells upon re-stimulation. Additionally, this resulted in sterile protection when challenged 14 days after blockade and immunisation; however, protection was greatly reduced when challenged after 45 days. Using mice deficient in IL-27R or using antibody blockade of PD-L1, PD-L2 and IL-10 with a non-protective single immunisation of radiation attenuated *Pb* ANKA sporozoites did not lead to significantly increased $CD8^+$ T cell activation upon re-stimulation. Neither did it result in increased protection from parasite load in the liver. These experiments are a proof of principle that certain regulatory pathways can significantly reduce protective $CD8^+$ T cell responses to sporozoite immunisation.

For my second hypothesis, I investigated $CD4^+$ and $CD8^+$ T cell responses to *Pb* ANKA blood stage infection in ECM resistant BALB/c mice treated with antibodies to block the IL-10R. I show that blockade of the IL-10R leads to increased $CD4^+$ and $CD8^+$ T cell production of IFNγ with blood stage *Pb* ANKA infection. Other work in this chapter shows that IL-10R blockade leads to increased ECM as a result of increased brain pathology. Additionally, I show that IL-10R blockade with *Pb* ANKA blood stage infection leads to an increase in expression of CTLA-4, but not PD-1 on $CD4^+$ $CD8^+$ T cells. This suggests that there may be a relationship between IL-10- and CTLA-4-mediated regulation in *Pb* ANKA blood stage infection of BALB/c mice.

To address my third hypothesis, I used a novel immunisation schedule using *Pb* ANKA sporozoites that express *Pf* CSP rather than *Pb* ANKA CSP. One immunisation with transgenic parasites followed by a booster immunisation with *Pb* ANKA was performed using C57BL/6 and BALB/c mice to boost non-CSP responses. This led to antibodies that recognised previously validated pre-erythrocytic antigens and functionally inhibited sporozoite invasion of hepatocytes in vitro. Using high-density microarray technology I investigated all proteins expressed during the pre-erythrocytic stages of *Pb* ANKA using serum from these immunised mice. Results show antibody responses to previously unidentified pre-erythrocytic antigens and therefore potential antigens for future vaccine research.

Table of Contents

List of Figures

Abbreviations

ACT	Artemisinin combination therapy
APC	Antigen presenting cell
ARDS	Acute respiratory distress syndrome
BFA	Brefeldin A
BSA	Bovine serum albumin
CD	Cluster of differentiation
cGY	Centigray
CM	Cerebral malaria
CSP	Circumsporozoite protein
CTLA-4	Cytotoxic T lymphocyte antigen 4
DAPI	4',6-diamidino-2-phenylindole
DC	Dendritic cell
EBi3	Epstein Barr induced gene 3
ECM	Experimental cerebral malaria
EEF	Exoerythrocytic form
ELISA	Enzyme linked immunosorbent assay
Fmoc	9-fluorenylmethoxycarbonyl
FOV	Field of view
GAP	Genetically attenuated parasite
GAPDH	Glyceraldehyde 3-phosphate dehydrogenase
GFP	Green fluorescent protein
GRB2	Growth factor receptor-bound protein 2
H&E	Hematoxylin and eosin
HCV	Hepatitis C virus
i.p.	Intraperitoneal
i.v.	Intravenous
ICAM1	Intercellular adhesion molecule 1
IFA	Immunofluorescence assay
IFNγ	Interferon gamma

Ig	Immunoglobulin
IL	Interleukin
IMC	Inner membrane complex
ITN	Insecticide treated net
Lck	Lymphocyte-specific protein tyrosine kinase
LCMV	Lymphocytic choriomeningitis virus
LFA1	Lymphocyte function associated protein 1
LSA-1	Liver stage antigen type 1
LSEC	Liver sinusoid endothelial cell
LSHTM	London school of hygiene and tropical medicine
MHC	Major histocompatibility complex
MSP	Merozoite surface protein
MVA	Modified vaccinia Ankara
NK	Natural killer
NO	Nitric oxide
NPPOC	3'-nitrophenylpropyloxycarbonyl
Pb	*Plasmodium berghei*
PBS	Phosphate buffered saline
PCR	Polymerase chain reaction
PD-1	Programmed cell death protein 1
PD-L1	Programmed death ligand 1
PD-L2	Programmed death ligand 2
Pf	*Plasmodium falciparum*
PFA	Paraformaldehyde
PI3K	Phosphatidylinositol-3-kinase
PKCϴ	Protein kinase C theta
PMA	Phorbol myristate acetate
pRBC	Parasitised red blood cell
PV	Parasitophorous vacuole
Py	*Plasmodium yoelii*
RAS	Radiation attenuated parasites
RBC	Red blood cell

RT-PCR	Reverse transcription polymerase chain reaction
S20	Sporozoite specific protein 20
SDS	Sodium dodecyl sulphate
SPPS	Solid phase protein synthesis
TCR	T cell receptor
Th1	T helper 1
Th2	T helper 2
TLR	Toll like receptor
TNFα	Tumour necrosis factor alpha
TRAP	Thrombospondin related adhesion protein
Treg	Regulatory T cell
WT	Wild type
ZAP70	Zeta chain associated protein kinase 70

1 | Introduction

1.1 Malaria and its global impact

Worldwide, 3.4 billion people are at risk of malaria infection, with 212 million new clinical cases (estimate range from 148-304 million) and 429,000 fatalities (estimate range from 235,000-639,000) in 2015[1]. This creates a huge global burden on health systems as rapid, effective diagnosis and treatment are required to address mild disease and to prevent potential cerebral complications, coma and death that can occur in severe disease. Due to the widespread nature of malaria, diagnosis and treatment are often required in remote and underdeveloped areas, further complicating the responsibility of government and regional health programmes. Malaria not only influences worldwide spending on public health, but also influences national and international economies as constant exposure to malaria leads to a reduction in the available national workforce. Between 1965 and 1990 the average growth of income per capita in countries with endemic malaria was 0.4% compared to an average of 2.3% in non-endemic countries[2]. Although establishing direct correlation between malaria and poverty is difficult, individual studies have found that malaria is related to reduced education[3], worker productivity[4], household savings[5] and international trade[4]. Both directly and indirectly, malaria impacts all levels of society from an individual to global scale. National and international efforts to tackle the burden of malaria have reduced the rate of new annual cases by 37% and death rates by 60%; however, a global reduction does not reflect fluctuations in malaria at a national level. Eradication of malaria has been seen in a number of countries but it is still possible to see resurgence in disease. Venezuela was the first country to eradicate malaria from its most populated areas in 1961; however since the late 1990's there has been a continued increase in malaria cases, showing poor control of the spread of malaria and other infectious diseases[6]. As eradication can be temporary, novel avenues of research should be explored to help maintain eradication and help achieve elimination.

Protozoan parasites of the *Plasmodium* genus are the aetiological agents of malaria, with *Plasmodium falciparum* (*Pf*)*, Plasmodium vivax* (*Pv*)*, Plasmodium knowlesi* (*Pk*)*, Plasmodium malariae* (*Pm*) and *Plasmodium ovale* (*Po*) species capable of infecting humans and causing disease. The *Plasmodium* genus is a member of the Hematozoa clade within the *Apicomplexa* phylum and is closely related to other apicomplexans including *Toxoplasma* in the coccidia clade, *Cryptosporidium* in the cryptosporidia

clade and *Eugregarinorida* in the gregarines clade. *Pf* is the most widely studied of the *Plasmodium* species and causes the most fatalities globally with the majority being infants and children under 5 years of age[7]. Death as a result of malaria infection can be due to several complications. These include severe anaemia and jaundice due to the loss of erythrocytes, organ failure (particularly renal failure) due to deposits of immune complexes, acidosis, respiratory distress including acute respiratory distress syndrome (ARDS) and cerebral malaria due to sequestration of infected erythrocytes in the microvasculature of the brain. *Pv* infection can also result in severe malaria; however it is not studied to the extent of *Pf,* despite it causing an estimated 50% of clinical cases outside of Africa[8]. Interestingly, it is able to cause relapse infections up to several months after clinical symptoms are treated. This is a result of the dormant hypnozoite life stage, unique to *Pv* and *Po* of the human infective species. Unfortunately the mechanisms by which the hypnozoite is formed and activated remain poorly understood. *Pk* is a predominantly primate pathogen that can infect humans via macaque monkeys[9] but to date no natural human to human transmission has yet been documented. *Pm* and *Po* infect humans but do not cause severe malaria and account for a comparatively small number of cases annually.

1.2 Malaria control

Unfortunately, the complexity and genetic plasticity of the malaria parasite has led to increasing drug resistance[10]. Chloroquine resistance was first reported at the border of Thailand and Cambodia in 1957 and proguanil resistance was observed as early as 1 year after its introduction[11]. Artemisinin has been more successful; however resistance was seen in 2009, again at the Thailand-Cambodia border[12]. In order to reduce the development of resistant parasites, artemisinins are usually given as part of Artemisinin Combination Therapy (ACT). This is beneficial for two reasons, firstly there is a much lower chance of a parasite spontaneously developing resistance to two antimalarial drugs at the same time and secondly, partnering artemisinins, which have short half-lives, with drugs that have a longer half-life helps prevent recrudescence.

In order to control the mosquito vector itself, large-scale spraying of DDT was introduced after WWII. Although further research confirmed DDT caused a detrimental effect on the environment[13], the use of novel and safer insecticides has resulted in much greater control of malaria transmission. The uses of insecticides include insecticide treated bed nets (ITN's) and indoor residual spraying, both of which significantly contribute to reductions in morbidity and mortality[7,14]. Although strategies exist that can significantly influence malaria prevalence and treatment, increasing resistance and changes in global politics and economies can in some cases quickly reverse the positive contributions these methods make to malaria eradication. As such, more research is required to discover novel drugs, novel insecticides and in particular to develop novel vaccines that could significantly contribute to international eradication and elimination programmes.

1.3 The *Plasmodium* life cycle

Members of the *Plasmodium* genus are protozoan parasites that have developed a complex life cycle, which requires vertebrate hosts and invertebrate vectors (Figure 1.1). Differentiation of the parasite allows for successive specificity to different tissues or cell types in order to successfully progress through the life cycle. Parasites are transferred from an infected female *Anopheles* mosquito to a vertebrate host during a blood meal, which is necessary for egg production in females. Motile invasive *Plasmodium* sporozoites exist within the distal areas of the lateral lobes of the salivary glands, primarily in extracellular secretory cavities[15]. Here they form aggregates; however individual parasites gradually relocate to the salivary ducts where they are susceptible to being ejected by the mosquito vector[15]. The female mosquito injects saliva during a blood feed to prevent clotting and with it an infected mosquito transmits sporozoites. Small numbers of roughly 10-100[15–18] are released into the dermis of the vertebrate host where they immediately encounter substrate for surface proteins involved in motility. Sporozoites use gliding motility and cell traversal to move through the dermis and enter the peripheral blood system[19] or lymphatic system[20]. Motility is largely via thrombospondin-related adhesion protein (TRAP), which recognises sulphated glycoconjugates in addition to other, as yet undescribed host proteins. TRAP is an abundant protein on the surface of the sporozoite; however it is mainly present within the micronemes[21] where it is secreted for motility and invasion. TRAP

binds to substrate present on the surface of host cells and travels towards the posterior end of the parasite via an actin-myosin system located at the inner membrane complex (IMC) where they are cleaved and released[22]. Salivary gland sporozoites have a tropism for the vertebrate liver and with 30% of the total blood volume passing through the liver every minute[23], sporozoites can rapidly sequester in the liver once they have entered the peripheral blood system[24]. Specificity to the liver is due to the circumsporozoite protein (CSP), the major surface protein of sporozoites and may be secreted from the apical end[25]**.** Heparan-sulphate proteoglycans are expressed at high levels on hepatocytes[26], projecting through the fenestrae of the liver sinusoids where they are recognised by CSP[27]. This has been confirmed through incubation of liver sections with recombinant CSP, showing preferential localisation at the hepatocyte surface[27]. An effective cell traversal mechanism allows the sporozoite to cross the liver sinusoid endothelial cells and space of Disse to eventually invade the liver parenchyma.

The pre-erythrocytic or liver stage involves the intra-hepatic development of sporozoites into merozoites that can bind to and invade red blood cells (RBCs). Sporozoites first traverse several hepatocytes before entering a final cell by forming an invagination of the host cell membrane and creating a parasitophorous vacuole (PV) that is subsequently altered to express *Plasmodium*-specific proteins. Through schizogony, thousands of merozoites that are specific to the next life stage are produced. Schizogony involves the asynchronous division of the nucleus multiple times to create a syncytium, followed by budding off of daughter cells[28]. In some *Plasmodium* species, including *Pv, Po* and the non-human primate parasite *P. cynomolgi*, another form called the hypnozoite is produced which can remain dormant in the liver for months before re-activation through as yet unknown mechanisms. Once schizogony is complete, groups of merozoites bud off the hepatocyte in merosomes and traverse to the blood circulation where they are released and can rapidly infect RBCs.

The erythrocytic or blood stage can result in the clinical symptoms of malaria. Merozoites bind to RBC membranes with stochastic orientation via recognition of erythrocyte surface proteins and re-orientate themselves to allow the apical end to form a tight junction for PV formation[29]. More merozoites or sexual stage gametocytes are generated within the PV again by schizogony. Once complete, the schizont and

RBC membranes rupture and merozoites are released, leading to febrile illness in the host. Reinfection and RBC rupture is repeated, giving recurrent episodes of fever ranging from 24 hours for *Pf, Pv* and *Po* (tertian fever) to 72 hours for *Pm* (quartan fever). Male microgametocytes and female macrogametocytes have been reported to survive in the blood circulation for between 3.4 days[30] and 6.5 days[31] and must be ingested by female *Anopheles* mosquitoes during a blood meal for successful transmission and continuation of the life cycle. In the mosquito gut the gametocytes develop into gametes as a result of a reduction in temperature, changes in pH and the presence of xanthurenic acid[32–34]. Gametes fuse to form zygotes and become motile ookinetes, which traverse the gut epithelium and sequester in the gut basal lamina. There they develop into oocysts and begin a phase of sporogony, which generates thousands of sporozoites. As ookinetes are diploid and sporozoites are haploid, sporogony occurs by the meiotic division of the ookinete nucleus to form a polyploid nucleus with 4 haploid nuclei. As an oocyst these nuclei divide as in schizogony by asynchronous mitosis to generate sporozoites. With oocyst rupture, sporozoites are released into the mosquito hemolymph and preferentially locate to the salivary glands, possibly through CSP recognition of proteins expressed by salivary gland cells[35]. Once in the salivary cavities they can be transmitted to a new host in the next blood meal.

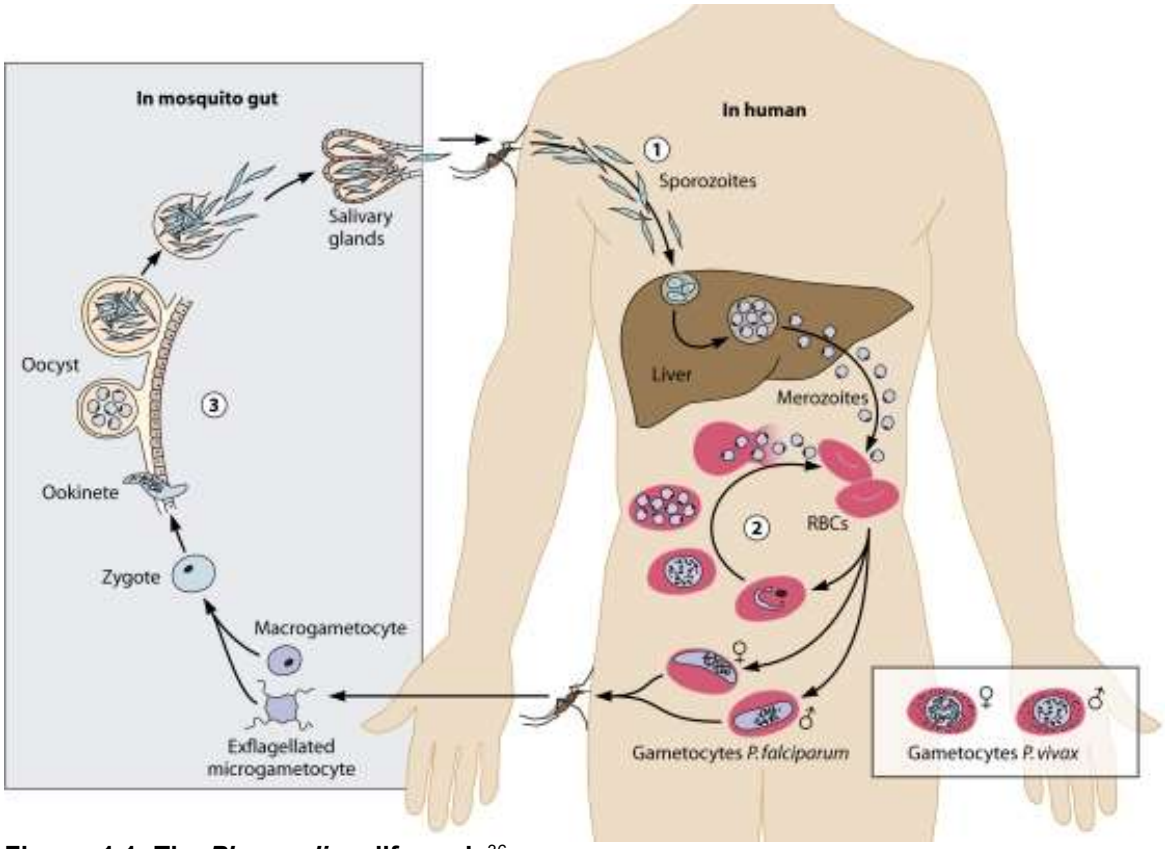

Figure. 1.1: The *Plasmodium* life cycle[36].

Sporozoites enter the vertebrate host via inoculation by an infected female *Anopheles* mosquito blood meal and localise to the liver where they infect hepatocytes and develop into thousands of merozoites (1). Merozoites enter the blood circulation and infect RBC's as part of the blood stage, where they cyclically proliferate, rupture the host cell and re-infect new RBC's (2). Some merozoites develop into sexual stage gametocytes, which remain in the blood and can be taken up by a female *Anopheles* mosquito during a blood meal. In the mosquito gametocytes develop into gametes and fuse to form an ookinete (3). In the gut basal lamina, sporogony occurs in the oocyst before the oocyst ruptures and releases sporozoites, which can enter the salivary gland, where they can be released into a new vertebrate host.

1.4 Whole sporozoite vaccination strategies for malaria pre-erythrocytic stages

Drug treatment and vector control strategies significantly contribute to decreased malaria incidence and have been sufficient to eradicate malaria in some areas of the world[37]; however eradication is increasingly difficult, particularly due to parasite resistance to drugs[38] and vector resistance to insecticides[39]. In order to supplement these strategies and add to the interventions available against malaria globally, an effective vaccine would significantly contribute to eradication and elimination programmes by eliciting extended sterile immunity in vaccinated individuals, reducing both disease and transmission.

Vaccination with radiation attenuated sporozoites (RAS) can elicit protection against subsequent challenge with infectious sporozoites. This was first identified in mice using x-radiation attenuated *P. berghei* (*Pb*) sporozoites as a vaccination in an A/J mouse model[40]. Using this strategy, patent infection was reduced from 90% in controls to 37% in mice vaccinated with a sufficient number of radiation attenuated sporozoites. Later studies using γ-radiation attenuated sporozoites were able to show complete protection using *Pb* as well as *P. yoelii* (*Py*) species[41]. Used in mice, *Pb* and *Py* provide good models of malaria infection as they can induce severe disease including experimental cerebral malaria (ECM) in susceptible mice such as C57BL/6 or non-lethal infection can be observed using certain parasite strains such as *Py* 17XNL. Further to mouse models, the same radiation attenuation strategy with *P. cynomolgi* sporozoites can also induce protection in rhesus monkeys[42]. The success of these investigations has been translated to humans using vaccines designed using γ-radiation attenuated *Pf* sporozoites[43,44] and has set a gold standard of immunisation in malaria vaccine research. Unfortunately, using RAS as a global vaccine would require overcoming several obstacles. Sporozoites must be isolated from mosquito salivary glands as there are no scalable methods for culturing infectious sporozoites *in vitro*. Mosquitoes must be grown in sterile conditions and the resulting sporozoites must be a pure suspension, which is expensive but has been achieved to a sufficient level for human vaccine trials[45]. Importantly, controlled irradiation is critical as insufficient attenuation can lead to patent malaria and excessive irradiation can prevent any sterilising immunity[46]. Even though this method of attenuation is very

effective, the risk of sub-optimal irradiation increases with increasing batch sizes, making scaling-up of this method more problematic than other strategies such as a sub-unit vaccine design.

From the positive results shown in early experiments of sporozoites attenuation by irradiation and its potential for eliciting protection, some research has progressed to investigating other methods of parasite attenuation. Sequencing of the *Plasmodium* genomes including *Pf* [47–49] and the murine species *Pb* [50] has led to greater understanding of these parasites and has enabled the generation of genetically attenuated parasites (GAPs), whose attenuation is controlled by genetic manipulation. The large number of genes available (over 5000) and their plasticity throughout the life cycle creates difficulties with identifying appropriate candidates. Good candidate genes for GAP must not be essential for parasite survival during the erythrocytic and mosquito stages (important for parasite generation), but must be required for complete, functional liver stage development. By following the progression of parasite development after a single gene deletion, GAPs facilitate an increased understanding of the biology of the parasite. Using GAP techniques, *Plasmodium* parasites can be generated that arrest in early liver stages[51,52] or arrest late in the liver stage[53]. Arresting parasites at different times during development leads to different advantages such as reduced risk of breakthrough infection if arrest is early compared to apparent increased antigen exposure if parasites arrest late in development. Further to this, multiple genes can be investigated simultaneously in one parasite to optimise vaccine candidates[54]. GAPs provide a promising avenue for future research as they allow for reliable, reproducible, specific attenuation of parasites; however they have several similar limitations to the gold standard as production of parasites still requires development in the vector. There is also a risk of future stochastic genetic changes that could reverse the attenuation, resulting in the generation of a virulent strain that could induce disease.

Another vaccine strategy uses sporozoite injection with concurrent anti-malarial drug treatment. This method allows for full liver stage development of the parasite before blood stage arrest as a result of chemotherapy. The advantage of this strategy is that the immune system is exposed to all antigens that are expressed in the liver stage, whereas irradiation or genetic manipulation attenuates the parasite before full liver stage development is completed. Immunisation with blood stage parasites under a

drug regimen can also induce protection from both blood and liver stage parasites, indicating cross-over protection[55].

Although most of today's vaccines rely on attenuation or inactivation of the pathogen itself, subunit vaccines are regarded as an optimal strategy for vaccine design. They are consistent, stable, scalable and non-infectious; however the subunit vaccination should generate a level of immune protection that is capable of preventing patent disease. The RTS, S vaccine, currently the most advanced malaria vaccine, consists of B and T cell epitopes to CSP with hepatitis antigen. It has 27% efficacy in infants and 39% efficacy for children between 5-17 months[45]. It is promising that we can now develop a vaccine that has some efficacy against malaria; however further research will be required to produce next generation vaccines that will assist in eradicating disease in endemic regions. The success of RTS, S depends on the CSP B and T cell epitopes as CSP is an immunodominant antigen during the pre-erythrocytic stages of infection. Towards the design of novel malaria vaccines; however, the addition of novel pre-erythrocytic antigens to CSP epitopes could increase the efficacy of a malaria vaccine and provide a much better tool for fighting disease and transmission.

1.5 The adaptive immune response to *Plasmodium* infection

1.5.1 Adaptive immune responses to pre-erythrocytic stage malaria

1.5.1.1 $CD8^+$ T cell responses to pre-erythrocytic stage malaria

Although the immune response to malaria infection is complex and not yet fully understood, several studies have shown that activation of $CD8^+$ T cell responses is non-redundant in protection against pre-erythrocytic malaria in mouse models, rhesus monkeys and humans[41,56–60]. Indeed, adoptive transfer of *Py* antigen-specific $CD8^+$ T cells from immunised BALB/c mice into naïve mice is sufficient to confer sterile protection against subsequent sporozoite challenge[61]. As the liver stage of malaria

infection is relatively short and the number of inoculated sporozoites during natural infection is low, these $CD8^+$ T cells must successfully eliminate a small number of infected hepatocytes (1 in $1x10^9$ in humans, 1 in $1x10^6$ in mice[62]) before blood stage infection. This requires a large number of antigen-specific effector memory $CD8^+$ T cells that are capable of mounting a rapid cytotoxic response after infection[59,63]. Unfortunately, natural infection with malaria does not lead to sterilising immunity and this level of protection is best induced by multiple immunisations with large numbers of attenuated sporozoites. Therefore, there is something inherent to natural sporozoite infection that restricts the magnitude of parasite-specific $CD8^+$ T cells to such an extent that sterile protection cannot be achieved. Further to this, understanding the mechanisms of protection is complicated by the fact that different strains of *Plasmodium* and different strains of mice lead to models that require subtly different immune responses for protection. This suggests that there is an added element to pre-erythrocytic protection that is context dependent. In mice, $CD8^+$ T cell-mediated protection against *Pb* is almost entirely dependent on interferon gamma (IFNγ) and tumour necrosis factor alpha (TNFα) production. Interestingly though, *Py* protection is additionally dependent on perforin[64]. In order to better understand why there are these differences in $CD8^+$ T cell responses and why protection is only achieved with very high doses of antigen at multiple intervals, an important avenue of investigation is $CD8^+$ T cell regulation. Unfortunately, there is currently a paucity of information regarding this.

An interesting limitation of previous research into protective pre-erythrocytic mechanisms is that it has largely focussed on CSP-specific responses due to the immunodominance of CSP[65]. Therefore, most of our current understanding of pre-erythrocytic immunity is a result of investigating CSP-mediated immune responses. To study the immune mechanisms further, a greater understanding of $CD8^+$ T cell epitopes is required to provide positive T cell activation readouts. Using bioinformatics, Hafalla et al. in 2013 identified 600 $CD8^+$ T cell *Pb* epitopes restricted to C57BL/6 alleles[66]. Using ELISPOT and intracellular staining of $CD8^+$ T cells they validated these peptides and discovered TRAP and S20 protein epitopes. TRAP and S20 are both expressed during the sporozoite stage of the life cycle. TRAP is crucial for sporozoite motility and is expressed on the surface of the parasite, possibly making it a good target for CD8+ T cell responses. S20 is as yet uncharacterised and its location in the sporozoite is unknown; however, it too appears to have

immunogenic properties. This is important as it allows for a broader understanding of $CD8^+$ T cell immune responses to pre-erythrocytic malaria.

An important consideration for pre-erythrocytic malaria infection is that the liver itself is a unique immunological organ, which promotes immune tolerance through a variety of mechanisms, creating an environment that is not conducive to $CD8^+$ T cell activation[67]. Blood arrives to the liver through the hepatic portal vein, transporting with it a multitude of exogenous digestive products generated in the gut. Due to this high presence of non-self antigen in the liver, there is a compensatory dampening of immune activation. The liver experiences constitutive expression of IL-10, particularly via dendritic cells (DCs)[68], which decreases major histocompatibility complex II (MHC II) and B7 molecule expression on liver sinusoid endothelial cells (LSEC)[69]. The liver also promotes an increase in expression of factors involved in inducing T cell tolerance. In a classic mouse model of liver damage, Wei et al. investigated the expression of cytotoxic T lymphocyte antigen 4 (CTLA-4) and transforming growth factor beta (TGFβ) on regulator T (Treg) cells after concavalin-A treatment and found expression to be significantly increased in the liver compared to the spleen[70]. Increased CTLA-4 expression has also been linked to liver resident $CD8^+$ T cells after RAS immunisation[71]. In separate investigations, Treg cells have been shown to promote T cell tolerance through the expression of CTLA-4[72,73]. There is also increased expression of programmed death ligand 1 (PD-L1) in the liver by antigen presenting cells (APCs)[74]. With low antigen expression the binding of T cell programmed death receptor 1 (PD-1) to APC PD-L1 results in expansion but a lack of effector function[75]; however at sufficiently high antigen concentrations function can be achieved[76]. As mentioned previously, a high dose of antigen in the form of RAS can elicit sterile protection; however this might not be necessary if the mechanisms that force the requirement of such a high dose are modulated.

Another method for liver immune suppression is through the action of resident APCs. The role of LSECs in malaria, if any, is largely unknown; however they are capable of antigen presentation and specifically activate $CD4^+$ T cells towards a regulatory phenotype and can prevent cytotoxic $CD8^+$ T cell activation[77]. In addition, the environment of the liver also influences DCs by preventing full differentiation, leading to an immature phenotype and preferential priming of regulatory T cells[67]. Maturation can be induced however by type I IFN, which are produced in response to viral

infection and which may be inhibited by other infections. This understanding of the liver environment shows that T cells in the liver are under constant negative regulation and therefore any changes could promote $CD8^+$ T cell activation and improved immune responses.

1.5.1.2 $CD4^+$ T cell responses to pre-erythrocytic malaria

With regard to the pre-erythrocytic stage, $CD4^+$ T cells are involved in protection through intrinsic and extrinsic mechanisms. Carvalho et al. showed that $CD4^+$ T cells were important in CSP-specific $CD8^+$ T cell responses by blocking CD4 in BALB/c mice immunised against a *Py* CSP epitope[78]. Blockade reduced the magnitude of CSP-specific $CD8^+$ T cells and this control of the $CD8^+$ T cell response was shown to be dependent on IL-4. A second extrinsic mechanism is through $CD4^+$ T cell induced B cell activation and secretion of neutralising antibody[79]; however $CD4^+$ T cells can intrinsically mediate protection through Th1 expression of IFNγ. Oliveira et al. in 2008 showed that immunisation of β2 microglobulin$^{-/-}$ mice with *Py* or *Pb* can still induce protection against challenge regardless of mouse genetic background[79]. When CD4 was blocked using anti-CD4 antibodies protection was significantly abrogated. Similarly, when IFNγ was blocked protection was also reduced, suggesting that (in addition to activating B cells) IFNγ produced by $CD4^+$ T cells in the absence of $CD8^+$ T cells may influence protection.

1.5.1.3 Antibody responses to pre-erythrocytic malaria

During pre-erythrocytic malaria, antibodies have a short window of time in which to successfully recognise sporozoites and prevent infection as they travel from the dermis to the liver. Despite this challenge, high titres of pre-erythrocytic stage-specific antibodies have been shown to correlate with protection[80]. Indeed, in mouse studies it has been shown that antibodies generated by liver stage *Py* immunisation are sufficient to prevent hepatocyte invasion in vitro (also seen in *Pb* immunisation[81,82]) and help reduce, but not eliminate parasitaemia after in vivo transfer to a naïve mouse[83]. Interestingly, the manner in which antibodies offer protection is also different between different stages of malaria infection. Sporozoite-specific antibodies have been shown to act independently from complement activation, agglutination and opsonisation[84,85], suggesting that antibodies could act by coating and neutralising parasites and impede host cell ingress. Although there is a clear shift in the salient adaptive immune mechanisms required as infection progresses from liver stage to

blood stages, antibodies continue to be an important avenue of research for both. CSP has been identified as a major immunodominant protein within the pre-erythrocytic stage. The RTS, S vaccine currently in phase III clinical trials uses the B cell epitope repeat region of CSP as well as CSP T cell epitopes; however, there has been little advancement in the identification of novel pre-erythrocytic malaria B cell epitopes. In order to increase our understanding of B cell protective mechanisms, more antigens and their respective epitopes must be identified and studied.

1.5.2 Adaptive immune responses to blood stage malaria

1.5.2.1 $CD8^+$ T cell responses to blood stage malaria

Contrary to their critical role in protective immunity during pre-erythrocytic *Plasmodium* infection, $CD8^+$ T cells show minimal contribution to protection against blood stage infection. Rather, they contribute towards immune-mediated pathology, particularly experimental cerebral malaria (ECM) in mouse models of blood stage infection of susceptible mice. Athymic nu/nu BALB/c mice that are infected with blood stage *Pb* ANKA do not show symptoms of ECM, unlike nu/+ BALB/c mice[86]. In another investigation, Yañez et al. showed the contribution of $CD4^+$ and $CD8^+$ T cells to ECM using both knock-out and antibody-mediated depletion mouse models[87]. C57BL/6 mice that do not express MHC II[88] and C57BL/6 mice that were depleted of CD4 by antibodies as well as β_2 microglobulin$^{-/-}$ and C57BL/6 mice that were depleted of CD8 by antibodies were all protected from ECM when infected with blood stage *Pb* ANKA parasites. Additionally, gene-targeted deficiency of IFNγ in mice also led to abrogation of ECM, highlighting it as a soluble mediator of ECM. Further research investigating the relationship of $CD4^+$ and $CD8^+$ T cells in ECM has suggested that $CD4^+$ T cells that produce IFNγ during blood stage infection leads to the accumulation of $CD8^+$ T cells in the brain, leading to $CD8^+$ T cell degranulation and breaching of the blood-brain barrier[89–92]. In this context, $CD8^+$ T cells are the principle mediator of ECM disease in mice but it is dependent on IFNγ producing $CD4^+$ T cells. As there is no human model for cerebral malaria investigation, it is important to note that the contribution of $CD8^+$ T cells to human cerebral malaria is not currently fully understood.

Although blood stage *Pb* infection of C57BL/6 mice leads to ECM, this is not the case in BALB/c mice. Indeed, the virulence of blood stage infection in mice can be different

depending on both the *Plasmodium* species and the mouse strain used[93]. As yet, the differing immune mechanisms involved in these models and how they influence $CD8^+$ T cell activation and pathology is poorly understood. Previous work by our group investigated CTLA-4 and PD-1 signalling during blood stage *Pb* ANKA infection in a C57BL/6 and a BALB/c mouse model[94]. Results showed that CTLA-4 and PD-1/PD-L1 signalling independently influence resistance to ECM during blood stage *Pb* ANKA infection in both models and blockade of either pathway resulted in increased T cell activation and susceptibility to ECM in BALB/c mice. Kossodo and colleagues also investigated regulation by showing that IL-10 and TGFβ possibly contribute to protection against cerebral malaria, suggesting that negative regulatory pathways could reduce pathogenic T cell activation[95]. Interestingly, the lab of John Harty has suggested that the progression to blood stage infection is the culprit for low numbers of parasite-specific effector memory $CD8^+$ T cells and therefore poor parasite control in endemic settings[96]. Regardless, it is clear that regulation has a significant impact on the course of blood stage infection and that understanding it will aid future therapeutic discovery.

1.5.2.2 $CD4^+$ T cell responses to blood stage malaria

As blood stage infection involves the recurrent infection of RBCs that do not express MHC, protection is largely dependent on antibodies and helper $CD4^+$ T cell activation of B cells[97,98]. As already mentioned, $CD4^+$ T cells appear to be involved in ECM via the production of IFNγ; however, there is also evidence for them having a protective role. Multiple $CD4^+$ T cell subgroups have been implicated in blood stage malaria[99–102]; however, Treg cells have been studied extensively with respect to blood stage regulation. Although they do appear to be involved in malaria protection, the specifics of their role in protection is not fully understood[96,103]. With *Py* infection of BALB/c mice, Treg cells increase expression of Socks2, IL-10 and CTLA-4 among other regulatory molecules[104]. PD-1 expression is also increased during human infection of *Pf* and if this is investigated further using a C57BL/6 mouse model of *Py* infection, blockade of PD-1 and LAG3 leads to improved immune responses against *Py* malaria[105]. Interestingly however, CTLA-4 blockade in C57BL/6 mouse models of blood stage *Pb* infection increases T cell activation and exacerbates disease[94,106]. Although regulatory pathways appear to be able to significantly influence $CD4^+$ T cell activation during blood stage malaria, further investigation is required in order to fully understand this complex system.

1.5.2.3 Antibody responses to blood stage malaria

In blood stage malaria infection, B cells are crucial for protection. Continuous infection and reinfection with malaria, which is common in holoendemic regions, increases protective antibody titres to levels where individuals can control parasitaemia without sterilising protection[80]. Indeed, transfer of serum from people with naturally acquired non-sterile immunity to naïve individuals is sufficient to reduce disease and parasitaemia[107]. Antibody-mediated control is particularly important during the blood stages of infection as merozoites cyclically infect non-nucleated RBCs, which do not express MHC and therefore cannot directly present antigen to T cells. It has been well established that antibodies against the blood stages of malaria alone are capable of controlling parasitaemia[108] and further research has revealed this protection can be through multiple mechanisms. These include merozoite neutralisation with[109] or without complement[110], antibody-dependent cell inhibition[111], phagocytosis of infected RBCs through antibody help[112] or antibody-dependent respiratory burst by neutrophils[113]. Our current understanding of the level of contribution of each of these mechanisms is; however, incomplete.

1.6 Using high-density peptide array design to identify novel antibody targets

In the post-genome era it has become possible to investigate biological mechanisms to a much greater resolution than ever before. Through technical developments in DNA sequencing it is now cheaper and quicker than ever before to predict all proteins that are encoded within a genome, allowing for unprecedented knowledge pertaining to possible drug and vaccine targets in pathogenic organisms. A technique that has become more and more sophisticated as –omics research has developed is the use of microarrays. Using microarrays allows for high-density, high-throughput investigation of thousands of molecular targets using chips as small as a glass slide. As proteins are encoded by the genome and dysregulation of proteins is inexorably linked to many diseases, the fields of transcriptomics and proteomics have become increasingly important in biomedical research.

As microarrays have gained in popularity their use has become increasingly diverse. Applications include protein expression profiling, molecular interaction mapping, biomarker discovery, drug target discovery, disease diagnosis and epitope mapping. In the discipline of vaccinology, the ability to probe thousands of possible vaccine targets at one time is particularly useful. Earlier research in vaccine development largely included isolating the pathogenic agent, attenuating it to the extent that it does not cause clinical symptoms but still induces immunity and injecting it to elicit protection. In order to identify specific targets proteins would have to be generated and investigated separately. To study multiple potential antigens on a miniaturised, parallel platform such as a microarray, the first and most time-consuming element is the synthesis of the peptide/protein library. A robust, multi-step process is to synthesise peptides/proteins first and then robotically transfer them to the array slide. Since the development of Solid Phase Protein Synthesis (SPPS) however[114], molecules can be built directly on the surface of beads coated in a specific linker. The advantage of this method is that it allows for the synthesis of peptides and proteins that cannot be produced through cellular mechanisms, for example sequences that bacteria cannot generate, sequences that incorporate unnatural amino acids or sequences that require a modified backbone. This strategy has since been expanded to allow for rapid, parallel synthesis of a large array of randomly sequenced peptides or proteins through the split-and-pool technique[115,116]. In terms of vaccine target discovery, these developments in array technology allow for the synthesis of an entire proteome that can fit onto array chips that can be relatively easily probed and investigated. Carmona et al. in their 2015 paper investigating *Trypanosoma cruzi* antigenic determinants used microarray technology to screen 457 proteins from the CL-Brener strain[117]. The peptide library consisted of peptides 15 amino acids in length with a 14 amino acid overlap of the previous peptides sequence, resulting in more than 175,000 individual peptides. Synthesis of the peptide library involved the direct *in situ* SPPS generation of sequences on the array slide itself with a high resolution permitted by the use of photolithography techniques[118]. In their paper they describe over 120 novel linear antigenic determinants through analysis of these peptides when probed sequentially with naïve control and Chagas disease positive human sera. This paper shows an unprecedented examination of the most antibody specificities identified in parallel for a single human infection.

The use of microarray design has clear advantages compared to its predecessors; however it is not a perfect system for identifying all epitopes within a biological

system. Other techniques such as ELISA are quicker and much simpler; however, they normally investigate antigenic determinants through non-covalent peptide immobilisation which does not specifically determine the orientation of the molecule on the slide, introducing variability. Even covalent immobilization could affect the molecular structure; however this is less of a concern for shorter peptides. Possibly the main disadvantage of peptide microarrays is that only linear epitopes can be identified, leaving non-linear epitopes that comprise approximately 95% of the potential antigenic regions unknown. In the context of malaria, microarrays have been used extensively to evaluate the immune response to malaria infection and to evaluate the efficacy of vaccination[119]. Interestingly though, they have not been utilised to identify novel pre-erythrocytic stage antigens using a mouse model of malaria. Here I will describe the use of microarray technology to investigate liver and sporozoite stage proteomes with the objective of vaccine target discovery.

1.7 Aims and research objectives

The work presented here concerns three main hypotheses. First that $CD8^+$ T cell inhibitory regulation during exposure to pre-erythrocytic malaria infection is capable of negatively influencing protective $CD8^+$ T cell responses. Secondly, that IL-10R signalling during blood stage infection of an ECM refractory mouse model of malaria is involved in ECM resistance. Finally, I hypothesised that protective pre-erythrocytic immunisation generates non-CSP antigen-specific antibody responses that may offer protective immunity towards pre-erythrocytic infection.

In order to investigate these hypotheses I used mouse models of malaria. From my hypotheses my first objective was to investigate CD8 T cell regulatory pathways and their contribution to $CD8^+$ T cell inhibition during a non-protective attenuated sporozoite immunisation. The pathways I chose to investigate were CTLA-4, PD-1, IL-27R and IL-10R signalling. My second objective was to confirm whether IL-10R signalling is involved in blood stage resistance to ECM using BALB/c mice that are normally resistant. My final objective was to validate a novel immunisation schedule that preferentially boosted non-CSP antibody responses and use serum from immunised mice to investigate novel pre-erythrocytic antigens using high-density microarray technology.

2 | Blockade of CTLA-4 Augments $CD8^+$ T Cell-Mediated Protection Against Malaria Pre-erythrocytic Stages

2.1 Introduction

Malaria infection is initiated by the inoculation of *Plasmodium* sporozoites into the vertebrate host by female *Anopheles* mosquito vectors. Sporozoites preferentially locate to the liver where they invade and develop in hepatocytes. This is the pre-erythrocytic stage of their life cycle, which is clinically silent and therefore a particularly interesting stage for drug and vaccine research. Immunisation with RAS elicits sterile protection against sporozoite challenge. By comparing protection in *Pb* immunised T cell deficient mice (thymectomised, irradiated, B cell reconstituted and anti-thymocyte serum treated) and B cell deficient mice (treated from birth with goat anti-mouse μ chain serum), Chen and colleagues showed that this protection is dependent on T cell, but not antibody responses[120]. Sporozoite challenge of immunised T cell deficient mice resulted in no protection but immunised μ-suppressed mice were still protected from challenge. Further to this, it has been shown that $CD8^+$ T cells in particular are critical mediators of protection during the pre-erythrocytic stage. In their experiments, Weiss et al. successfully immunised BALB/c mice against *Py* sporozoite challenge by multiple immunisations with radiation attenuated *Py* sporozoites; however, this protection could be completely removed with the antibody-mediated depletion of CD8 but not CD4 prior to challenge[121]. The sporozoite surface exhibits a high density of CSP, which is immunodominant and offers a considerable contribution to pre-erythrocytic immunity. Rodrigues and colleagues generated *Py*-specific spleen derived $CD8^+$ T cell clones using a BALB/c model of immunisation with γ-radiation attenuated *Py* sporozoites[61]. They found that clones specific for the region between amino acids 277 and 288 of *Py* CSP became highly cytotoxic upon exposure to MHC compatible cells that had previously been cultured with *Py* CSP peptide. The potency of this response was further investigated by adoptively transferring these clones into naïve BALB/c mice before challenge with *Py* sporozoites. Incredibly, adoptive transfer of two clones was sufficient to elicit complete sterile protection against challenge and this protection was through inhibition of liver stage parasite development. Work done by the Harty lab further supports the importance of cytotoxic T cell responses in protection against liver stage malaria through immunisation of BALB/c mice against *Pb* CSP[122]. Immunisation specifically targeted the development of memory $CD8^+$ T cells through the use of DCs that were coated in CSP peptide, followed by a boosting immunisation with attenuated *L. monocytogenes* (*actA* and *inlB* deficient[123]) expressing the same peptide. This led

to sterile protection against *Pb* sporozoite infection with 5 separate challenges between 7 and 19 months after immunisation. Subsequent work by the Hill group supports the importance of focusing malaria vaccine research on the generation of $CD8^+$ T cell responses through their development of the Adenovirus prime and Modified Vaccinia Ankara (MVA) boost regimen[124]. Protective $CD8^+$ T cell responses generated against *Pb* ANKA CSP peptide were sufficient to elicit protection against *Pb* sporozoite challenge. Interestingly, protection was also elicited through immunisation against a TRAP peptide. These experiments highlight that antigen experienced $CD8^+$ T cells are capable of recognising sporozoite antigens and responding with functional immunity, even in the absence of any other parasite-specific immune mechanisms.

Currently the gold standard in malaria immunisation requires multiple vaccinations with large numbers of whole, attenuated parasites, eliciting sterile immunity against the pre-erythrocytic stages of *Plasmodium* species[40,43,125,126] . This exposes the immune system to a level of antigen that is many times greater than what is normally experienced in an endemic setting, eliciting sterile protection that cannot be achieved naturally. Why a single immunisation of RAS does not promote a sufficient protective $CD8^+$ T cell immune response is an important question as a greater understanding of this would allow for the design of more efficacious RAS vaccines. It would seem that regulation of $CD8^+$ T cell responses could account for the requirement of such high doses of vaccine at multiple intervals; however, there is a paucity of research that has addressed this facet of the pre-erythrocytic immune response.

Promotion of appropriate immunological responses prevents uncontrolled atypical lymphoproliferation and activation in response to foreign antigens[127,128] as well as autoimmune disease due to self-reactive T cells[129]. Due to the possible pathological outcomes of T cell stimulation, successful activation requires a series of signals that must occur within appropriate temporal and spatial boundaries. The first signal required is T cell receptor (TCR) recognition of exogenous peptide bound to a MHC molecule on an APC. This non-covalent interaction initiates the recruitment of co-receptors that are crucial for eliciting an appropriate response and provides the site at which consequent stimulatory signals must occur. The second activating signal consists of costimulatory receptors that associate with the TCR and bind their cognate molecules, facilitating lowering the threshold of T cell activation and forming the

immune synapse. CD28 is a particularly potent costimulatory receptor that associates with the TCR. Successful binding of CD28 to the B7 molecules CD80 and CD86 promotes intracellular phosphorylation of CD28, leading to activation of lymphocyte-specific protein tyrosine kinase (Lck), growth factor receptor-bound protein 2 (GRB2) and phosphatidylinositol-3-kinase (PI3K) signalling pathways in mice[130–133] . There is also evidence that CD28 has a temporal influence on T cell activation as it reduces the amount of time required for activation after TCR recognition of peptide bound to MHC[134,135].

After initial TCR activation, expression of inhibitory receptors including CTLA-4 (CD152) and PD-1 (CD279) are upregulated in order to control the strength and duration of T cell activation[136,137]. CTLA-4 is normally present as a dimer at low concentrations on the $CD8^+$ T cell surface due to clathrin-mediated endocytosis[138]; however, TCR activation drives the production of protein and translocation of intracellular CTLA-4 to the cell membrane. CTLA-4 co-inhibition of the TCR is not fully understood; however several studies show its potent effects are the result of both cell intrinsic and extrinsic mechanisms. CTLA-4 shares its MYPPPY binding motif with CD28 and has a higher affinity for their cognate molecules CD80 and CD86[139], allowing it to directly compete with CD28 at the immune synapse and prevent prolonged TCR excitation. After binding to B7 molecules, CTLA-4 produces a negative cell intrinsic signal through the dephosphorylation of proteins involved in TCR signalling, including CD3ζ, zeta chain associated protein kinase 70 (ZAP70), and Lck[140]. Furthermore, Treg cells are able to influence the activation of effector T cells via their CTLA-4 in a cell extrinsic manner. Treg cells can recognize MHC-peptide complexes and bind their CTLA-4 receptor to B7 molecules on the APC surface. Due to the higher expression of CTLA-4 on Treg cells compared to effector T cells, this competition prevents CD28-mediated activation of non-regulatory T cells[141]. It has also been shown that by transendocytosis, T cells can completely remove B7 molecules from the APC and degrade them in intracellular lysosomes[142].

PD-1 signalling is distinct from CTLA-4 signalling; however, it is also capable of dephosphorylating molecules downstream of the TCR. It is largely associated with $CD8^+$ T cell exhaustion, particularly in chronic infection[143]. PD-1 monomers on the T cell surface bind to PD-L1 (CD274), which is expressed on B and T cells, macrophages and dendritic cells; and PD-L2 (CD273), which is expressed

constitutively on macrophages and dendritic cells[144]. Binding leads to PD-1 localisation to the TCR and de-phosphorylation of CD3ζ, ZAP70 and protein kinase C Θ (PKCΘ) via recruitment of SHP2[145–147]. Recruitment of SHP2 can also inhibit CD28 signalling as well as TCR signalling due to blocking PI3K activation downstream of CD28[148].

Due to the efficiency with which these inhibitory receptors can regulate T cell activation, they have been investigated extensively as targets for therapeutic interventions. Blockade of PD-1 signalling has been shown to have a positive effect on resolving infection in chronic, but not acute disease [143]. CTLA-4 blockade however; can increase the action of antigen-specific T cells in both acute and chronic infection[149–151]. Further research has investigated the outcome of infection if inhibitory receptors are blocked concurrently with vaccination. In their investigations into improving vaccines against chronic viral infection, Sang-Jun Ha and others used a C57BL/6 mouse model in which mice were immunised with recombinant vaccinia virus that expresses a Lymphocytic choriomeningitis virus (LCMV) $CD8^+$ T cell epitope[152]. On and following the day of immunisation, mice were given doses of PD-L1 blocking antibody to prevent PD-1 signalling. Upon challenge with LCMV, it was observed that there was a synergistic effect of immunisation and blockade, increasing epitope-specific $CD8^+$ T cell function which subsequently protected against infection, even in the absence of $CD4^+$ T cells. With regard to CTLA-4 blockade with immunisation, the Allison group have used a *Listeria monocytogenes* mouse model[153]. OT-1 $CD8^+$ T cells were adoptively transferred into C57BL/6 mice, followed by a vaccination dose of *L. monocytogenes* that expressed the ovalbumin $CD8^+$ T cell epitope SIINFEKL. Blockade of CTLA-4 during vaccination resulted in an increase in the number of epitope-specific effector memory OT-1 $CD8^+$ T cells and increased TNFα production upon re-stimulation with SIINFEKL peptide. These discoveries have led to continued animal and human research into cancer immunotherapy, showing clearance of tumours after vaccination concurrently with blockade of CTLA-4[154–156], PD-1 and in combination[157,158].

During blood stage infection, T cell responses have multiple potential functions of both protection and pathology. As the clinical symptoms of malaria occur during blood stage infection, it is important to understand how these responses are regulated and this has led to some research into pathways including CTLA-4 and PD-1. Both CTLA-

4 and PD-1 are upregulated during blood stage malaria infection in humans and non-human animals[106,159–162]; however, their effects appear to be context dependent. In a study by Lepenies et al. infection of BALB/c mice with blood stage non-lethal *Py* (17NL) or lethal *Py* (17L) parasites resulted in increased CTLA-4 expression on $CD4^+$ T cells but blockade of CTLA-4 during infection led to strikingly contrasting results[163]. CTLA-4 blockade with non-lethal *Py* infection led to reduced peak parasitaemia and early clearance of infection but CTLA-4 blockade with lethal infection resulted in increased liver pathology. It is also important to note that expression of CTLA-4 and PD-1 differs with models of *Plasmodium* infection. Blood stage infection of ECM resistant BALB/c mice with *Pb* ANKA results, paradoxically, in lower expression of CTLA-4 and PD-1 on $CD4^+$ and $CD8^+$ T cells compared to ECM susceptible C57BL/6 mice; however, blockade of CTLA-4 or PD-1/PD-L1 but not PD-1/PD-L2 leads to BALB/c mice becoming susceptible to ECM[94].

Unfortunately, there is little understanding as to the importance of CTLA-4 or PD-1 signalling in pre-erythrocytic malaria infection. In this study I investigate this question using a C57BL/6 mouse model of pre-erythrocytic γ-radiation attenuated *Pb* sporozoite immunisation and subsequent challenge. I gave a normally non-protective single immunisation with γ-radiation attenuated *Pb* sporozoites to C57BL/6 mice concurrently with or without blocking antibodies against CTLA-4, PD-L1 or PD-L2. Using flow cytometry and antibody-mediated blockade I show that immunisation with CTLA-4 blockade, but not PD-L1 or PD-L2 blockade significantly induces the production of IFNγ by $CD8^+$ T cells upon peptide re-stimulation. Challenge of these mice *in vivo* resulted in a significant number of mice from the CTLA-4 group having sterile protection after infection, which was not observed in PD-L1 or control groups. Through the depletion of IFNγ, CD4 and CD8 I show that CTLA-4 blockade-mediated protection is through both $CD4^+$ and $CD8^+$ T cells and their production of IFNγ. Using flow cytometry and antibody-mediated blockade I show that immunisation with CTLA-4 blockade, but not PD-L1 blockade significantly induces the production of IFNγ by $CD8^+$ T cells upon sporozoite peptide re-stimulation. This is a proof of principle that immune modulation of CTLA-4 can augment $CD8^+$ T cell-mediated protection in a normally non-protective single immunisation of γ-radiation attenuated *Pb* ANKA sporozoites in a mouse model of ECM.

2.2 Materials and Methods

2.2.1 Mosquito and mouse conditions

C57BL/6 mice between 5-8 weeks were bred in-house at London School of Hygiene and Tropical Medicine (LSHTM) or by Charles River Laboratories (UK). They were housed in filter-topped cages up to 6 per cage with absorbent bedding, nesting material and enrichment. Their diet consisted of autoclaved water and food pellets. Procedures were performed under license from the United Kingdom Home Office under the Animals (Scientific Procedures) Act 1986 and approved by the Animal Care and Ethical Review Committee.

Pb ANKA infected *Anopheles stephensi* mosquitoes grown either at LSHTM or the Max Planck Institute for Infection Biology, Berlin were kept at 22°C with 80% humidity and fed on 10% glucose solution (10% D-Glucose [Sigma-Aldrich] in distilled water). In order to generate infectious *Pb* sporozoites, blood stage parasites were first collected from infected C57BL/6 mice via cardiac puncture into 1.5ml Eppendorf tubes (Sigma) with heparin (Sigma) and kept on ice. Blood was diluted 1:2 in freezing media made from 7.5% Glycerol (Sigma) in RPMI complete (RPMI 1640 [Gibco] with 10% FCS [Gibco], 2% L-Glutamine [Gibco] and 1% Penicillin and Streptomycin [Gibco]) and kept at -80°C. When required, blood stage parasites were thawed and 200µl was injected intravenously (i.v.) into a naïve C57BL/6 mouse. After three days, blood was collected from the infected mouse via cardiac puncture and 100,000 infected RBCs were passaged into two naïve C57BL/6 mice. 4 days after passage, mice were given a terminal dose (100-150µl) of anaesthesia consisting of 50% phosphate buffered saline (PBS) (Gibco), 33% ketamine (Ketamidor, 100mg/ml [National Veterinary Services Limited]) and 17% xylazine (Rompun, 2% w/v [National Veterinary Services Limited]) intraperitoneally (i.p.) and placed on a cage of mosquitoes (70 mosquitoes per mouse) for a 30 minute blood feed. Ketamidor and Rompun were purchased under prescription through LSHTM's Named Veterinary Surgeon. 18-20 days after blood feed, mosquitoes were judged to be positive for sporozoites in the salivary glands.

2.2.2 Whole sporozoite immunisation and challenge

Female *Anopheles stephensi* salivary glands were dissected from infected mosquitoes in RPMI complete and *Pb* ANKA sporozoites were isolated through salivary gland homogenisation and centrifugation. Glands were homogenised using autoclaved plastic pestles in Eppendorf tubes and centrifuged at 10,000 rpm for 3 minutes. The pellet was re-suspended in 200µl of RPMI complete and *Pb* ANKA sporozoites were counted on a C-chip haemocytometer (Digital bio). For immunisations, *Pb* ANKA sporozoites were diluted to 50,000/ml in RPMI complete. To attenuate by irradiation for immunisation, the suspension was exposed to gamma radiation at $1.2x10^4$ centigray (cGY) for 20.5 minutes. C57BL/6 mice were immunised by an i.v. injection of 10,000 attenuated *Pb* ANKA sporozoites per mouse. For challenge, *Pb* ANKA sporozoites were diluted to 5,000 per ml in RPMI and 1,000 parasites were given i.v. per mouse. Parasitaemia (%) was measured by microscopy using thin blood smears from mouse tail blood that were fixed in methanol and stained for 15 minutes with Giemsa (VWR Chemical) diluted 1:5 in water.

2.2.3 Antibody blockade

Antibodies were diluted from stock solutions to 1mg/ml in PBS. 0.2ml of α-CTLA-4 [UC10-4F10-11], α-PD-L1 [9G2] or α-PD-L2 [TY5] antibodies (BioXcell) were given i.p. per mouse concurrently with γ-radiation attenuated *Pb* ANKA sporozoite immunisation. For experiments in which they were used for neutralisation (α-IFNγ [XMG1.2]) or depletion (α-CD4 [GK1.5] and α-CD8 [53.6.72]) (BioXcell) antibodies were given 3 days and 1 day before *Pb* ANKA sporozoite challenge. Immunised controls were given 0.2ml of PBS i.p. per mouse and no antibodies. Previous work by our group has shown that rat IgG isotype controls do not provide any protection against malaria challenge [94].

2.2.4 Flow cytometry

Spleens were passed through a 70nm pore nylon cell strainer (BD) and centrifuged at 1,800 rpm for 4 minutes. To lyse RBC's the pellet was re-suspended in 1ml of 1x lysis buffer (10x lysis buffer [BD] diluted 1:10 in autoclaved distilled water) and incubated for 10 minutes. Splenocytes were washed by diluting to 10ml in RPMI

complete followed by centrifugation at 1,800 rpm for 4 minutes, discarding the supernatant and diluted to 2 million cells per well. Livers were perfused with PBS during dissection and also passed through a 70nm nylon cell strainer. The homogenate was centrifuged at 1,800rpm for 4 minutes and the pellet was re-suspended in Percoll gradient (4% 10x PBS [Gibco], 36% Percoll[GE Healthcare] and 60% RPMI) and centrifuged at 2,000rpm for 10 minutes. Supernatant was discarded and RBC's were lysed using lysis buffer for 5 minutes and washed in RPMI using the same protocol as for splenocytes before being re-suspended to 180µl per condition.

Sporozoite peptides from TRAP (SALLNVDNL) and S20 (VNYSFLYLF) were synthesised by Mimotopes (Melbourne, Australia) using 9-fluorenylmethoxycarbonyl (Fmoc) chemistry and pseudoprolines to prevent unwanted coupling[164]. Lymphocytes were re-stimulated with 10µg of peptide and brefeldin A (BFA) (ebioscience). Lymphocytes were incubated for 6 hours at 37°C with 5% CO_2. Cells were stained with α-CD3 (V500), α-CD4 (APC), α-CD8a (PerCP Cy5.5), α-CD11a (e450), α-IFNγ (PE Cy7), α-TNFα (FITC), α-CTLA-4 (PE) or α-PD-1 (PE Cy7) as required (ebioscience).

2.2.5 Real Time PCR (RT-PCR)

Liver sections were added to 3ml of TRIzol (Fisher Scientific) in a 15ml Falcon tube (Fisher Scientific) and homogenised using a Power Gen 125 tissue homogenizer (Fisher Scientific). Between samples the homogeniser was washed in distilled water and between groups it was washed in a 1% sodium dodecyl sulphate (SDS) (Sigma) solution. 200µl of sample was mixed with 300µl of TRIzol and stored at -80°C until RNA extraction. For RNA extraction 200µl of chloroform was added to the 500µl sample and centrifuged at 13,000 rpm for 15 minutes at 4°C. The upper layer was then transferred into 1.5ml RNAse free eppendorf tubes (ThermoFisher). 250µl of isopropanol, 60µl of 3M Sodium Acetate and 0.5µl glycoblue (5mg/ml) was added per sample and all samples were left at -20°C overnight. Tubes were spun at 13,000 rpm for 15 minutes at 4°C and the supernatant was removed. Pellets were washed with 400µl of ice-cold ethanol and re-suspended before spinning at 13,000 rpm for 10 minutes at 4°C. 80µl of RNAse/DNAse-free water (Sigma) was added per sample and all tubes were heated to 65°C until pellets had dissolved. To 5µl of RNA sample, 5µl of Oligo dT-Primers and 0.5µl random primers (Retroscript kit, Ambion) were added.

Tubes were centrifuged, put at 75°C for 3 minutes and centrifuged again before being put on ice. To each sample a mix of 10x RT buffer, dNTP, 4x RNAse inhibitor and MMLV-RT enzyme (Retroscript kit, Ambion) was added before centrifugation. Samples were heated to 42°C for 60 minutes followed by 90°C for 10 minutes. cDNA was diluted and primers for the mouse endogenous control glyceraldehyde 3-phosphate dehydrogenase (GAPDH) (forward 5'-CGTCCCGTAGACAAAATGGT-3', reverse 5'-TTGATGGCAACAATCTCCAC-3') (Eurofins) and *Pb* ANKA 18S (forward 5'-TGAGGCCGGTGCTGAGTATGTCG-3', reverse 5'-CCACAGTCTTCTGGGTGGCAGTG-3') (Eurofins) were added with SYBR Green I Master Mix (ThermoFisher). Samples were run for 15 minutes at 95°C as an initial denaturing stage. Amplification was 40 repetitions at 95°C (denaturation) for 15 seconds, 55°C (annealing temp) for 15 seconds and 65°C (data collection) for 45 seconds. The final sequence collected melting curve data, beginning at 95°C (denaturation) for 15 seconds then increasing from 60°C by 1°C per minute to a final temperature of 95°C. A 7500 Fast & 7500 Real-Time PCR System (Applied Biosystems) was used and analysed using 7500 Software version 2.0.6 (Applied Biosystems).

2.3 Results

In response to the pre-erythrocytic stage of malaria, T cell-mediated responses are crucial in resolving infection. Adoptive transfer of BALB/c parasite-specific effector memory $CD8^+$ T cells ($CD62L^-CD127^+$) alone is sufficient to elicit sterile protection against *Pb* ANKA sporozoite challenge in naïve BALB/c mice[124], showing that $CD8^+$ T cells can independently clear infection. Although regulation of $CD8^+$ T cells through pathways including CTLA-4 and PD-1 have been shown to be involved in blood stage malaria, little is known with regard to these pathways during liver stage malaria infection and how they may influence $CD8^+$ T cell responses to sporozoite infection. To address this, I investigated whether CTLA-4 and PD-1 production is upregulated by T cells in response to a single immunisation with γ-radiation attenuated *Pb* ANKA sporozoite immunisation in C57BL/6 mice. Following from this I used a C57BL/6 mouse model to determine whether modulation of these pathways can influence the magnitude of antigen-specific $CD8^+$ T cell responses after a single, normally non-

protective vaccination and whether this contributes towards immune protection from sporozoite challenge.

I first investigated CTLA-4 and PD-1 expression on $CD4^+$ and $CD8^+$ T cells using a C57BL/6 mouse model of immunisation. 2 weeks after a γ-radiation attenuated *Pb* ANKA sporozoite immunisation, spleens and livers were taken and lymphocytes were stained for T cell markers CD3a, CD4 and CD8 as well as PD-1 and intracellular CTLA-4 (Figure 2.1). These two organs were chosen for study as the spleen is an important secondary lymphoid organ and a site for T cell activation to blood borne antigens and the liver is the site of pre-erythrocytic infection and therefore local T cell responses. Using flow cytometry I was able to distinguish any differences in expression of these regulatory molecules between immunised and naïve mice. The histograms showing median fluorescence intensity (MFI) for CTLA-4 showed small shifts towards higher levels of CTLA-4 on $CD4^+$ and $CD8^+$ T cells with immunisation (Figure 2.1). This trend was much more apparent when I compared the numbers of T cells expressing CTLA-4 with or without immunisation. Indeed, with immunisation there was significantly higher expression of CTLA-4 in the spleen and liver for $CD8^+$ T cells and in the liver for $CD4^+$ T cells. Similarly, for PD-1 expression there appeared to be a shift towards more $CD4^+$ and $CD8^+$ T cells expressing PD-1 after immunisation and this achieved significance in the spleen and liver for both $CD4^+$ and $CD8^+$ T cells. These experiments show that immunisation with γ-radiation attenuated *Pb* ANKA sporozoites followed by *ex vivo* sporozoite antigen re-stimulation leads to an increase in the production of PD-1 and CTLA-4 by $CD4^+$ and $CD8^+$ T cells in both liver and spleen T cells, suggesting a possible involvement of both pathways in regulating T cell responses to subsequent *Pb* sporozoite antigen exposure.

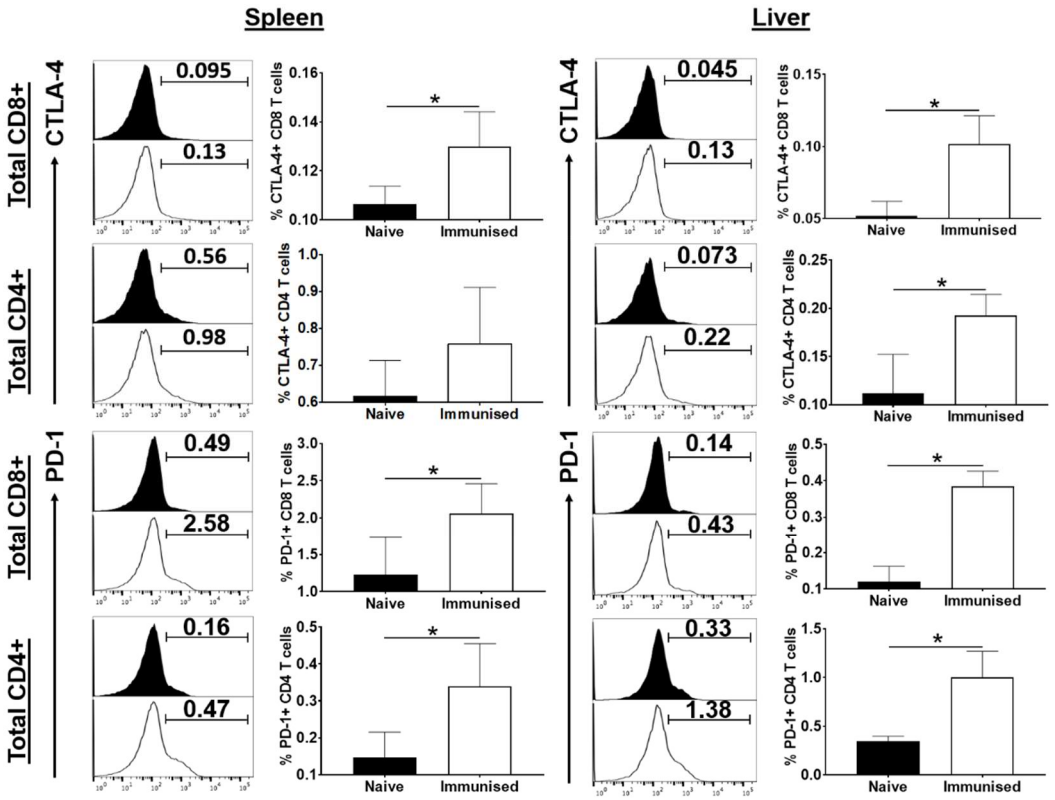

Figure 2.1. Attenuated *Pb* sporozoite immunisation increases the expression of CTLA-4 and PD-1 on CD4⁺ and CD8⁺ T cells.

C57BL/6 mice were either naïve or immunised with 10,000 γ-radiation attenuated *Pb* ANKA sporozoites i.v. After 2 weeks spleens and livers were taken and lymphocytes were stimulated with 10μg/ml of TRAP peptide (SALLNVDNL) for 6 hours with BFA. After stimulation, cells were stained for CD4, CD8 and PD-1 and intracellularly stained for CTLA-4. Statistics performed using Mann-Whitney t test, data from three experiments with n=4 mice per group.

Showing that *Pb* sporozoite immunisation leads to an increase in T cell expression of PD-1 and CTLA-4 led to my next question, how strongly does increased expression of CTLA-4 and PD-1 influence functional T cell responses to sporozoite peptide antigen re-stimulation? C57BL/6 mice were given a single immunisation of γ-radiation attenuated *Pb* ANKA sporozoites i.v. concurrently with CTLA-4 or PD-L1 blockade. This was done by giving an additional injection of blocking antibodies (α-CTLA-4 and α-PD-L1 respectively) i.p. at the time of immunisation. The rationale for using blocking antibodies is that genetically knocking out CTLA-4 is fatal and knocking out PD-1 results in spontaneous autoimmunity. By using blocking antibodies the function of these proteins can be inhibited for a determined amount of time in isolation in WT mice. Furthermore, using blocking antibodies in this way inhibits T cell activation during the initial immunisation, but when mice are subsequently challenged, these proteins are functional and T cell activation is restored. Therefore, the absence of

CTLA-4 or PD-1 signalling during sporozoite exposure alone can be investigated. Although not performed in this investigation, confirmation of blocking antibody specificity could be done by performing a western blot using recombinant protein that is to be blocked and targeting it with blocking antibody, finally using a secondary antibody to detect successful binding.

In order to examine changes in the total number of antigen experienced T cells using flow cytometry, I gated $CD3^+CD4^+$ and $CD3^+CD8^+$ populations using CD11a (Figure 2.2). CD11a is a marker for antigen experienced T cells, co-localising with CD18 to form lymphocyte function associated protein 1 (LFA1), which binds to intercellular adhesion molecule 1 (ICAM1), increasing adhesion and the frequency of antigen recognition. As positive readouts for $CD8^+$ T cell activation, previously identified pre-erythrocytic stage linear antigen sequences originating in thrombospondin-related adhesion protein (TRAP) (SALLNVDNL)[66] and sporozoite-specific protein 20 (S20) (VNYSFLYLF)[66] were used. 2 weeks after a single sporozoite immunisation with or without α-PD-L1 or α-CTLA-4, spleens and livers were taken and lymphocytes were re-stimulated with the TRAP or S20 peptides. After a 6 hour incubation with peptide, cells were fixed and stained for T cell markers CD3a, CD4, CD8 and CD11a and effector cytokine IFNγ for flow cytometric analysis. Secretion of IFNγ is critical for protective $CD8^+$ T cell responses against pre-erythrocytic malaria infection[57].

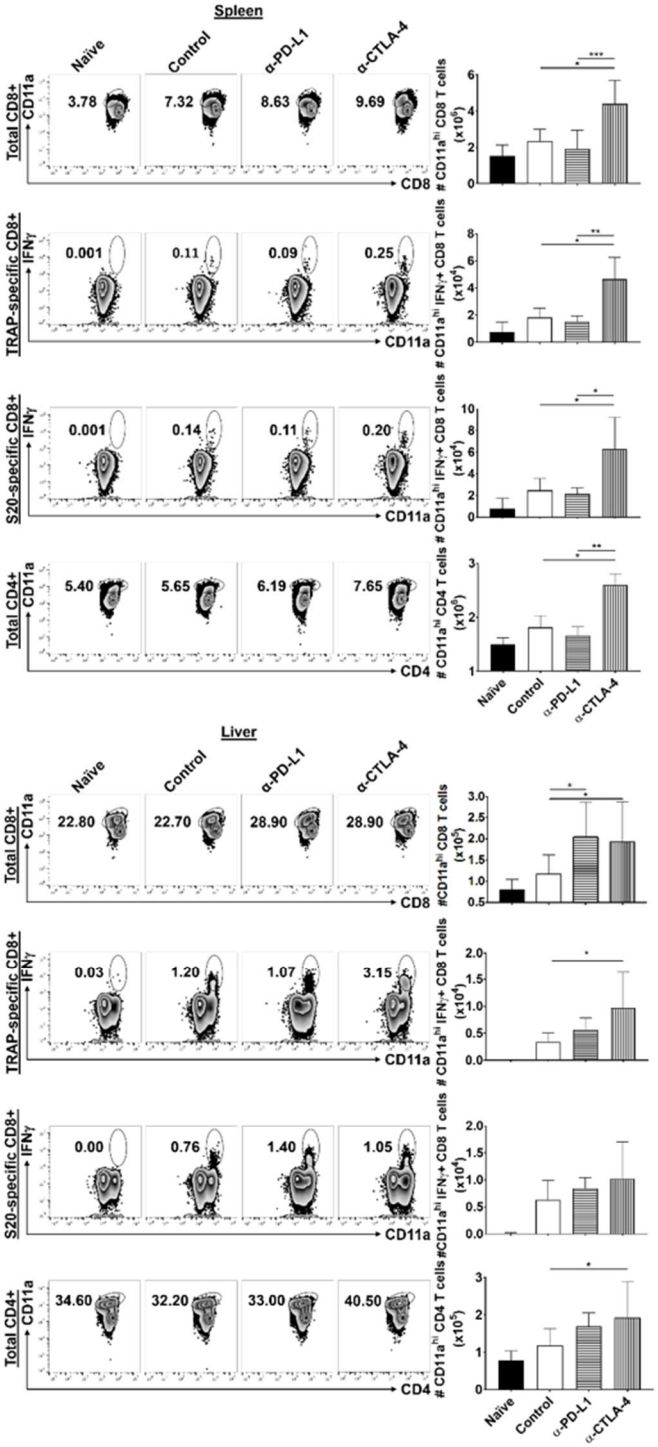

Figure 2.2. CTLA-4 blockade with immunisation influences the number of parasite-specific CD8⁺ T cells in the spleen and liver; however PD-L1 blockade does not.

C57BL/6 mice were either naïve or immunised with 10,000 γ-radiation attenuated *Pb* ANKA sporozoites i.v. with or without 200μg of blocking antibody (α-CTLA-4 or α-PD-L1) i.p. After 2 weeks spleens and livers were taken and lymphocytes were stimulated with 10μg/ml of TRAP (SALLNVDNL) or S20 (VNYSFLYLF) peptide for 6 hours with BFA. After stimulation, cells were stained for T cell markers CD3a, CD4, CD8a, CD11a and IFNγ. Total numbers of antigen experienced ($CD11a^+$) $CD8^+$ and $CD4^+$ T cells are shown as well as total numbers of IFNγ-producing $CD8^+$ T cells after peptide re-stimulation ($IFN\gamma^+$ $CD11a^{hi}$). Statistics performed using Kruskal-Wallis test with Dunn's multiple comparisons post-test. Pooled data from three experiments with n=5 mice per group per experiment.

In the spleen CTLA-4 blockade with a single γ-radiation attenuated *Pb* ANKA sporozoite immunisation consistently increased the total number of TRAP and S20 peptide-specific, antigen experienced T cells ($CD8^+CD11a^{hi}$ and $CD4^+CD11a^{hi}$ T cells) compared to immunised and naïve controls. Most importantly, there is a clear difference in the spleen between the effect of CTLA-4 blockade with immunisation and the effect of PD-L1 blockade with immunisation on antigen experienced $CD4^+$ and $CD8^+$ T cell populations (p=0.0035 and p=0.0003 respectively). Compared to immunised control groups, PD-L1 blockade with immunisation did not significantly increase the total number of antigen experienced $CD4^+$ or $CD8^+$ T cells. In contrast, if mice received CTLA-4 blockade with immunisation there was a significant increase in antigen experienced $CD4^+$ and $CD8^+$ T cell numbers compared to immunised controls (p=0.0112 and p=0.0309 respectively). This observation was also true when functional production of IFNγ was measured. In the spleen, CTLA-4 blockade significantly increased the number of TRAP-specific IFNγ producing cells compared to PD-L1 blockade (p=0.018) and naïve and immunised controls (p=0.0001 and p=0.0415 respectively). After S20 re-stimulation, α-CTLA-4 treated mice also had significantly more peptide-specific, IFNγ producing $CD8^+$ T cells compared to α-PD-L1 treated or immunised or naïve controls (p=0.0167, p=0.0465 and p=0.0001 respectively).

In the liver, total numbers of antigen experienced $CD8^+$ and $CD4^+$ T cells appear to be similar whether immunisation was accompanied by CTLA-4 or PD-L1 blockade, although there is a trend towards higher numbers of antigen experienced $CD4^+$ T cells if α-CTLA-4 was given at immunisation. Even though statistical significance was not observed, there was also a trend towards more IFNγ-producing $CD8^+$ T cells after peptide re-stimulation if CTLA-4 was blocked at immunisation.

Taken together, these results show that immunisation with blockade of CTLA-4 but not PD-L1 can result in an increase in the capacity to generate antigen experienced $CD8^+$ and $CD4^+$ T cells compared to mice that only received immunisation. With regard to functional responses, it would also appear that CTLA-4 blockade with γ-radiation attenuated *Pb* sporozoite immunisation increases the number of TRAP- and S20-specific, IFNγ-producing $CD8^+$ T cells. As TNFα is also an important $CD8^+$ T cell cytokine that is associated with protection in pre-erythrocytic malaria, TNFα production by $CD8^+$ T cells after stimulation with TRAP and S20 peptides was also

investigated; however, although there was a small trend towards higher levels of TNFα with CTLA-4 blockade and immunisation compared to other groups, this was not significant (Figure 2.S1). For this reason future experiments focused on $CD8^+$ T cell production of IFNγ.

Although PD-L1 signalling is much more widely studied than PD-L2 signalling, I also investigated the effect of blocking PD-L2 with a single immunisation (Figure 2.3). PD-L1 and PD-L2 do not have identical signalling pathways and act independently; however, the results show that PD-L2 blockade also has no effect on IFNγ production by antigen-experienced $CD8^+$ T cells compared to CTLA-4 blockade with immunisation. Following these results I decided to focus on CTLA-4 signalling and PD-L1 signalling as PD-L1 blockade is much more extensively described in relation to $CD8^+$ T cell regulation.

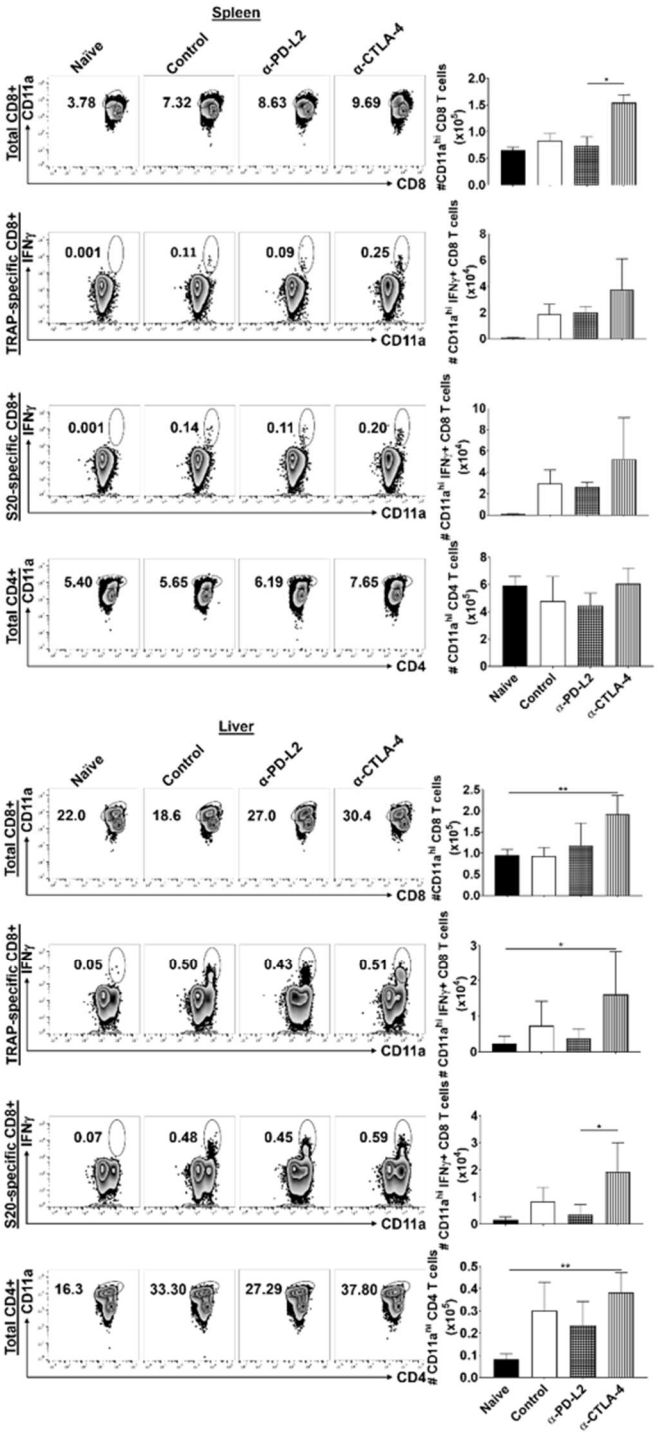

Figure 2.3. CTLA-4 blockade with immunisation increases the number of parasite-specific CD8⁺ T cells in the spleen and liver; however PD-L2 blockade does not.

C57BL/6 mice were either naïve or immunised with 10,000 γ-radiation attenuated *Pb* ANKA sporozoites i.v. with or without 200μg of blocking antibody (α-CTLA-4 or α-PD-L2) i.p. After 2 weeks spleens and livers were taken and lymphocytes were stimulated with 10μg/ml of TRAP (SALLNVDNL) or S20 (VNYSFLYLF) peptide for 6 hours with BFA. After stimulation, cells were stained for T cell markers CD3a, CD4, CD8a, CD11a and IFNγ. Total numbers of antigen experienced ($CD11a^+$) $CD8^+$ and $CD4^+$ T cells are shown as well as total numbers of IFNγ-producing $CD8^+$ T cells after peptide re-stimulation ($IFN\gamma^+$ $CD11a^{hi}$). Statistics performed using Kruskal-Wallis test with Dunn's multiple comparisons post-test. N=5 mice per group.

The main beneficial function of sporozoite-specific $CD8^+$ T cells is their ability to recognise and kill exoerythrocytic form (EEF) infected cells. Therefore, my next question was whether CTLA-4 significantly reduces the capacity of $CD8^+$ T cells to control parasitaemia *in vivo* in my C57BL/6 mouse model. As immunisations were performed with γ-radiation attenuated *Pb* ANKA sporozoites that experience arrested development in the liver, any sterile protection elicited by CTLA-4 blockade would be due to increased immune responses against pre-erythrocytic stage parasites. C57BL/6 mice that were immunised with or without blocking antibodies were challenged with 10,000 *Pb* sporozoites 14 days after immunisation by i.v. injection.

Figure 2.4 shows the liver burden of *Pb* ANKA after challenge by measuring the presence of *Pb* ANKA 18S RNA in the liver relative to the mouse endogenous control GAPDH 40 hours after challenge. 18S expression was chosen as it is ubiquitously expressed throughout the *Plasmodium* life cycle and mouse GAPDH was chosen as it is a classic housekeeping gene that is expressed in abundance and constitutively in mouse tissue. With α-CTLA-4 treatment at immunisation, there is a striking reduction of parasite load in the liver after *Pb* sporozoite challenge compared to α-PD-L1 treatment at immunisation and naïve and immunised controls (p=0002, p=<0.0001 and p=0.0084 respectively). It is also clear that PD-L1 blockade with immunisation does not elicit improved parasite control in the liver compared to controls. This provides strong evidence that CTLA-4, but not PD-L1 regulates T cell responses during γ-radiation attenuated *Pb* ANKA sporozoite immunisation and inhibits the protective capacity of sporozoite-specific T cells.

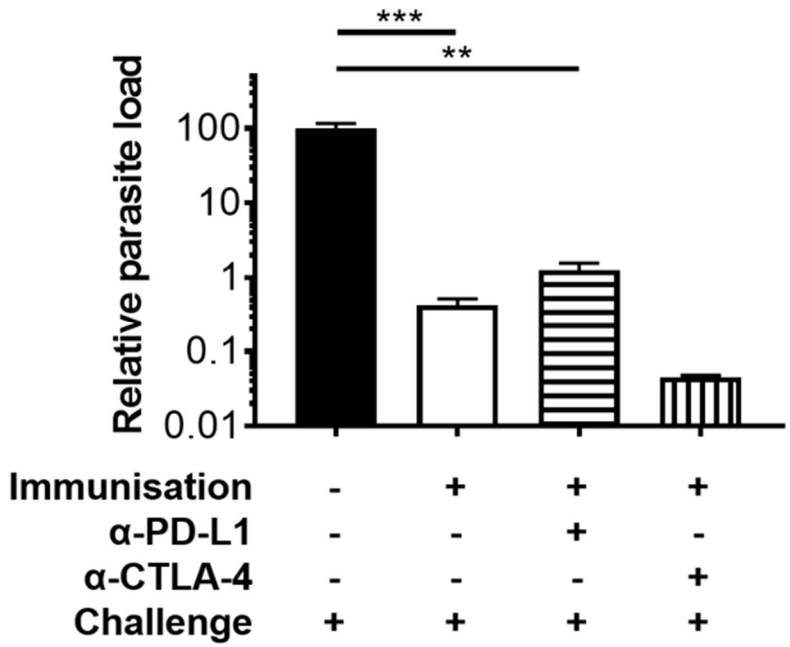

Figure 2.4. Blockade of CTLA-4 but not PD-L1 significantly reduces the liver load of parasites.

C57BL/6 mice were immunised with 10,000 γ-radiation attenuated *Pb* ANKA sporozoites i.v. with or without 200μg of blocking antibody (α-CTLA-4 or α-PD-L1) i.p. Naïve and immunised mice were challenged with 10,000 *Pb* sporozoites two weeks after immunisations were performed. Parasite liver load was measured by RT-PCR using primers for the *Pb* 18S gene and control mouse GAPDH gene. Results are shown as target expression relative to mouse GAPDH expression. Statistics performed using Kruskal-Wallis test with Dunn's multiple comparisons post-test with n=8 mice per group.

Sporozoite challenge of naïve C57BL/6 mice results in patent parasitaemia in 100% of mice between day 3 and day 5 post-infection. If no further treatment is given, between days 7 and 10 the parasitaemia and the subsequent pathological immune responses result in ECM[165]. Therefore, if there is no patent parasitaemia in mice by day 7, mice are considered to have sterile protection from blood stage infection. Antibody blockade of CTLA-4 with a single, normally non-protective, immunisation of γ-radiation attenuated *Pb* ANKA sporozoites in C57BL/6 mice elicited 60-100% sterile protection up to 1 week after challenge; however, only 1 mouse in all experiments had sterile protection with PD-L1 blockade (Figure 2.5). This shows that signalling through the CTLA-4 pathway has a potent effect on naïve T cell activation and subsequent responses to parasite infection. Although PD-L1 treatment resulted in a parasitaemia that was lower than immunised controls, this was not sufficient to be statistically significant.

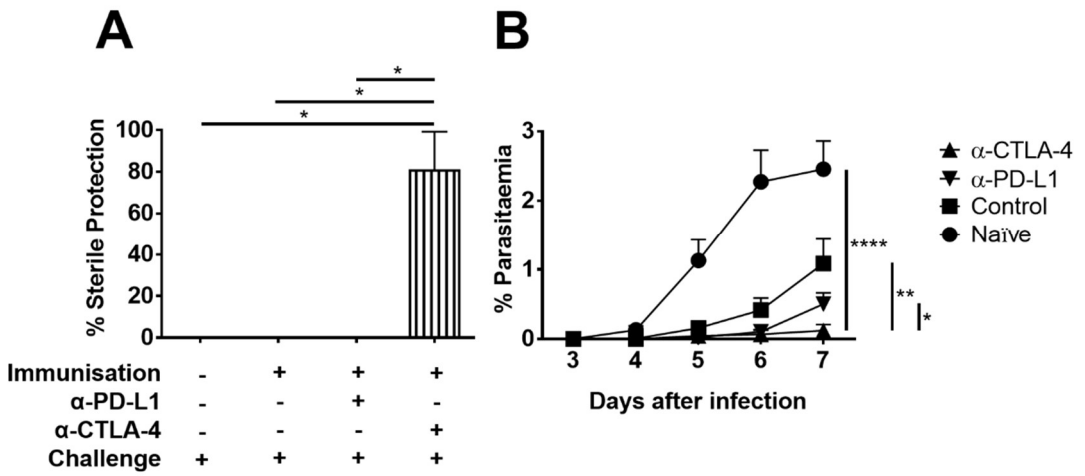

Figure 2.5. α-CTLA-4, but not α-PD-L1 treatment elicits sterile protection from challenge

C57BL/6 mice were immunised with 10,000 γ-radiation attenuated *Pb* ANKA sporozoites i.v. with or without 200μg of blocking antibody (α-CTLA-4 or α-PD-L1) i.p. and all mice were challenged 2 weeks later with 1,000 *Pb* ANKA sporozoites. Sterile protection (A) and parasitaemia (B) were determined by microscopy with thin tail blood smears. Statistics performed using Kruskal-Wallis followed by Dunn's multiple comparisons post-test for sterile protection and day 7 post-infection parasitaemia. Pooled data from 4 experiments with n=4 to 7 mice per group.

The experiments previously described show that CTLA-4 blockade with a single non-protective immunisation of γ-radiation attenuated *Pb* ANKA sporozoites increases the numbers of sporozoite antigen-specific $CD8^+$ T cells and additionally, it significantly increases sterile protection and reduces parasitaemia upon sporozoite challenge. In order to further investigate the mechanism of protection with CTLA-4 blockade concurrently with γ-radiation attenuated *Pb* ANKA sporozoites, I additionally depleted CD4, CD8 or IFNγ with antibodies at the same time as *Pb* ANKA sporozoite challenge (Figure 2.6). By depleting CD8, CD4 or IFNγ immediately prior to peptide re-stimulation, it is possible to investigate the immune response in the absence of the influence of these molecules. Blockade of CTLA-4 followed by depletion of CD8 or CD4 resulted in patent parasitaemia in all mice. This shows that the protection elicited by CTLA-4 blockade during attenuated sporozoite immunisation is mediated by both $CD8^+$ T cell and $CD4^+$ T cell mechanisms and that neither of these T cell compartments can elicit sterile protection without the other. Blockade of IFNγ resulted in a single mouse in a single experiment (14.2%) maintaining sterile protection, highlighting the importance of IFNγ in the production of T cell-mediated immunity with CTLA-4 blockade. As Th1 $CD4^+$ T cells and $CD8^+$ T cells are jointly capable of producing IFNγ it is perhaps not surprising that both are involved in the protection elicited by CTLA-4 blockade. Interestingly, these experiments do not show the relative

contribution of $CD4^+$ or $CD8^+$ T cell mechanisms to protection. Although the majority of liver stage protection has previously been attributed to $CD8^+$ T cells, we cannot confirm here whether this is also true in the absence of CTLA-4 signalling. It would perhaps be interesting to adoptively transfer $CD8^+$ and $CD4^+$ T cells from mice vaccinated with CTLA-4 blockade into naïve mice to investigate this.

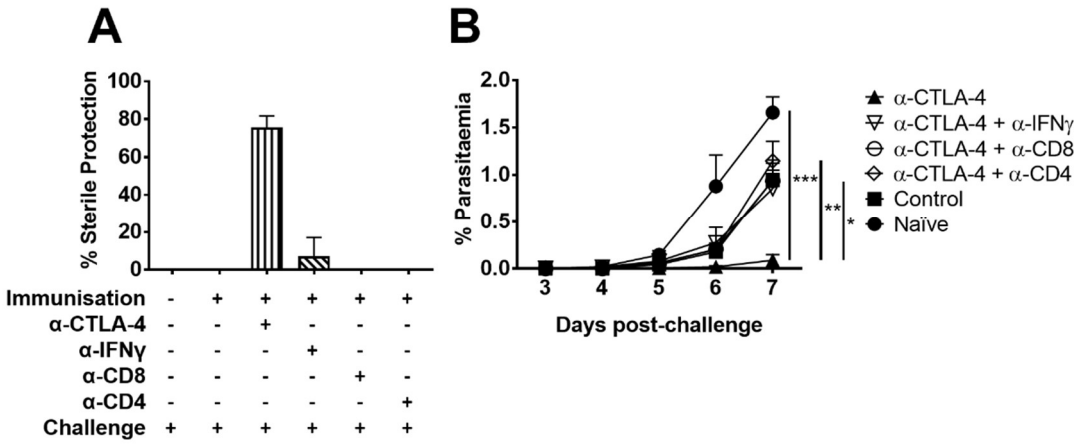

Figure 2.6. $CD8^+$ T cells as well as $CD4^+$ T cells are involved in α-CTLA-4-mediated sterile protection and this is at least in part due to IFNγ signalling.

C57BL/6 mice were immunised with 10,000 γ-irradiation attenuated *Pb* ANKA sporozoites i.v. with or without 200μg of blocking antibody (α-CTLA-4 or α-PD-L1) i.p. On days 11 and 13 after immunisation, mice either received no treatment or were given 200μg of blocking antibody (α-IFNγ, α-CD8 or α-CD4) i.v. On day 14 post immunisation, all C57BL/6 mice were challenged with 1,000 *Pb* ANKA sporozoites i.v. Sterile protection (A) and parasitaemia (B) were determined by microscopy from thin tail blood smears. Statistics performed using Kruskal-Wallis with Dunn's multiple comparisons post-test. Pooled data from 2 experiments with n=6 mice per group.

As the magnitude of $CD8^+$ T cell responses to malaria pre-erythrocytic stage antigens after sporozoite immunisation is dependent on IL-4 secreting $CD4^+$ T cells[78], it is perhaps unsurprising that blockade of CD4 results in patent parasitaemia with challenge in mice given a non-protective sporozoite immunisation with CTLA-4 blockade. Due to the loss of protection when CD8 is blocked with CTLA-4, it appears that CTLA-4 blockade alone increases antigen experienced, $IFN\gamma^+$ $CD8^+$ T cells which have a direct functional consequence on eliciting sterile protection in C57BL/6 mice.

The experiments described so far solely investigate short term immune responses after a single sporozoite immunisation. In order to investigate the significance of long-

term protection mediated by CTLA-4 blockade with immunisation, mice were left for 45 days after γ-radiation attenuated *Pb* ANKA sporozoite immunisation with or without CTLA-4 or PD-L1 blockade before being challenged with wild type (WT) *Pb* ANKA sporozoites (Figure 2.7). In contrast to challenge 14 days after immunisation, if mice were given α-CTLA-4 with γ-radiation attenuated *Pb* ANKA sporozoite immunisation and challenged 45 days later, the majority of mice became positive for blood stage parasites (Figure 2.7A). A single mouse still showed no blood stage parasites in the group treated with α-PD-L1 with γ-radiation attenuated *Pb* ANKA sporozoite immunisation. As with the previous experiments, all mice in the immunisation only and naïve groups became positive for parasites. Another similarity was the differences in the development of parasitaemia between groups. Parasitaemias in mice given an immunisation alone or concurrently with α-PD-L1 treatment developed with very similar % parasitaemia values (Figure 2.7B). These groups had consistently higher parasitaemias than mice treated with α-CTLA-4 and immunisation. This led to parasitaemias at day 7 being significantly different between α-CTLA-4 treated mice with immunisation and control mice given only the immunisation.

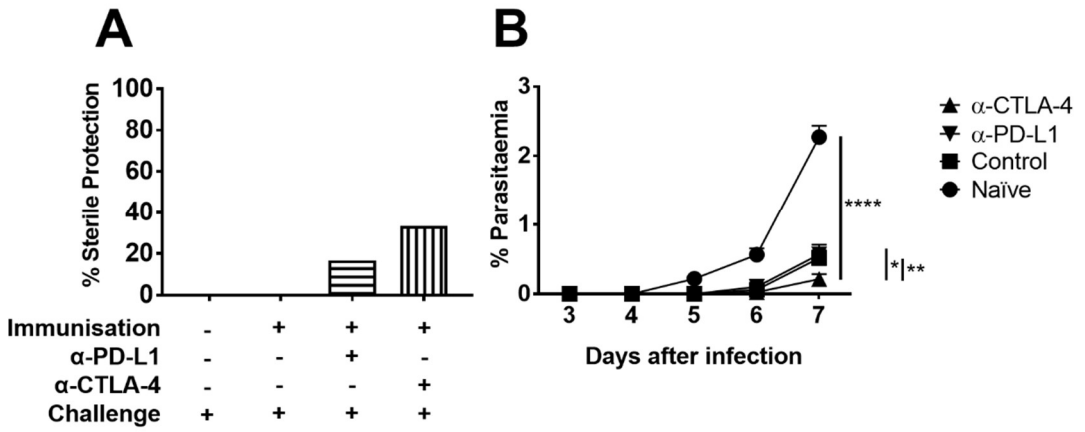

Figure 2.7. Memory responses to challenge after CTLA-4 or PDL-1 blockade does not elicit sterile protection

C57BL/6 mice were immunised with 10,000 γ-irradiation attenuated *Pb* sporozoites i.v. with or without 200μg of blocking antibody i.p. 45 days later all mice were challenged with 1,000 *Pb* ANKA sporozoites i.v. and parasitaemia was measured by microscopy of thin blood smears. A) Frequency of sterile protection measured by microscopic analysis of thick blood smears. B) Parasitaemia calculated as a % of RBCs infected with parasites in thin blood smears. Statistics performed using Kruskal-Wallis test with Dunn's multiple comparisons post-test for sterile protection and one-way ANOVA followed by Turkey's multiple comparisons test for % parasitaemia. N=5 mice per group.

All naïve mice were positive for parasites by day 5 and began showing early signs of ECM by day 7. Mice that were given a γ-radiation attenuated *Pb* ANKA sporozoite immunisation alone or with α-PD-L1 treatment were very similar in their daily progression to patency. All mice in these two groups became positive by day 7. Interestingly, unlike in the 2 week experiments, the majority of mice in the α-CTLA-4 group succumbed to patency (Figure 2.8); however, the progression in this group was protracted compared to the other groups. The progression to patency with CTLA-4 blockade was significantly reduced compared to the control group, but not the α-PD-L1 group. There was no significant difference in progression to patency between control and α-PD-L1 groups.

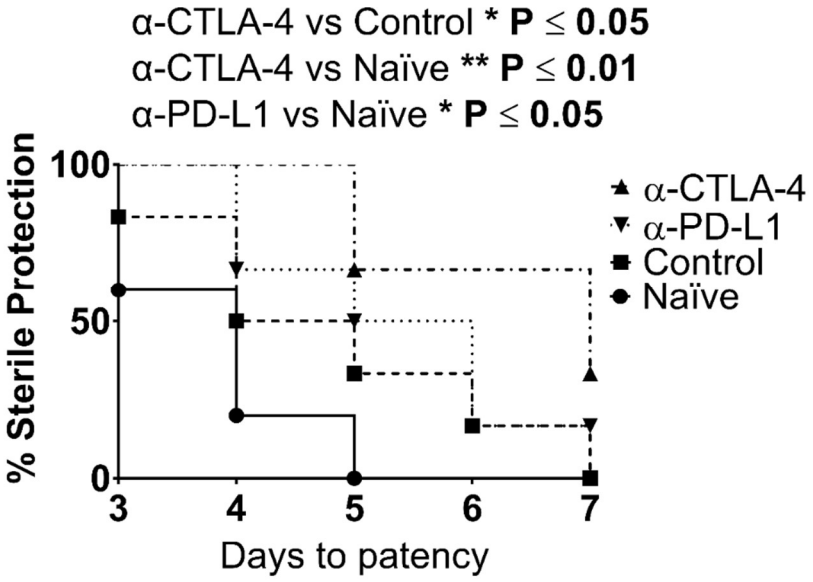

Figure 2.8. CTLA-4 blockade can delay the onset of patency through long-term memory responses.

C57BL/6 mice were either naïve or given a single i.v. immunisation of 10,000 γ–irradiation attenuated *Pb* ANKA sporozoites with or without PD-L1 or CTLA-4 blocking antibodies. After 45 days mice were challenged with 1,000 *Pb* ANKA sporozoites i.v. and monitored for the onset of parasitaemia through microscopy of thin blood smears. N=6 mice per group. Statistics performed using Mantel-Cox test.

These results show that the addition of CTLA-4 blockade into a normally non-protective single vaccination strategy with attenuated sporozoites is able to generate sterile immunity. This protection from challenge involves both $CD4^+$ and $CD8^+$ T cell mechanisms and is mediated at least in part by IFNγ production. CTLA-4 blockade with immunisation also significantly increases the number of parasite-specific $CD8^+$ T cells. These T cells can functionally respond to antigen stimulation by producing IFNγ. Interestingly, this is not seen with PD-L1 blockade, highlighting the different mechanisms by which they inhibit T cell activation.

2.4 Discussion

T cell regulation has been shown to influence both immunopathologies and clearance during parasite infections. In malaria, signalling through the co-inhibitory receptors CTLA-4 and PD-1 has been shown to be non-redundant in blood stage infection[94]; however, there is a paucity of understanding regarding these pathways during pre-erythrocytic stage malaria infection. Normal responses to TCR activation, in addition to conventional excitatory signalling, includes the upregulation of co-inhibitory receptors to the cell surface, which act to reduce T cell activation through mechanisms including the reduction of IL-2 signalling[166], which helps to prevent atypical lymphoproliferation and pathologies including autoimmunity. In acute blood stage *Pb* infection, blockade of CTLA-4 is capable of inducing ECM in normally refractory mouse strains[94]. This is a result of increased T cell activation during blood stage infection, leading to localized inflammation in the brain and reduced integrity of the blood-brain barrier. With vaccination, blockade of CTLA-4 has been shown to increase the number of pathogen-specific effector T cells prior to infection, allowing effective protection from patent infection. To investigate the contribution of co-inhibitory receptor pathways in liver stage malaria immunisation, a C57BL/6 mouse model was used. C57BL/6 mice are non-resistant to malaria and are susceptible to ECM[167], making them a good model for severe malaria.

I hypothesized that there is an upregulation of CTLA-4 and PD-L1 on T cells during pre-erythrocytic malaria and that they can also modulate responses to pre-erythrocytic infection. To do this, upregulation of CTLA-4 and PD-1 after sporozoite immunisation was investigated. By re-stimulating with our TRAP peptide, I could measure the expression of CTLA-4 and PD-1 on $CD8^+$ and $CD4^+$ T cells that can protect against patent infection (Figure 2.1). A significant increase in CTLA-4 and PD-1 expressing T cells in immunised mice compared to naïve controls suggested that both may be influenced by sporozoite immunisation. This confirms a relationship between the liver stage immune response and CTLA-4 and PD-1 pathways but it does not confirm whether these increases in expression result in a significant functional response. In order to investigate this, I used antibody-mediated blockade of CTLA-4 PD-L1 or PD-L2 concurrently with a non-protective γ-radiation attenuated *Pb* ANKA sporozoite immunisation. By measuring T cell responses to re-stimulation, I

investigated the contribution of CTLA-4, PD-L1 and PD-L2 to the pre-erythrocytic stage immune response (Figure 2.2). Previous research has identified linear sporozoite epitopes that can be utilized as positive readouts in *ex vivo* experiments with C57BL/6 mouse models to show pre-erythrocytic stage parasite-specific $CD8^+$ T cell activation[66]. Unfortunately this is not yet possible for dissecting the $CD4^+$ T cell response so this study focused on $CD8^+$ T cell functional responses and their contribution to protection.

Antigen experienced effector and memory T cells upregulate expression of CD11a on their surface and has been shown to accurately distinguish these populations from naïve T cells[168]. By using the same strategy, I investigated the total antigen experienced T cell populations with or without CTLA-4, PD-L1 or PD-L2 blockade. In the spleen, PD-L1 or PD-L2 blockade did not significantly increase the number of antigen experienced $CD8^+$ or $CD4^+$ T cells compared to controls; however blockade of CTLA-4 did. Interestingly, this was not observed in the liver as there was no significant increase in $CD11a^{hi}CD4^+$ or $CD11a^{hi}CD8^+$ T cell populations between PD-L1, PD-L2 and CTLA-4 blockade groups. CTLA-4 blockade did significantly increase the number of $CD11a^{hi}CD4^+$ and $CD11a^{hi}CD8^+$ T cells compared to immunised controls, whereas PD-L1 blockade only achieved significance for $CD11a^{hi}CD8^+$ T cells. This discrepancy between the spleen and liver could be due to the tolerogenic environment of the liver. An important mechanism in preventing undesired T cell activation is through PD-1 signalling via LSECs[74]. As the liver is capable of soliciting naïve T cell activation[169,170], blockade of PD-L1 or PD-L2 would reduce this inhibition and increase naïve T cell activation. Therefore blockade of PD-L1 or PD-L2 in the liver would result in an increase in naïve T cell activation to a variety of antigens arriving from the large intestine, antigens that would be largely non-sporozoite-specific. This would also explain how we see comparable CD11a positive $CD8^+$ T cells; however there is a clear difference in functional IFNγ production after peptide re-stimulation.

Parasite-specific CD11a positive $CD8^+$ T cells produced IFNγ upon re-stimulation, indicating that these antigen experienced cells could specifically recognize immunogenic antigens on the sporozoite and respond by generating functional cytokines associated with resolving infection. In the spleen, CTLA-4 blockade resulted in a significant increase in IFNγ production compared to naïve and

immunised controls as well as the PD-L1 blockade group. Even with the additional blockade of PD-L1 at immunisation, there was no increase in the number of IFNγ positive $CD8^+$ T cells, suggesting this pathway is not salient in inhibiting naïve T cell activation during sporozoite immunisation. In the liver there is also a clear trend towards an increase in IFNγ positive $CD8^+$ T cells with CTLA-4 blockade; however this is not significantly different from PD-L1 or PD-L2 blockade. Indeed, only with TRAP re-stimulation does CTLA-4 blockade show a significant increase compared to immunised controls. Together, these data show that blockade of CTLA-4 increases the capacity for T cells to become antigen experienced and subsequently increases functional responses to pre-erythrocytic malaria antigens through IFNγ production.

Although blockade of CTLA-4 and PD-L1 can lead to pathogenic T cell activation in the context of blood stage malaria infection, blockade with an immunisation can help to improve vaccine efficacy. After showing an increased T cell functional response, I wanted to investigate whether blockade of these pathways could improve the efficacy of a non-protective pre-erythrocytic vaccination. In my mouse model, a single vaccination with attenuated sporozoites was unable to produce sterilizing protection in any C57BL/6 mice when challenged with *Pb* WT parasites (Figure 2.4). By giving this immunisation concurrently with a blockade of CTLA-4 I observed a significant increase in mice that could control parasite challenge and prevent patent parasitaemia up to 7 days after challenge. This level of protection was not seen with blockade of PD-L1, suggesting it is not as influential in negatively regulating naïve T cell activation in response to sporozoite antigens. This is interesting because we saw a significant difference in $CD8^+$ T cell production of IFNγ in response to sporozoite antigen with α-CTLA-4 compared to α-PD-L1 groups in the spleen, but not in the liver. It would appear that blockade of CTLA-4 increases $CD8^+$ T cell responses above a protective threshold with attenuated sporozoite vaccination; however PD-L1 blockade does not.

To confirm that protection elicited by CTLA-4 blockade with a single sporozoite immunisation is due to immune responses towards liver stage infection, we measured the liver load of parasites after challenge (Figure 2.4). 40 hours after challenge there was a significant reduction in parasite load with CTLA-4 blockade compared to control and α-PD-L1 groups. This confirms that the increased sterile protection seen in Figures 2.5 and 2.6 with CTLA-4 blockade is due to detection and clearance of the

parasite in the liver, preventing patent infection. Whether the $CD8^+$ T cell populations responsible for this are circulating or liver resident T cells is unknown and warrants further investigation.

To further understand the mechanism of protection, I investigated the contribution of $CD8^+$ T cells, $CD4^+$ T cells and IFNγ to CTLA-4-mediated protection (Figure 2.7). By blocking CTLA-4 with immunisation, followed by blocking CD8, CD4 or IFNγ 3 days and 1 day before challenge, I was able to identify the contribution of each to protection. Interestingly, both CD8 and CD4 blockade resulted in reversal of the sterile protection elicited by CTLA-4 blockade, showing that both T cell populations are required in CTLA-4 blockade-mediated sterile immunity. Patent parasitaemia was also seen with neutralisation of IFNγ, highlighting its importance in the generation of effector responses in T cells. Therefore, sterile immunity elicited by CTLA-4 blockade with a single γ-radiation attenuated *Pb* ANKA sporozoite immunisation requires both $CD4^+$ and $CD8^+$ T cells and is mediated at least in part by IFNγ. Interestingly, the sterile protection offered by CTLA-4 blockade with sporozoite immunisation is not as effective in the context of long term memory responses. Although I show a significant delay in the onset of parasitaemia compared to immunised controls, I saw blood stage infection in 66.7% of mice in the α-CTLA-4 group by day 7 post-challenge.

Taken together, the results of this study are a proof of principle that blockade of co-inhibitory T cell signalling pathways can significantly improve the efficacy of pre-erythrocytic vaccine responses in mice. It is important to note however; that this protection can only be achieved through targeting specific pathways as not all are equally involved in regulating pre-erythrocytic malaria immune responses.

2.5 Conclusion

There is a clear global need to improve the efficacy of vaccines for both infectious and non-infectious diseases. Modulating regulation of T cell responses is increasingly becoming a focus of vaccinology as it has been shown to improve vaccine efficacy in both human and non-human trials. In malaria, T cell regulation in pre-erythrocytic infection is poorly understood; however, co-inhibitory receptors including CTLA-4 and

PD-1 have been shown to be non-redundant in blood stage infection. In this study, I show that it is possible to improve a normally non-protective single immunisation with attenuated whole sporozoites by concurrently blocking CTLA-4. This protection is mediated by $CD8^+$ and $CD4^+$ T cells and is dependent on production of IFNγ. These data provide strong evidence for a proof of principle that blockade of co-inhibitory receptors concurrently with a normally non-protective pre-erythrocytic vaccination can elicit sterile protection. Further research into other potential inhibitory or stimulatory receptors that could be targeted to improve pre-erythrocytic vaccine efficacy is critical to improve our understanding of T cell regulation and to identify pathways that could be utilised in human pre-erythrocytic malaria vaccine development.

2.6 Supplementary Data

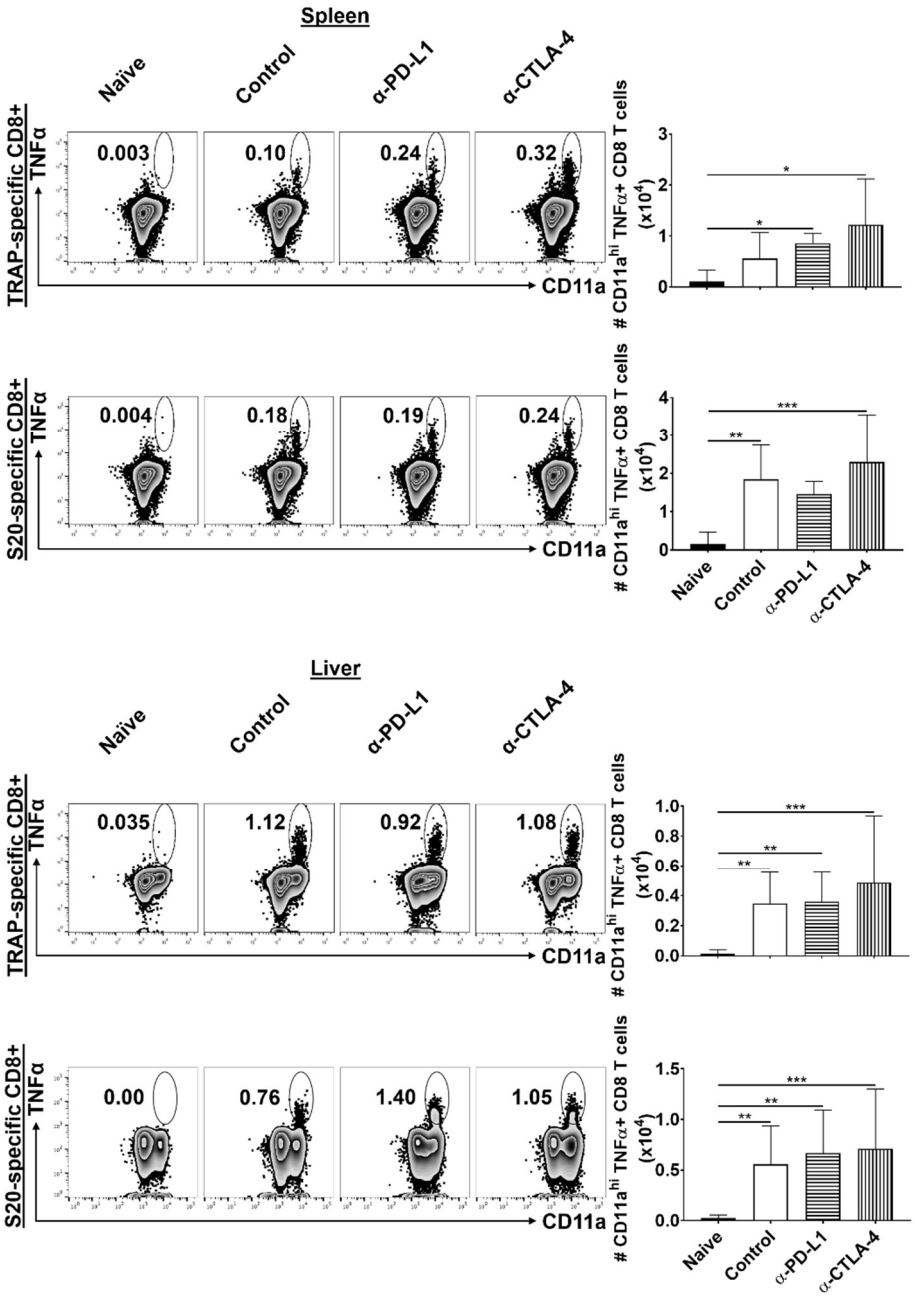

Figure 2.S1. Both CTLA-4 or PD-L1 blockade with immunisation do not increase TNFα production by parasite-specific CD8⁺ T cells in the spleen and liver.

C57BL/6 mice were either naïve or immunised with 10,000 γ-radiation attenuated *Pb* ANKA sporozoites i.v. with or without 200μg of blocking antibody (α-CTLA-4 or α-PD-L1) i.p. After 2 weeks spleens and livers were taken and lymphocytes were stimulated with 10μg/ml of TRAP (SALLNVDNL) or S20 (VNYSFLYLF) peptide for 6 hours with BFA. After stimulation, cells were stained for T cell markers CD3a, CD4, CD8a, CD11a and TNFα. Total numbers of antigen experienced ($CD11a^+$) $CD8^+$ and $CD4^+$ T cells producing TNFα after peptide re-stimulation ($TNFα^+$ $CD11a^{hi}$). Statistics performed using Kruskal-Wallis test with Dunn's multiple comparisons post-test. Pooled data from three experiments with n=5 mice per group per experiment.

3 | IL-27R and IL-10R Signalling Pathways are Dispensable for Protective $CD8^+$ T Cell Immune Responses to *Plasmodium berghei* Infection

3.1 Introduction

Protection against malaria requires a complex collection of immune responses that must adapt as infection progresses from the pre-erythrocytic stages to the blood stage. During the clinically silent pre-erythrocytic stage of infection, *Plasmodium* sporozoites that enter the vertebrate host via a blood meal from an infected female *Anopheles* mosquito quickly localise to the liver and begin hepatic development, which ultimately results in patent, clinical blood stage infection. While infection is limited to the pre-erythrocytic stage, the principle mediators of protection are parasite antigen-specific $CD8^+$ T cells[41,56]. Their mechanism of protection is so significant that depleting $CD8^+$ T cells by antibody depletion before sporozoite challenge can completely abrogate any protection elicited by immunisation in both mice and rhesus monkeys[42,171]. This further supports evidence that successful immunisation of humans, either by whole sporozoite immunisation or subunit immunisation, results in increased functional, IFNγ producing $CD8^+$ T cells that are associated with protection[56,172]. Unfortunately, although protective $CD8^+$ T cell responses can be induced against pre-erythrocytic malaria, the current gold standard requires multiple immunisations with very high numbers of attenuated sporozoites as a single immunisation is not sufficient. Therefore the question is, what mechanisms are regulating $CD8^+$ T cell responses to pre-erythrocytic malaria in order to necessitate multiple exposures to high concentrations of antigen.

Due to the potential pathogenic consequences of T cell activation during blood stage malaria, regulatory pathways have been investigated to a much greater extent than for the pre-erythrocytic stage. Using a model of blood stage malaria infection, Kimura and colleagues identified $FoxP3^-$ $CD4^+$ T cells that performed a regulatory role through IL-27 cytokine production leading to reduced proliferation of effector T cells[173]. Using RT-PCR they showed that infection of $FoxP3^{hCD2}$ knock-in mice with blood stage *Pb* parasites resulted in a significant increase in the expression of the IL-27 subunits IL27p28 and Epstein Barr virus induced gene 3 (EBi3) by $FoxP3^-CD11a^+CD4^+$ T cells when stimulated with *Pb* antigen and anti-TCR. The negative regulatory function of IL-27 in blood stage malaria has also been shown through its promotion of increased production of IL-10 by $CD4^+$ T cells during infection[174,175], reduction in the capacity of $CD4^+$ T cells to migrate to the liver[176] and the non-redundant role of IL-27 in inhibiting

pathogenic Th1 activation during blood stage malaria as shown in the work of Gwyer Findlay et al., using mice that do not express WSX-1, the alpha subunit of IL-27R[102]. As WSX1$^{-/-}$ mice cannot express the full IL-27R, signalling through this receptor is prevented and the effects of its absence can be investigated. Interestingly, Gwyer Findlay et al. showed that, although depletion of CD4^{+} T cells in WSX1$^{-/-}$ mice reduced liver pathology in blood stage infection, depletion of CD8^{+} T cells did not. Additionally, they showed that there was no difference in CD8^{+} T cell production of IFNγ in their model of infection between IL-27 signalling deficient or WT mice. This suggests that CD8^{+} T cell activation may not be regulated by IL-27 in blood stage *Pb* infection. Despite the expression of WSX-1 and gp130 on CD8^{+} T cells[177] and the protective function of IFNγ production, the role of IL-27 signalling on CD8^{+} T cell regulation during liver stage malaria infection has not been fully investigated.

In humans, it has been shown that individuals with circulating CD4^{+} T cells that produce higher levels of IL-10 are more likely to have had a greater number of malaria episodes[99]; however, these individuals also experience more asymptomatic infections. This trend was confirmed by de Mendonca et al. whilst investigating *Pv* infections[178]. These investigations highlight that the severity of malaria infections is at least partially dependent on the inflammatory phenotype of T cells and that IL-10 expression by CD4^{+} T cells correlates with control of clinical disease. This has also been shown in mouse models during blood stage malaria infection. IL-10 signalling has been shown in a BALB/c model to be a regulatory factor that reduces immune pathology[95] and a C57BL/6 infection model of lethal and non-lethal *Py* showed that the likely source for IL-10 is from regulatory type I T cells and that classical regulatory T cells do not influence the outcome of infection[179]. These studies show that IL-10 is non-redundant in regulating CD4^{+} T cell activation and immune pathology during blood stage infection; however it's regulation of CD8^{+} T cells during infection is unknown.

IL-27 is a member of the IL-12 family, a group of type I cytokines including IL-12, IL-23, IL-27 and IL-35. These cytokines are heterodimeric and their subunits have been shown to be capable of promiscuity between different binding partners to form the different cytokines. IL-12 itself consists of the subunits IL-12p40 and IL-12p35; however the p40 subunit is also used in IL-23 (IL-12p40 binding to IL-12p19)[180] and the p35 subunit is required for IL-35 (IL-12p35 binding to EBi3)[181]. IL-27 is the result

of a heterodimer between IL-27p28 and EBi3[182] and has a complex role in the immune response. The majority of IL-27 production is via innate myeloid cells, particularly monocytes, macrophages and dendritic cells[183] after activation of Toll-like receptors (TLR), CD40, CD137[184,185] or stimulation with type I or type III interferons following infection[186–190].

IL-27 is recognized by its receptor IL-27R, which consists of IL-27Rα and the shared receptor subunit gp130[182], which is also used in several other cytokine receptors including IL-6R and IL-11R. Recognition of IL-27 by its receptor has been shown to influence both innate and adaptive immunity. Signalling promotes activation of natural killer (NK) cells[191], increases the survival of eosinophils[192] and indirectly reduces the activity of neutrophils[193]. For adaptive immune responses, IL-27 appears to be particularly important in $CD4^+$ T cell responses as it polarizes the population towards a type I $CD4^+$ helper T cell (Th1) phenotype. This is achieved through activation of the transcription factor T-bet and increasing ICAM1 and IL12Rβ2 expression while also actively inhibiting GATA-binding protein 3 expression[194], which is responsible for Th2 differentiation. In addition to $CD4^+$ T cells, $CD8^+$ T cells are also activated via IL-27 stimulation of T-bet leading to increased IFNγ secretion and the production of granzyme B and perforin to promote cytotoxic activity[195]. Interestingly, IL-27 is also associated with negative regulation of immune responses. Signalling increases production of the anti-inflammatory cytokine IL-10[196], inhibits the production of IL-2[197,198] and promotes regulatory T cell differentiation[199]. In particular, type I regulatory $CD4^+$ T cell differentiation is promoted, leading to suppression of effector T cell activation, increased tolerance through IL-10 secretion, removal of APC's through perforin and granzyme B secretion and reduction of the capacity of APC's to activate effector cells[200].

The apparent dichotomy of IL-27 signalling outcomes with infection is largely attributed to the inflammatory environment. Early studies suggested IL-27 signalling as pro-inflammatory due to its ability to promote Th1 responses with peptide stimulation[201,202] or during infection with *Listeria monocytogenes* [182,202] and *Leishmania major* [203]. More recently however, a mouse model showed that *Toxoplasma gondii* infection in the absence of IL-27 prevents downregulation of $CD4^+$ T cell responses following the acute phase, leading to lethal inflammatory disease[204]. Similarly, with *Mycobacterium tuberculosis* the absence of IL-27 leads to a decrease

in the bacterial load and severe lung pathology[205] and with *Trypanosoma cruzi* infection, IL-27 is responsible for regulating excessive production of the pro-inflammatory cytokines IL-6, TNFα and IFNγ[206]. Together, these studies suggest that IL-27 can promote early pro-inflammatory immune responses and polarize T cell differentiation; however it also limits the duration and intensity of inflammatory responses. It would appear that these properties have greater or lesser effects on immunity depending on the infectious agent. Interestingly, it has been suggested that the particular cellular source of IL-27 could have some contribution to the apparent diversity of IL-27 signalling consequences[183].

IL-10, unlike IL-27 is associated with purely anti-inflammatory immune regulation and is the original member of the IL-10 family of class II cytokines (also including IL-19, IL-20, IL-22, IL-24 and IL-26). As a major mediator of anti-inflammatory signalling its expression is tightly regulated as over expression can lead to poorer responses to cancer[207] and deficiency leads to uncontrolled inflammation[208–214]. IL-10 is produced as a homodimer by the majority of leukocytes[215] and acts through Jak1/STAT3 signalling. Upon recognition of IL-10 by the IL-10R Jak1 is recruited and phosphorylated, allowing the activation of STAT3 and its formation of homodimers. Translocation of STAT3 homodimers to the nucleus allows for transcriptional inhibition of factors involved in inflammation including TNFα, IFNγ, IL-4, IL-5 and IL-2[216–218] and the activation of mechanisms that inhibit inflammatory responses such as apoptosis. Due to the importance of IL-10 in negatively regulating T cell activation and the protective nature of $CD8^+$ T cell activation during pre-erythrocytic stage infection, an important area of investigation is whether this pathway can modulate $CD8^+$ T cells and their capacity to protect against patent blood stage infection.

As the field of T cell regulation becomes increasingly complex, it is crucial to understand how different pathways are employed in different pathogenic contexts. This is particularly important for infections that are known to require T cell activation for protection, such as liver stage infection in malaria. By understanding the influence of the multitude of regulatory mechanisms available, we can greater understand protective immune responses to malaria and inform vaccine development for the future.

3.2 Materials and Methods

3.2.1 Mosquito and mouse conditions

C57BL/6 and WSX-1$^{-/-}$ mice between 5-8 weeks were bred in-house at London School of Hygiene and Tropical Medicine (LSHTM) or by Charles River Laboratories (UK). They were housed in filter-topped cages up to 6 per cage with absorbent bedding, nesting material and enrichment. Their diet consisted of autoclaved water and food pellets. Procedures were performed under license from the United Kingdom Home Office under the Animals (Scientific Procedures) Act 1986 and approved by the Animal Care and Ethical Review Committee.

Pb ANKA infected *Anopheles stephensi* mosquitoes grown at LSHTM were kept at 22°C with 80% humidity and fed on 10% glucose solution (10% D-Glucose [Sigma] in distilled water). In order to generate infectious *Pb* ANKA sporozoites, blood stage parasites were first collected from infected C57BL/6 mice via cardiac puncture into 1.5ml Eppendorf tubes (Sigma) with heparin (Sigma) and kept on ice. Blood was diluted 1:2 in freezing media made from 7.5% Glycerol (Sigma) in RPMI complete (RPMI 1640 [Gibco] with 10% FCS [Gibco], 2% L-Glutamine [Gibco] and 1% Penicillin and Streptomycin [Gibco]) and kept at -80C. When required, blood stage parasites were thawed and 200µl was injected i.v. into a naïve C57BL/6 mouse. After three days, blood was collected from the infected mouse via cardiac puncture and 100,000 parasites were passaged into two naïve C57BL/6 mice. 4 days after passage, mice were given a terminal dose (100-150µl) of anaesthesia consisting of 50% PBS, 33% ketamine (Ketamidor, 100mg/ml [National Veterinary Services Limited]) and 17% xylazine (Rompun, 2% w/v [National Veterinary Services Limited]) i.p. and placed on a cage of mosquitoes (70 mosquitoes per mouse) for a 30 minute blood feed. Ketamidor and Rompun were purchased under prescription through LSHTM's Named Veterinary Surgeon. 18-20 days after blood feed, mosquitoes were judged to be positive for sporozoites in the salivary glands.

3.2.2 Whole sporozoite immunisation and challenge

Female *Anopheles stephensi* salivary glands were dissected from infected mosquitoes in RPMI complete and *Pb* ANKA sporozoites were isolated through homogenisation and centrifugation. Glands were homogenised using autoclaved plastic pestles in Eppendorf tubes and centrifuged at 10,000 rpm for 3 minutes. The pellet was re-suspended in 200µl of RPMI complete and *Pb* ANKA sporozoites were counted on a C-chip haemocytometer (Digital bio). For immunisations, *Pb* ANKA sporozoites were diluted to 50,000/ml in RPMI complete. To attenuate by irradiation for immunisation, the suspension was exposed to gamma radiation at $1.2x10^4$ centigray (cGY) for 20.5 minutes. C57BL/6 mice were immunised by an i.v. injection of 10,000 attenuated *Pb* ANKA sporozoites per mouse. For challenge, *Pb* ANKA sporozoites were diluted to 5,000 per ml and 1,000 were given i.v. per mouse. Parasitaemia (%) was measured by microscopy using thin blood smears from mouse tail blood that were fixed in methanol and stained for 15 minutes with Giemsa (VWR Chemical) diluted 1:5 in water.

3.2.3 Antibody blockade

Antibodies were diluted from stock solutions to 1mg/ml in PBS. 0.2ml of α-IL-10R [JES5-2A5] (BioXcell) was given i.p. per mouse concurrently with γ-radiation attenuated *Pb* ANKA sporozoite immunisation. WSX-$1^{-/-}$ controls were given 0.2ml of PBS i.p. per mouse and no antibodies. Previous work by our group has shown that rat IgG isotype controls do not provide any protection against malaria challenge [94].

3.2.4 Flow cytometry

Spleens were passed through a 70nm pore nylon cell strainer (BD) and centrifuged at 1,800 rpm for 4 minutes. To lyse RBC's the pellet was re-suspended in 1ml of 1x lysis buffer (10x lysis buffer [BD] diluted 1:10 in autoclaved distilled water) and incubated for 10 minutes. Splenocytes were washed by diluting to 10ml in RPMI complete followed by centrifugation at 1,800 rpm for 4 minutes, discarding the supernatant and diluted to 2 million cells per well. Livers were perfused with PBS during dissection and also passed through a 70nm nylon cell strainer. The

homogenate was centrifuged at 1,800 rpm for 4 minutes and the pellet was re-suspended in Percoll gradient (4% 10x PBS [Gibco], 36% Percoll[GE Healthcare] and 60% RPMI) and centrifuged at 2,000rpm for 10 minutes. Supernatant was discarded and RBC's were lysed using lysis buffer for 5 minutes and washed in RPMI as with splenocytes before being re-suspended to 180µl per condition.

Sporozoite peptides from TRAP (SALLNVDNL) and S20 (VNYSFLYLF) were synthesised by Mimotopes (Melbourne, Australia) using Fmoc chemistry and pseudoprolines to prevent unwanted coupling[164]. Lymphocytes were re-stimulated with 10µg of peptide and BFA (ebioscience). Lymphocytes were incubated for 6 hours at 37°C with 5% CO_2. Cells were stained with α-CD3 (V500), α-CD4 (APC), α-CD8a (PerCP Cy5.5), α-CD11a (e450) or α-IFNy (PE Cy7) as required (ebioscience).

3.2.5 Real Time PCR (RT-PCR)

Liver sections were added to 3ml of TRIzol (Fisher Scientific) in a 15ml Falcon tube (Fisher Scientific) and homogenised using a Power Gen 125 tissue homogenizer (Fisher Scientific). Between samples the homogeniser was washed in distilled water and between groups it was washed in a 1% SDS (Sigma) solution. 200µl of sample was mixed with 300µl of TRIzol and stored at -80°C until RNA extraction. For RNA extraction 200µl of chloroform was added to the 500µl sample and centrifuged at 13,000 rpm for 15 minutes at 4°C. The upper layer was then transferred into 1.5ml RNAse free eppendorf tubes (ThermoFisher). 250µl of isopropanol, 60µl of 3M Sodium Acetate and 0.5µl glycoblue (5mg/ml) was added per sample and all samples were left at -20°C overnight. Tubes were spun at 13,000 rpm for 15 minutes at 4°C and the supernatant was removed. Pellets were washed with 400µl of ice-cold ethanol and re-suspended before spinning at 13,000 rpm for 10 minutes at 4°C. 80µl of RNAse/DNAse-free water (Sigma) was added per sample and all tubes were heated to 65°C until pellets had dissolved. To 5µl of RNA sample, 5µl of Oligo dT-Primers and 0.5µl random primers (Retroscript kit, Ambion) were added. Tubes were centrifuged, put at 75°C for 3 minutes and centrifuged again before being put on ice. To each sample a mix of 10x RT buffer, dNTP, 4x RNAse inhibitor and MMLV-RT enzyme (Retroscript kit, Ambion) was added before centrifugation. Samples were heated to 42°C for 60 minutes followed by 90°C for 10 minutes. cDNA was diluted and primers for the mouse endogenous control glyceraldehyde 3-phosphate

dehydrogenase (GAPDH) (forward 5'-CGTCCCGTAGACAAAATGGT-3', reverse 5'-TTGATGGCAACAATCTCCAC-3') and *Pb* ANKA 18S (forward 5'-TGAGGCCGGTGCTGAGTATGTCG-3', reverse 5'-CCACAGTCTTCTGGGTGGCAGTG-3'), *Pb* ANKA IL-10 (forward 5'-ATGCTGCCTGCTCTTACTGACTG-3', reverse 5'-CCCAAGTAACCCTTAAAGTCCTGC-3'), *Pb* ANKA IL-27p28 (forward 5'-CTGGTACAAGCTGGTTCCTG-3', reverse 5'- CTCCAGGGAGTGAAGGAGCT-3'), *Pb* ANKA EBi3 (forward 5'- CAGAGTGCAATGCCATGCTTCTC, reverse 5'-CTGTGAGGTCCTGAGCTGAC-3'), *Pb* ANKA WSX-1 (forward 5'-CAAGAAGAGGTCCCGTGCTG-3', reverse 5'-TTGAGCCCAGTCCACCACAT-3') (Eurofins) were added with SYBR Green I Master Mix (ThermoFisher). Samples were run for 15 minutes at 95°C as an initial denaturing stage. Amplification was 40 repetitions at 95°C (denaturation) for 15 seconds, 55°C (annealing temp) for 15 seconds and 65°C (data collection) for 45 seconds. The final sequence collected melting curve data, beginning at 95°C (denaturation) for 15 seconds then increasing from 60°C by 1°C per minute to a final temperature of 95°C. A 7500 Fast & 7500 Real-Time PCR System (Applied Biosystems) was used and analysed using 7500 Software version 2.0.6 (Applied Biosystems).

3.3 Results

Deletion of the *wsx-1* gene in mice abrogates IL-27R signalling[203] by preventing the expression of the WSX-1 subunit of the IL-27R. As these mice were generated on a C57BL/6 genetic background, the use of this KO strain with C57BL/6 WT controls has been extensively used in mouse models to investigate IL-27R signalling in relation to immune responses. The outcome of IL-27R signalling during *Plasmodium* infection has been investigated primarily in relation to $CD4^+$ T cell responses in blood stage infection due to its involvement in regulatory T cell development and function. Regarding cytotoxic responses, Gwyer Findlay and colleagues showed that blockade of $CD8^+$ T cells during infection of WSX-$1^{-/-}$ KO mice did not lead to reduced pathology as mentioned previously[102]. In addition to this, $CD8^+$ T cells in WSX-$1^{-/-}$ KO mice did not produce different levels of IFNγ in relation to WT during infection (data not shown). These results suggest that IL-27R signalling is not required for $CD8^+$ T cell responses

during blood stage infection; however, its effect during liver stages has not been investigated. Although IFNγ production is associated with both blood and liver stage malaria[57,219–221] its action is largely through different mechanisms, raising the question whether other immune pathways such as IL-10 and IL-27 could have differing influences on blood and liver stage responses.

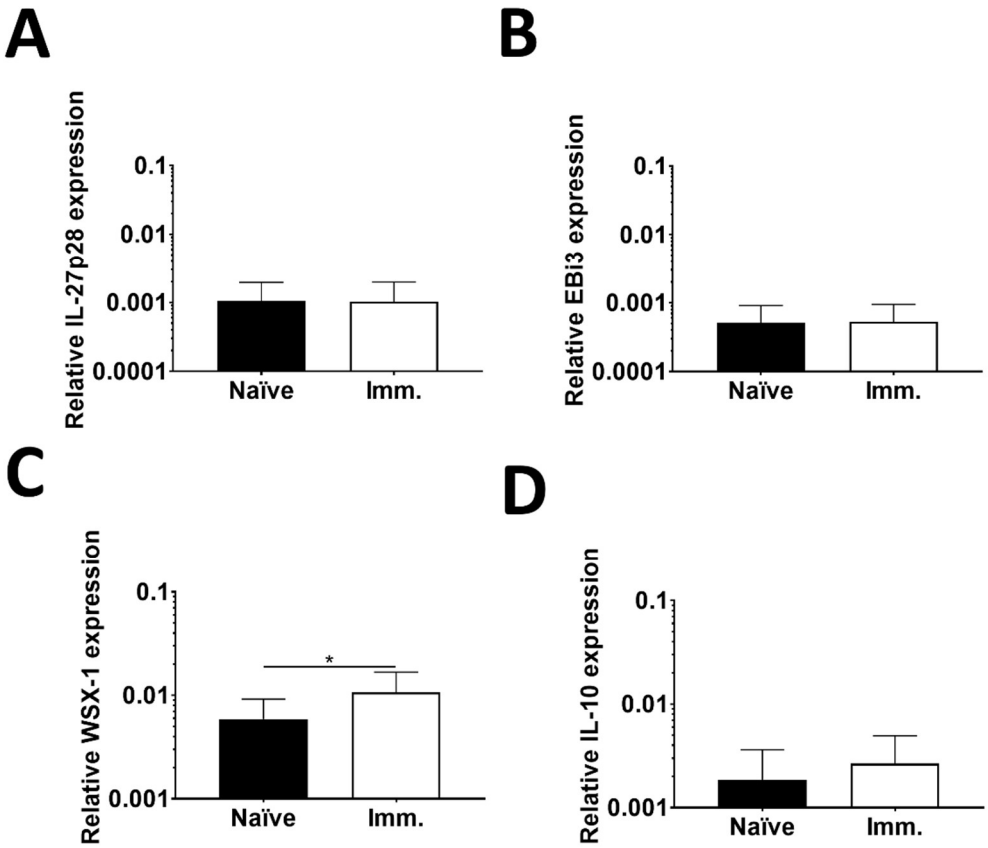

Figure 3.1. *Pb* ANKA sporozoite immunisation does not influence IL-10 or IL-27 cytokine expression, but does increase WSX-1 expression.

C57BL/6 mice were either naïve or immunised with y-radiation attenuated *Pb* ANKA sporozoites i.v.. 14 days after immunisation, all mice were challenged with 1,000 *Pb* ANKA sporozoites and livers were collected 40 hours later. Expression of IL-27p28 (A), EBi3 (B), WSX-1 (C), IL-10 (D) and control mouse GAPDH RNA was measured by RT-PCR. Results are shown as target expression relative to mouse GAPDH expression. Data taken from two experiments with 4-6 mice per experiment. Statistics were performed using the Mann-Whitney t test.

Using RT-PCR I first investigated the amount of IL-10 RNA as well as WSX-1, IL27p28 and EBi3 RNA in naïve and immunised C57BL/6 mouse livers. Challenge with *Pb* sporozoites after immunisation did not lead to a significant increase in IL-27 cytokine subunits IL-27p28 and EBi3 were not increased significantly (Figure 3.1A and Figure 3.1B respectively); however, there was a small but significant increase in the expression of WSX-1 (Figure 3.1C), which suggests there may be some influence of sporozoite immunisation on IL-27R expression in the liver. Regarding IL-10 expression, there was not a significant increase after challenge with Pb sporozoites (Figure 3.1D).

In this study WSX-1$^{-/-}$ mice and C57BL/6 WT controls were given a single non-protective immunisation of γ-radiation attenuated *Pb* ANKA sporozoites to generate pre-erythrocytic stage immune responses. In C57BL/6 mouse models of malaria vaccination using radiation attenuated sporozoites, challenge after one immunisation is insufficient to elicit sterile protection[59]; however, 2 or more immunisations can. In my experiments, lymphocytes isolated from spleens and livers of C57BL/6 mice that were given a single immunisation were cultured with TRAP or S20 peptides, which allowed for the re-stimulation of *Pb* ANKA sporozoite-specific CD8$^+$ T cells. It has been shown that antigen experienced T cells can be gated using CD11a as a marker of previous antigen exposure[168]. In order to compare the total numbers of antigen experienced CD8$^+$ and CD4$^+$ T cells, they were gated on CD11a as shown in figure 3.2.

There were no significant differences in the total numbers of CD8$^+$ and CD4$^+$ T cells between WT controls and WSX-1$^{-/-}$ mice that were immunised in both the spleen and the liver (Figure 3.2). This shows that with immunisation and re-stimulation, there is no significant increase or decrease in T cell expansion when IL-27R signalling is absent. As an increased population of T cells is expected with improved sporozoite vaccine-induced responses[222], this suggests that IL-27R signalling is not critical in regulating functional pre-erythrocytic stage T cell responses in the spleen or the liver. Although there were no apparent differences in the size of CD8$^+$ or CD4$^+$ T cell populations, I wanted to further investigate functional antigen experienced CD8$^+$ T cell responses by measuring the production of IFNγ upon exposure to *Pb* ANKA sporozoite peptides from TRAP and S20.

Figure 3.2 shows the capacity for $CD8^+$ T cells to produce IFNγ after re-stimulation, also measured by flow cytometry. With TRAP peptide stimulation there was a slight trend towards more $CD8^+$ T cells producing IFNγ in both the spleen and the liver for the WSX-$1^{-/-}$ compared to WT controls; however this did not achieve statistical significance in any of my experiments. By contrast, there was a significant difference in splenic and liver $IFN\gamma^+$ $CD8^+$ T cells between WSX-$1^{-/-}$ and WT immunised groups after S20 peptide re-stimulation (p=0.0217 and p=0.0213 respectively). This is interesting as it highlights the differing magnitude of $CD8^+$ T cell responses to antigen; however, it is important to understand whether there is an improvement in the total functional response to challenge after whole sporozoite immunisation in the absence of IL-27R signalling.

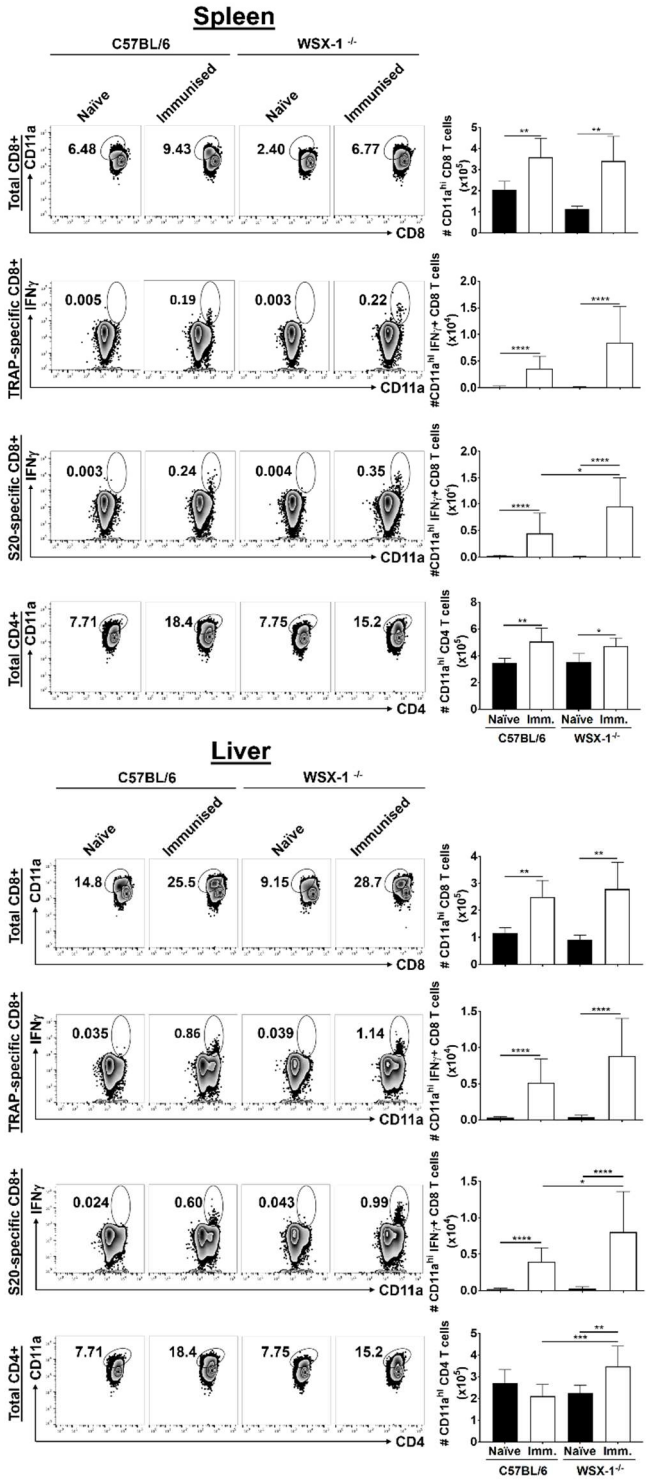

Figure 3.2. Immunisation in the absence of IL-27R does not significantly influence the number of parasite-specific CD8⁺ T cells in the spleen and liver.

C57BL/6 and WSX-1$^{-/-}$ mice were either naïve or immunised (Imm.) with 10,000 γ-radiation attenuated *Pb* ANKA sporozoites i.v. After 2 weeks spleens and livers were taken and lymphocytes were stimulated with 10μg/ml of TRAP or S20 peptide for 6 hours with BFA. After stimulation, lymphocytes were stained for activated T cell markers CD3a, CD4, CD8a, CD11a and intracellular IFNγ. Total antigen experienced (CD11a^{hi}) CD8^{+} and CD4^{+} T cells are shown as well as activated CD8^{+} T cells after re-stimulation (IFNγ^{+} CD11a^{+}). Statistics were performed using Kruskal-Wallis test with Dunn's multiple comparisons post-test. Pooled data from 2 experiments, n=5 per group.

As there was a trend towards higher $CD8^+$ T cell responses in WSX-$1^{-/-}$ immunised mice, I investigated their potential to reduce *Pb* ANKA parasite load in the liver after sporozoite challenge. I challenged WT and WSX-$1^{-/-}$ mice with 1,000 infectious *Pb* ANKA sporozoites i.v. and measured parasite load in the liver after 40 hours. By performing RT-PCR I measured the presence of the *Pb* gene 18S and calculated liver load in comparison to the expression of mouse GAPDH endogenous control (Figure 3.3). Even though innate immune responses can contribute, sterile protection requires a substantial increase in parasite-specific $CD8^+$ T cells after immunisation[59,122]. The results of figure 3.2 suggest a general trend; however, in the absence of a strong significant difference, I hypothesized there would be no increased reduction in parasite liver load in WSX-$1^{-/-}$ immunised mice compared to WT immunised mice after *Pb* ANKA sporozoite challenge. As expected, between immunised groups there was no significant difference, confirming my hypothesis. A single immunisation did decrease the relative parasite load in the liver of immunised mice vs naïve mice, but this is not sufficient for protection. These data show that, even though there may be a slight increase in functional $CD8^+$ T cell responses, blockade of IL-27R signalling does not improve the protective capacity of a single sporozoite immunisation against challenge.

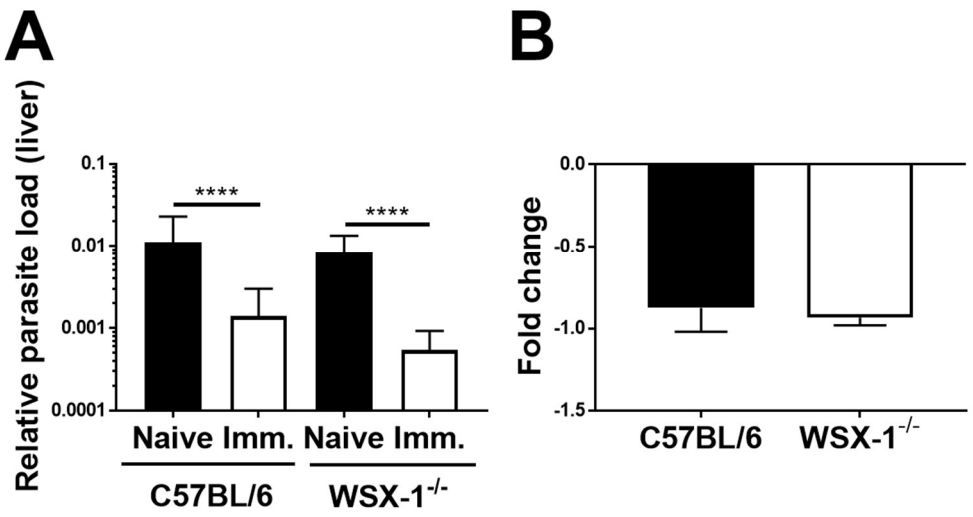

Figure 3.3. IL-27R signalling does not significantly inhibit the reduction of parasites in the liver.

C57BL/6 and WSX-1$^{-/-}$ mice were immunised with 10,000 γ-radiation attenuated *Pb* ANKA sporozoites i.v. followed by challenge 2 weeks later with 1,000 *Pb* ANKA sporozoites i.v. Livers were taken 40 hours after challenge and parasite load was measured by measuring *Pb* 18S DNA using RT-PCR. Relative parasite load is shown (A), calculated by comparing the amount of 18S DNA relative to a control endogenous mouse gene GAPDH DNA for each sample. Fold change in relative parasite load between naïve and immunised groups for each strain is also shown (B). Pooled data from 2 experiments with n=5 per group. Statistics were performed using the Mann-Whitney t test.

The experiments described so far have shown that IL-27R signalling blockade with immunisation compared to WT controls results in a trend, but not a significant increase in the magnitude of the functional CD8$^+$ T cell response to liver stage malaria antigen (Figure 3.2). Additionally, IL-27R blockade with a single γ-radiation attenuated *Pb* ANKA immunisation does not lead to a significant increase in protection from *Pb* ANKA sporozoite challenge (Figure 3.3). However, the data provided so far does not address IL-27R signalling blockade with regard to memory CD8$^+$ T cell responses. To investigate this; mice were similarly given a single immunisation of radiation attenuated *Pb* ANKA sporozoites but spleens and livers were not harvested until 45 days after immunisation. In this way, the long term CD8$^+$ T cell response could be investigated by *ex vivo* re-stimulation. As with the previous experiments, there was no difference in the total number of antigen experienced CD8$^+$ and CD4$^+$ T cells (Figure 3.4). It is interesting that the trend in functional CD8$^+$ T cell responses were also similar. With TRAP peptide re-stimulation there was a non-significant trend towards more IFNγ$^+$ CD8$^+$ T cells in the spleen and liver. A trend was also apparent with S20 re-stimulation but in contrast to the previous experiments,

there was no significant difference. These results suggest that the small but consistent increase in IFNγ^+ CD8$^+$ T cells after immunisation is still apparent in CD8$^+$ T cell populations long-term.

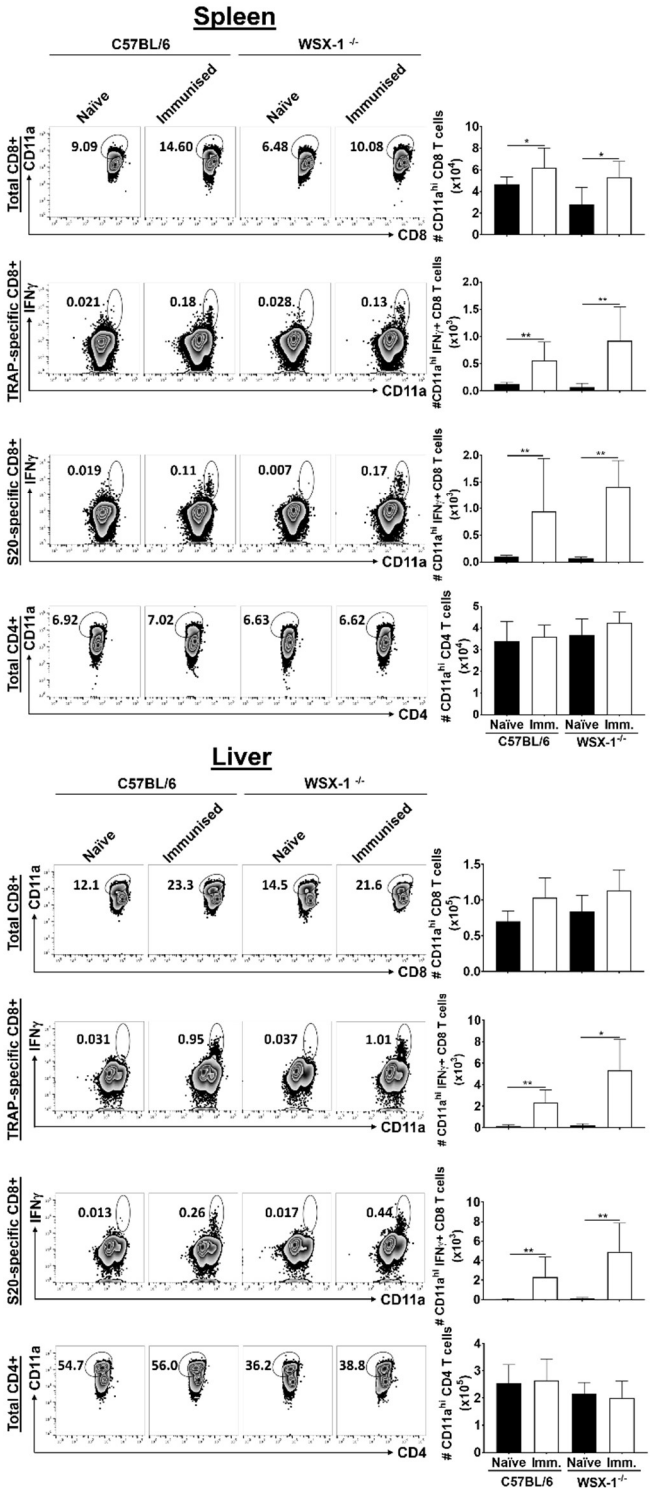

Figure 3.4. Immunisation in the absence of IL-27R does not significantly influence responses by parasite-specific memory CD8⁺ T cells in the spleen and liver.

C57BL/6 and WSX-1$^{-/-}$ mice were either naïve or immunised with 10,000 γ-radiation attenuated *Pb* ANKA sporozoites i.v. After 45 days spleens and livers were taken and lymphocytes were stimulated with 10μg/ml of TRAP or S20 peptide for 6 hours with BFA. After stimulation, lymphocytes were stained for activated T cell markers CD3a, CD4, CD8a, CD11a and intracellular IFNγ. Total antigen experienced (CD11a^{hi}) CD8^{+} and CD4^{+} T cells are shown as well as activated CD8^{+} T cells after re-stimulation (CD11a^{hi} IFNγ^{+}). N=6 per group. Statistics were performed using Kruskal-Wallis test with Dunn's multiple comparisons post-test.

As with my previous experiments, I also investigated whether the absence of IL-27R signalling led to an increased protection against *Pb* ANKA sporozoite challenge by measuring liver load (Figure 3.5). Perhaps unsurprisingly, after 45 days there was still no significant difference in the relative parasite load between naïve and immunised C57BL/6 and WSX-1$^{-/-}$ mice (Figure 3.5B).

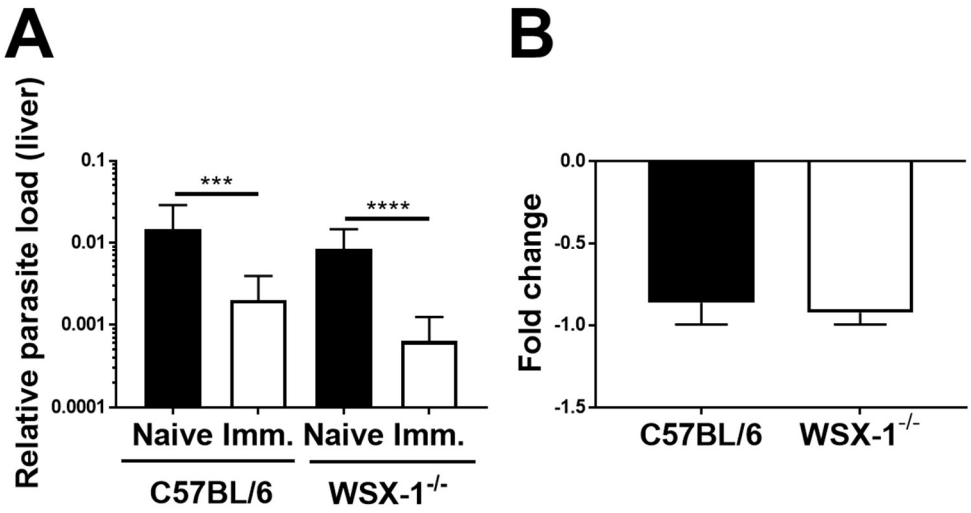

Figure 3.5. IL-27R signalling does not significantly inhibit the reduction of parasites in the liver long-term after immunisation.

C57BL/6 and WSX-1$^{-/-}$ mice were immunised with 10,000 γ-radiation attenuated *Pb* ANKA sporozoites i.v. followed by challenge 45 days later with 1,000 *Pb* ANKA sporozoites i.v. Livers were taken 40 hours after challenge and parasite load was measured by measuring *Pb* 18S DNA using RT-PCR. Relative parasite load is shown (A), calculated by comparing the amount of 18S DNA relative to a control endogenous mouse gene GAPDH DNA for each sample. Fold change between naïve and immunised groups for each strain is also shown (B). N=6 per group. Statistics were performed using the Mann-Whitney t test.

Together with these investigations into IL-27R signalling and liver stage *Plasmodium* infection, I examined the importance of IL-10R signalling in regulating the CD8$^+$ T cell response. Rather than using a knockout strain of mouse, I used blocking antibodies that selectively block the IL-10R alongside a single immunisation of γ-radiation attenuated *Pb* ANKA sporozoites to C57BL/6 mice. As with my IL-27R investigation, CD8$^+$ T cells were re-stimulated with TRAP or S20 peptide and stained for flow cytometry (Figure 3.6). With regard to total numbers of antigen experienced CD11a^{hi}CD8$^+$ T cells, immunisation increased numbers significantly compared to naïve mice in the spleen and liver; however, there was no difference between immunised controls and IL-10R blockade with immunisation. The same relationship was seen when comparing IFNγ$^+$ CD8$^+$ T cells after both TRAP and S20 peptide re-

stimulation, suggesting that blockade of IL-10R signalling does not influence $CD8^+$ T cell responses to liver stage malaria. This does not however inform us as to the protective capacity of the immune response to challenge with the blockade of IL-10R.

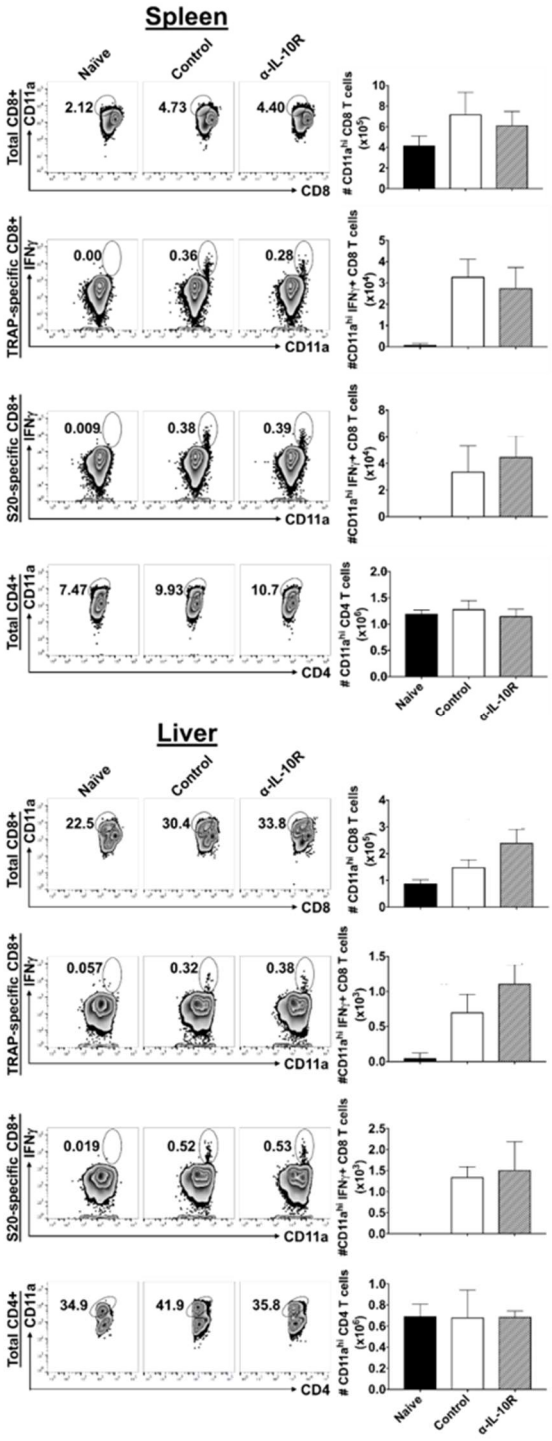

Figure 3.6. IL-10R blockade with immunisation does not significantly influence the number of parasite-specific CD8⁺ T cells in the spleen and liver.

C57BL/6 mice were either naïve or immunised with 10,000 γ-radiation attenuated *Pb* ANKA sporozoites i.v. with or without 200μg of blocking antibody in PBS (α-IL-10R) i.p. After 14 days spleens and livers were taken and lymphocytes were stimulated with 10μg/ml of TRAP or S20 peptide for 6 hours with BFA. After stimulation, lymphocytes were stained for activated T cell markers CD3a, CD4, CD8a, CD11a and intracellular IFNγ. Total antigen experienced ($CD11a^+$) $CD8^+$ and $CD4^+$ T cells are shown as well as activated $CD8^+$ T cells after re-stimulation ($IFN\gamma^+$ $CD11a^+$). Statistics performed using Kruskal-Wallis test with Dunn's multiple comparisons post-test. Pooled data from two experiments with 4 mice per group per experiment.

As with our investigation of IL-27R signalling, we challenged mice 14 days after immunisation concurrently with or without IL-10R blockade to discern any possible protection in the liver compared to immunised controls (Figure 3.7). It is clear that the parasite load for the immunised control and α-IL-10R groups is comparable, with no significant increased protection with IL-10R blockade. This confirms that the absence of IL-10R signalling does not improve the protective immune response to pre-erythrocytic malaria infection and, with the data from figure 3.6, does not increase the number of functional $CD8^+$ T cells which produce IFNγ in response to pre-erythrocytic antigens.

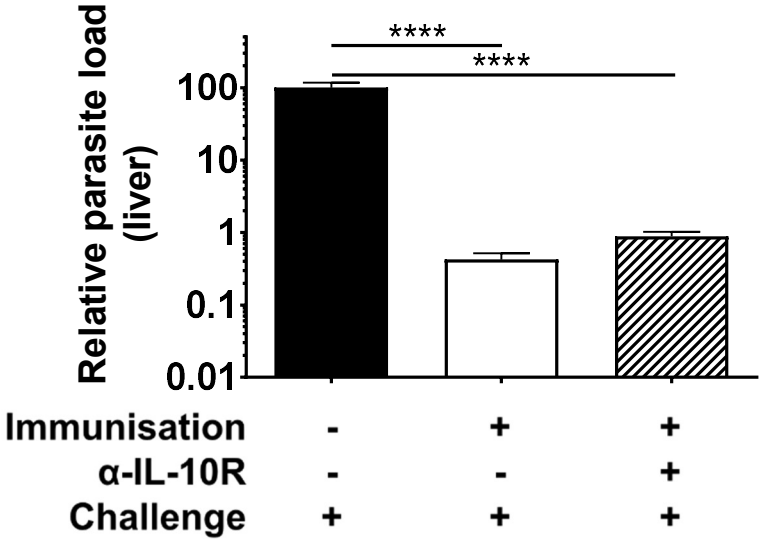

Figure 3.7. Blockade of IL-10R does not reduce the liver load of parasites.

C57BL/6 mice were naïve or immunised with 10,000 γ-radiation attenuated *Pb* ANKA sporozoites i.v. with or without 200μg of blocking antibody in PBS (α-IL-10R) i.p. After 14 days all mice were challenged with 10,000 *Pb* ANKA sporozoites i.v. Livers were taken 40 hours after challenge and parasite load was measured by measuring *Pb* 18S RNA using RT-PCR. Relative parasite load is shown, calculated by comparing the amount of 18S cDNA relative to a control endogenous mouse gene GAPDH cDNA for each sample. Statistics performed using Kruskal-Wallis test with Dunn's multiple comparisons post-test, n=8 per group.

3.4 Discussion

Immune responses to malaria infection are not sufficient to induce sterile protection in subsequent exposure. This is at least in part due to regulatory mechanisms that reduce the capacity for immune cell activation and memory. As regulation is a crucial aspect of immune activation and function, increasing our understanding of these pathways allows us to better appreciate what mechanisms are involved in infection resolution. In addition it also provides insight into pathways that could potentially be utilised to the benefit of the individual. Two pathways that have been extensively investigated with regard to T cell regulation are IL-27 and IL-10, both of which have been implicated in blood stage immune responses to malaria. Interestingly, their involvement in immune responses to sporozoite infection has not been previously investigated. IL-27 has a complex role in immune regulation, in a study performed by Matsui and colleagues, concomitant administration of recombinant IL-27 and IL-23 was given during a prime-boost immunisation regimen for hepatitis C virus (HCV)[223]. This resulted in an increase in virus-specific, IFNγ producing $CD8^+$ T cells. In contrast to this, Pennock et al. investigated subunit vaccination of *Listeria monocytogenes* or vaccinia virus and discovered that there were no significant differences in $CD8^+$ T cell activation upon challenge between control mice and IL-27Rα knockout mice[224]. The role of IL-10 in immune regulation on the other hand, is much more binary. It is a master negative regulator of immune function, inhibiting pathogen clearance and reducing inflammatory pathology[225]. In this study, I have investigated the influence of these pathways using two mouse models for severe malaria. Interestingly, I have shown that IL-27R and IL-10R signalling appear to not be involved in $CD8^+$ T cell regulation during responses to liver stage infection. As both of these pathways influence T cell activation during blood stage infection it is important to note that here I show regulation during blood stage infection cannot lead to assumptions of regulation during the liver stage.

As IL-27R signalling is capable of inducing both pro- and anti-inflammatory immune responses to infection, an important question for this study was whether it influenced liver stage infection and, if so, how. By running flow cytometry on spleens and livers from immunised C57BL/6 and WSX-$1^{-/-}$ mice, I aimed to answer this question. After a single non-protective immunisation, followed by peptide re-stimulation I investigated

the magnitude of $CD11a^{hi}CD4^{+}$ and $CD11a^{hi}CD8^{+}$ T cell populations and the functional responses of antigen experienced $CD8^{+}$ T cells. The size of both T cell populations was not significantly different 14 days after the single sporozoite immunisation, suggesting that there was no additional positive or negative influence of IL-27R signalling on antigen experienced T cell expansion. To measure functional responses, $CD8^{+}$ T cells were stimulated *ex vivo* with TRAP or S20 peptides. Re-stimulation by the sporozoite TRAP peptide resulted in a trend towards higher IFNγ $CD8^{+}$ T cell numbers in the absence of IL-27R but this was not significant in both experiments (Figure 3.2). In contrast, with S20 peptide re-stimulation of both spleen and liver $CD8^{+}$ T cells, there was a significant increase in WSX-$1^{-/-}$ IFNγ $CD8^{+}$ T cell numbers (p=0.0217 and p=0.0213 respectively). Previous work by this group has shown that Th2 $CD4^{+}$ T cells are required to control the magnitude of the $CD8^{+}$ T cell responses in liver stage malaria[78]. The trend seen in my experiments could suggest a small, indirect influence of IL-27R signalling via a decrease in the proportion of Th2 cells as the absence of IL-27 leads to an increase in the magnitude of the $CD8^{+}$ T cell population. It is interesting that the S20 peptide would induce a stronger $CD8^{+}$ T cell response than TRAP but the salient question from these experiments was whether the total $CD8^{+}$ T cell response was sufficiently increased in WSX-$1^{-/-}$ mice to elicit increased protection from sporozoite challenge.

The possibility that IL-27R signalling does influence the immune response to liver stage malaria was investigated by measuring parasite liver load after sporozoite challenge. A single immunisation with irradiated *Pb* ANKA sporozoites was again given to C57BL/6 and WSX-$1^{-/-}$ mice and 14 days later all were challenged i.v. with *Pb* sporozoites. EEF development in the liver occurs within 50 hours after infection[226–229] so livers were dissected between 40 and 42 hours after sporozoite challenge for RT-PCR quantification of parasitaemia. The rationale for 40-42 hours after challenge was that it is sufficient for successful hepatocyte invasion but not long enough for full schizont maturation, which has been similarly used in previous publications[230]. Immunisation elicited a significant reduction in parasite liver loads in both mouse conditions. Importantly however, even a two log reduction in parasite liver load is insufficient to elicit sterile protective responses. As a reliable CD4+ T cell epitope for liver stage infection isn't available at the current time it is difficult to accurately measure $CD4^{+}$ T cell activation in response to peptide re-stimulation; however, once a candidate is discovered, it would be interesting to investigate how IL-27R signalling

influences $CD4^+$ T cell activation as well as $CD8^+$ T cells using the methods described here.

IL-27 has also been shown to be a regulator of long term T cell responses[224,231]. In order to fully understand whether IL-27 influences T cell memory, I repeated the single immunisation with C57BL/6 and WSX-$1^{-/-}$ that was performed in the experiments for figure 3.2, followed by a period of 45 days before dissecting livers and spleens for lymphocyte re-stimulation. Following initial exposure to an infectious agent, antigen-specific T cell populations expand and differentiate to control infection. After resolution of infection, these T cell populations contract to prevent atypical activation. This leaves long-lived T cells that can respond to subsequent infection more rapidly and with greater avidity than the primary response[232]. Therefore, it is perhaps not surprising that there is almost a log reduction in the size of $CD8^+$ and $CD4^+$ T cell populations between 14 and 45 days. Similarly, there is a reduction in IFNγ producing $CD8^+$ T cells following peptide re-stimulation, which is proportional across all experimental groups. Importantly, there is an additional contrast with experiments from figure 3.2 as there is no significant difference between WT and WSX-$1^{-/-}$ immunised groups after S20 peptide re-stimulation. It is interesting that a trend towards higher IFNγ production by parasite-specific $CD8^+$ T cells persists with memory populations. As there is not a similar trend between naïve groups it would appear unlikely that this is the result of innate differences in the size of T cell populations between strains. It would seem that IL-27R signalling may have a small influence on functional $CD8^+$ T cell responses to liver stage malaria; however, alone is not sufficient to significantly regulate them.

Extensive research into IL-10 in the context of infectious disease has shown that it is capable of strong negative regulation of immune responses. During infection with malaria, IL-10 has been associated with protection against blood stage pathologies, which are at least in part a result of $CD8^+$ T cell-mediated inflammation, leading to liver pathology, cerebral malaria, and other organ failures attributed to severe disease. As with IL-27R signalling, IL-10 is capable of influencing multiple cell types of both immune and non-immune lineages. Interestingly, again there is a paucity of information available regarding the influence of IL-10 signalling during the liver stage of malaria and specifically how it influences different T cell populations.

In this study I attempted to increase our understanding of IL-10-mediated regulation during liver stage infection. Using similar methods as for my investigation of IL-27R signalling, I immunised C57BL/6 mice with a single non-protective γ-radiation attenuated *Pb* ANKA sporozoite immunisation; however, rather than using a KO mouse strain, I blocked the IL-10R at immunisation using α-IL10R antibodies. Using flow cytometry to investigate T cell populations and functional responses, I observed no difference between control groups and mice that were given IL-10R blocking antibodies. This is interesting as IL-10 signalling has been implicated in T cell responses to blood stage malaria infection however, in the context of liver stage infection this does not appear to be the case. From these results, I also investigated whether blockade of IL-10R with immunisation offers any protection against Pb ANKA sporozoite challenge. As expected, there was no reduction in parasite liver load with IL-10R blockade compared to controls.

3.5 Conclusion

Regulatory signalling through IL-27 and IL-10 have been widely studied; however, until now they have not been investigated in the context of $CD8^+$ T cell responses to pre-erythrocytic stage malaria infection in a mouse model of ECM. With regard to IL-27R signalling, there was a non-significant and non-protective increase in functional $CD8^+$ T cells in WSX-$1^{-/-}$ mice compared to C57BL/6. This is interesting and could be further investigated in combination with other regulatory or excitatory pathways. IL-10 signalling is also not involved in regulation of $CD8^+$ T cells during liver stage infection but, by showing this I have increased our understanding of the complex subject of regulation in pre-erythrocytic stage malaria. Although both pathways have been implicated in T cell responses during blood stage infection, it is interesting that I have not found any significant contribution of either pathway to regulating protective $CD8^+$ T cell responses. This shows that our understanding of regulation for blood stage malaria cannot lead to assumptions of regulation during the pre-erythrocytic stages and it is crucial to investigate both systems individually.

4 | Host Resistance to *Plasmodium*-Induced Acute Immune Pathology Is Regulated by Interleukin-10 Receptor Signalling

The work presented in this chapter is adapted and extended from the following publication[233] with permission:

Carla Claser, J. Brian De Souza, **Samuel G. Thorburn**, Georges Emile Grau, Eleanor M. Riley, Laurent Rénia and Julius C. R. Hafalla. Host Resistance to Plasmodium-Induced Acute Immune Pathology Is Regulated by Interleukin-10 Receptor Signaling. *Infect. Immun.* **85,** e00941-16 (2017)

My contribution to this investigation includes flow cytometric analysis of T cell responses to blood stage *Pb* malaria infection of BALB/c mice with IL-10R blockade as presented in Figures 4.4, 4.5 and 4.7.

4.1 Introduction

The regulation of pathological mechanisms leading to cerebral malaria (CM), a severe complication of infection with the malaria parasite *Plasmodium falciparum*, remains obscure. ECM due to *Pb* ANKA infection in susceptible C57BL/6 mice mimics the neurological signs observed during human CM, including ataxia and/or paralysis, which rapidly deteriorate to convulsions, coma, and death 7 to 10 days postinfection[234,235]. Histological examination of both CM and ECM brain sections reveals the presence of petechial hemorrhages[236–238]. Furthermore, both CM and ECM are characterized by the accumulation of parasitized red blood cells (pRBCs) and leukocytes in the cerebral microvasculature.

In C57BL/6 mice, the development of ECM is associated with CD8 Clec9A DCs, which prime naive CD4 and $CD8^+$ T cells to become effector cells and secrete pro-inflammatory cytokines such as IFNy[239,240]. The production of IFNy by $CD4^+$ T cells is thought to enhance the recruitment of effector $CD8^+$ T cells to brain microvessels, where pRBCs also accumulate[89,241]. These effector $CD8^+$ T cells, upon recognition of the parasite-derived epitopes presented by the brain endothelial cells[242,243], secrete perforin and granzymes, leading to breaching of the blood-brain barrier[90–92] and causing hemorrhages. Besides neurological impairment, *Pb* ANKA-infected C57BL/6 mice develop a multiorgan disease, and in the absence of cerebral pathology, animals die at a later time point because of anaemia and hyperparasitemia[241].

In contrast, *Pb* ANKA infection of BALB/c mice does not generally lead to ECM and therefore this strain is considered ECM resistant, although the infected animals succumb to anaemia and hyperparasitemia 2 to 3 weeks postinfection[94,234]. However, the immune mechanisms that confer resistance to ECM remain poorly understood. We previously showed that T cell inhibitory pathways, CTLA-4, and PD-1/PD-L1 independently regulate host resistance to ECM[94]. Blockade of the CTLA-4 or PD-1/ PD-L1 pathway in *Pb* ANKA-infected BALB/c mice led to the development of ECM with characteristics similar to those observed in C57BL/6 mice.

IL-10, an anti-inflammatory cytokine, is a principal regulator of immunity to infection. IL-10 signalling through its receptor (IL-10R, CD210) is known to attenuate the production of IFNy and other pro-inflammatory responses[244,245], which may otherwise induce immune pathology during acute infections. In the nonlethal models of *P. chabaudi* and *Py* blood stage malaria infection, deficiency in IL-10 signalling is associated with increased IFNy secretion and good parasite control at the expense of exacerbated immune pathology[246–248]. Likewise, IL-10 deficiency is fatal in the avirulent murine models of both *Toxoplasma gondii* and *Trypanosoma cruzi*[210,249]. Together, these studies clearly indicate a critical role for the IL-10R signalling pathway in preventing pathology. IL-10R signalling attenuates the production of IFNγ and other pro-inflammatory responses responsible for inducing immune-mediated pathology during acute parasitic infections.

In the present study, we hypothesized that IL-10R signalling also regulates T-cell-mediated inflammatory responses in ECM-resistant BALB/c mice, thereby preventing the onset of ECM. Blockade of the IL-10R during *Pb* ANKA infection of BALB/c mice results in acute immune-mediated pathology with features resembling those of ECM in susceptible mice. Therefore, the IL-10R signalling pathway appears to effectively maintain the equilibrium between pathogen clearance and tissue damage during the early stages of a lethal malaria infection in BALB/c mice.

4.2 Materials and Methods

4.2.1 Animals

In the United Kingdom, 6- to 12-week-old female BALB/cAnNCrl mice were purchased from Charles Rivers UK Ltd. and maintained under barrier conditions. Animal experiments were approved by the London School of Hygiene and Tropical Medicine Animal Welfare and Ethical Review Board and performed under Animals (Scientific Procedures) Act 1986. In Singapore, 6- to 7-week-old female BALB/cJ mice were bred and kept under specific-pathogen-free conditions in the Biomedical Resource Center of A*STAR. Animal experiments were approved by the A*STAR

Institutional Animal Care and Use Committee in accordance with the rules and regulations of the Singaporean Agri-Food and Veterinary Authority and the National Advisory Committee for Laboratory Animal Research.

4.2.2 Parasites and experimental infections

Experimental infections were initiated by i.v. inoculation of 10^4 pRBCs. In the United Kingdom, *Pb* ANKA parasites (*Pb* ANKA clone 15cy1[250], referred to here simply as *Pb* ANKA) expressing green fluorescent protein were used. In Singapore, transgenic parasite *Pb* ANKA line 231cl1 expressing luciferase and green fluorescent protein (referred to here as *Pb* ANKA *luc*) was provided by Christian Engwerda (QIMR Berghofer Medical Research Institute, Brisbane, Australia). Infected mice were monitored for neurological signs (uncoordinated and reduced locomotion, paralysis, deviation of the head, ataxia, convulsions, and coma). Parasitemia levels were monitored by the examination of Giemsa-stained thin blood smears or by flow cytometry[251]. In some experiments, day 7 infected mice were sacrificed and perfused and their brains and livers were removed for histology or imaging (see below). Serum was stored at 70°C for cytokine quantification (see below).

4.2.3 *In vivo* administration of antibodies

All antibodies were administered by intraperitoneal injection. Blocking antibody to IL-10R [1B1.3A] was administered at 0.3 mg/mouse on day 1 postinfection and at 0.2 mg/mouse on days 1, 4, and 6 postinfection. Neutralizing antibody to IFNγ [XMG1.2] was administered at 0.4 mg/mouse on days 4 and 6 postinfection, and depleting antibodies to CD4 [GK1.5] and CD8 [53.6.72] were administered at 1 mg/mouse on day 6 postinfection. All antibodies were rat anti-mouse IgG, obtained from BioXCell (USA); control rat IgG was obtained from Pierce.

4.2.4 Flow cytometry

The antibodies (clones) used for cell surface staining were (obtained from eBioscience) anti-mouse CD4 (GK1.5), CD8 (53.6-7), CD11a (M17/4), and CD62L (MEL-14) or (obtained from BD Biosciences) anti-mouse CD3 (145-2C11), CD4 (RM4-5), and CD8 (53-6.7). Isolated brain and splenic leukocytes were directly stained in accordance with standard protocols[94]. Antibodies used for intracellular staining were obtained from eBioscience (IFNγ [XMG1.2]). Intracellular staining was per- formed by permeabilizing cells with 0.1% saponin–PBS. Cells were analyzed with a FACSCalibur or LSR II (BD Immunocytometry Systems) and FlowJo software (TreeStar). Gating strategies were performed as previously described, where T cells are gated from singlets/live and lymphocyte populations[94]. Absolute numbers of lymphocytes were calculated from cell counts.

4.2.5 Cytokine quantification

Serum cytokine levels were assayed with the IFNγ Quantikine kit and the Quantikine ELISA mouse IL-10 kit (both from R&D Systems) in accordance with the manufacturer's protocol. Intracellular IFNγ levels were measured by flow cytometry (as described above) following 5 h of spleen cell culturing in the presence of phorbol myristate acetate (PMA; 50 ng/ml), ionomycin (1 g/ml), and brefeldin A (1 g/ml).

4.2.6 Bioluminescent imaging

Daily *in vivo* imaging was done to monitor the *Pb* ANKA *luc* parasite distribution (IVIS; Xenogen, Alameda, CA). Infected mice were shaved, anesthetized, and injected subcutaneously with 100 l of D-luciferin potassium salt (5 mg/ml in PBS; Caliper Life Sciences). Two minutes later, bioluminescence images were acquired with a medium binning factor and a field of view (FOV) of 21.7 cm for the whole body (ventral) or 4 cm for the head (dorsal). The exposure imaging time was 5 to 60 s. For *ex vivo* imaging, mice were given a second injection of luciferin and anesthetized and 3 min later perfused and sacrificed. Brains were removed and imaged with a 10-cm FOV. To allow comparisons of images from different days, uninfected mice injected with luciferin were imaged for background subtraction.

Bioluminescence quantification was done by using Living Imaging 4.2 software and expressed in average radiance units (photons per second per square centimeter per steradian).

4.2.7 Histology

Infected mice were sacrificed on day 7 postinfection. Mice were perfused with PBS, and their isolated brains and livers were immersed in 4% formaldehyde and embedded in paraffin. Sagittal sectioning was performed to obtain 5- m-thick brain and liver sections, which were stained with hematoxylin and eosin (H&E). Slides were acquired on a Metafer4 (MetaSystems), and numbers of hemorrhages, leukocytes, and necroses (of the liver) were manually determined.

4.2.8 Statistical analysis

Differences in survival were assessed with the log rank (Mantel-Cox) test, and Bonferroni correction was used to adjust for multiple comparisons within the log rank (Mantel-Cox) test. The cumulative ECM incidence between two groups was analyzed with Fisher's exact test. Comparisons of two groups were made with the Mann-Whitney test, and for multiple comparisons (more than two groups), statistical significance was determined with the Kruskal-Wallis test with Dunn's multiple comparisons post-test. For log-transformed values to allow normal distribution of the data, analysis of variance with Bonferroni's posttest for multiple groups was used. The data were analyzed with GraphPad Prism software (version 6.0) with *P* 0.05 as the level of significance.

4.3 Results

To establish whether IL-10R signalling regulates ECM pathogenesis in an otherwise ECM- resistant mouse strain, the outcomes of *Pb* ANKA infection in control mice and mice treated with blocking antibodies to IL-10R were compared. While control BALB/c

mice (treated with rat IgG or phosphate-buffered saline [PBS]) survived for up to 2 weeks postinfection, mice treated with anti-IL-10R antibody developed classical neurological signs of ECM and were euthanized on day 7 or 8 postinfection (Figure 4.1A and B). Both the survival curve and the cumulative ECM incidence of anti-IL-10R antibody- treated mice differ significantly from those of control mice. Strikingly, anti-IL-10R antibody-treated mice presented significantly lower parasitemia levels on days 5 and 7 postinfection than control mice (Figure 4.1C). Consistent with the development of ECM, the number of accumulated intravascular $CD8^+$ T cells was higher in the brains of anti-IL- 10R antibody-treated mice than in those of control mice (Figure 4.1D). A key feature of human CM and ECM in mice is the accumulation of pRBCs in the brain microvasculature. To determine the effects of IL-10R signalling on parasite accumulation, control and anti-IL-10R antibody-treated mice were infected with *Pb* ANKA *luc* parasites that express luciferase. The survival curve and cumulative ECM incidence (Figure 4.2A and B) of *Pb* ANKA *luc*-infected control and anti-IL-10R antibody-treated mice were similar to those of *Pb* ANKA-infected mice, although the onset of ECM was somewhat delayed. Anti-IL-10R antibody-treated *P. berghei* ANKA *luc*-infected mice developed ECM between days 7 and 12 postinfection, and control mice survived until day 25. *Pb* ANKA *luc*-infected anti-IL-10R antibody-treated mice presented with significantly lower parasitemia values on days 5 and 7 postinfection than control mice (Figure 4.2C). However, when parasite accumulation was measured by luminescence in the whole body (Figure 4.2D), head (Figure 4.2E), and isolated brain (Figure 4.2F and G), the values were significantly higher in anti-IL-10R antibody-treated mice than in control mice. These results indicate that despite a lighter peripheral parasite burden in anti-IL-10R antibody-treated mice than in control mice, the generalized parasite biomass is significantly elevated when the IL-10R signalling pathway is blocked.

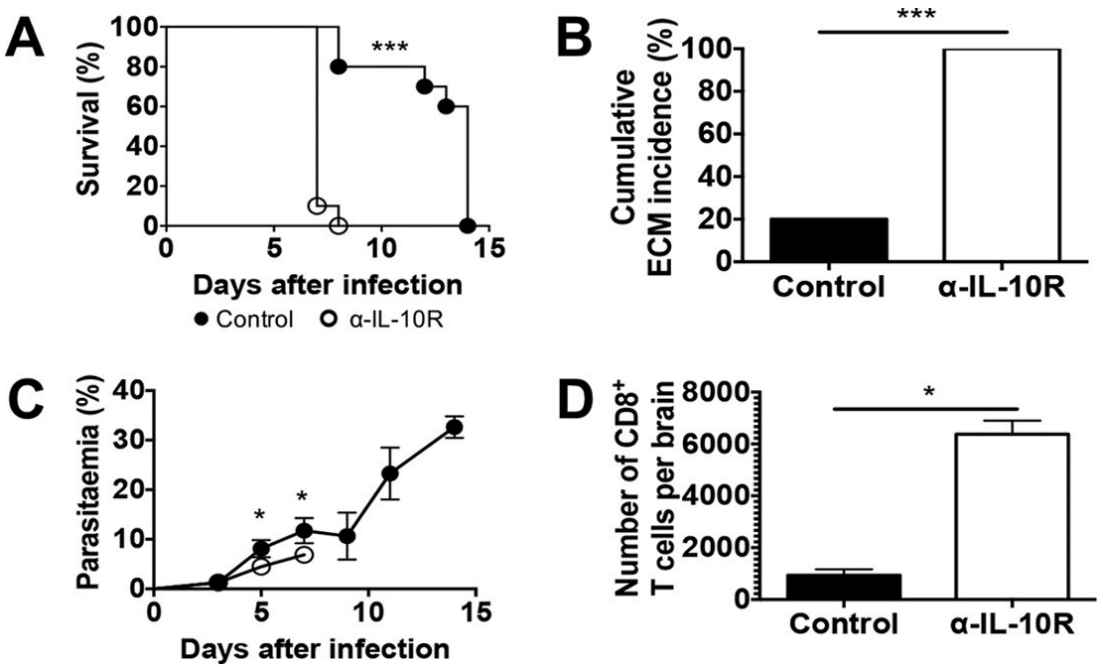

Figure 4.1: IL-10R blockade in *Pb* ANKA-infected BALB/c mice results in ECM.

BALB/c mice were infected i.v. with 10^4 *Pb* ANKA pRBCs and treated with anti-IL-10R antibodies. Control mice received either no antibody or rat IgG. (A) Cumulative survival curve. Closed circles, control (*n* 12); open circles, anti-IL-10R antibody (*n* 12). ***, *P* 0.0001 (log rank [Mantel-Cox] test). (B) Cumulative incidence of mice developing ECM (based on neurological signs, i.e., ataxia and paralysis). ***, *P* 0.0001 (Fisher's exact test). Mice that survived were euthanized on day 14 because of high parasitemia and anaemia. (C) Parasitemia levels, shown as the mean the standard deviation, of *Pb* ANKA-infected mice. Closed circles, control; open circles, anti-IL-10R antibody. The data shown are representative of three independent experiments with four to six mice per group. *, *P* 0.05 (Mann-Whitney U test). (D) Absolute numbers of CD8 T lymphocytes that have accumulated in the brain. The data shown (mean standard deviation) are representative of two independent experiments with four mice per group. *, *P* 0.05 (Mann-Whitney U test).

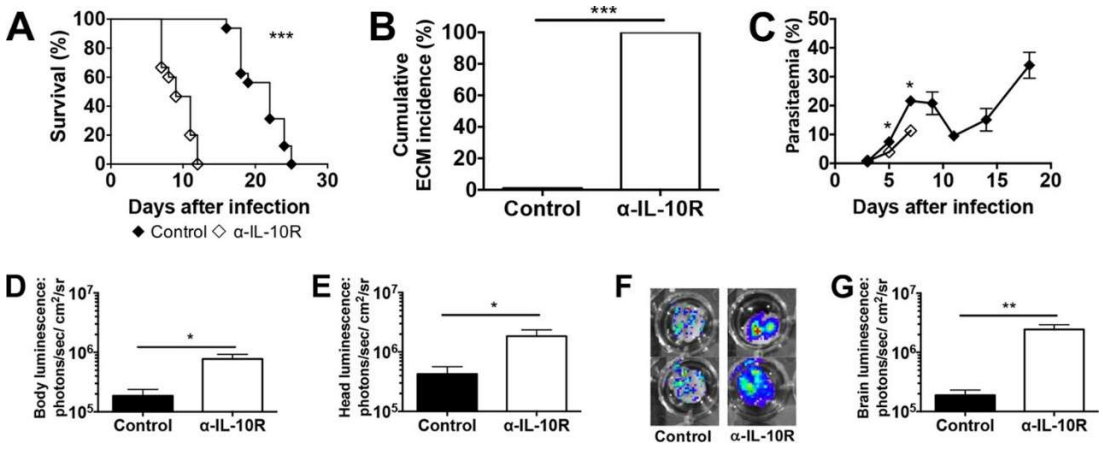

Figure 4.2: ECM after IL-10R blockade in *Pb* ANKA-infected BALB/c mice is associated with parasite accumulation in the brain.

BALB/c mice were infected i.v. with 10^4 *Pb* ANKA *luc* pRBCs and either left untreated (control) or treated with anti-IL-10R antibodies. (A) Cumulative survival curve. Closed diamonds, control (*n* 16); open diamonds, anti-IL-10R antibody (*n* 15); ***, *P* 0.0001 (log rank [Mantel-Cox] test). (B) Cumulative incidence of mice developing ECM. ***, *P* 0.0001 (Fisher's exact test). Similar to Figure 4.1, mice that survived were euthanized because of high levels of parasitemia and anaemia. (C) Parasitemia levels, shown as the mean the standard deviation, of *Pb* ANKA-infected mice. The data shown are representative of two independent experiments performed with five mice per group. *, *P* 0.05 (Mann-Whitney U test). (D to G) Parasite accumulation in the whole body (D), head (E), and isolated brain (F, G) as measured by luciferase activity on day 7 postinfection. The data shown are representative of two independent experiments performed with five mice per group. In panels D, E, and G, the data shown are the mean the standard deviation. *, *P* 0.05; **, *P* 0.001 (Mann-Whitney U test).

Histological examination of the brains and livers of *Pb* ANKA *luc*-infected control and anti-IL-10R antibody-treated mice was also performed. The numbers of brain petechial hemorrhages were significantly higher in anti-IL-10R antibody-treated mice than in control mice (Figure 4.3A, B), while the numbers of microvessels with leukocytes did not differ between the two groups (Figure 4.3C). Moreover, there was also no difference between the numbers of perivascular infiltrates in the liver in the two groups (Figure 4.3E), although there was a trend of finding necrosis in anti-IL-10R antibody-treated mice but not in control mice (Figure 4.3D and F). Taken together, these findings signify that blocking IL-10R signalling in otherwise ECM-resistant mice results in the development of immune pathology with all of the features of ECM.

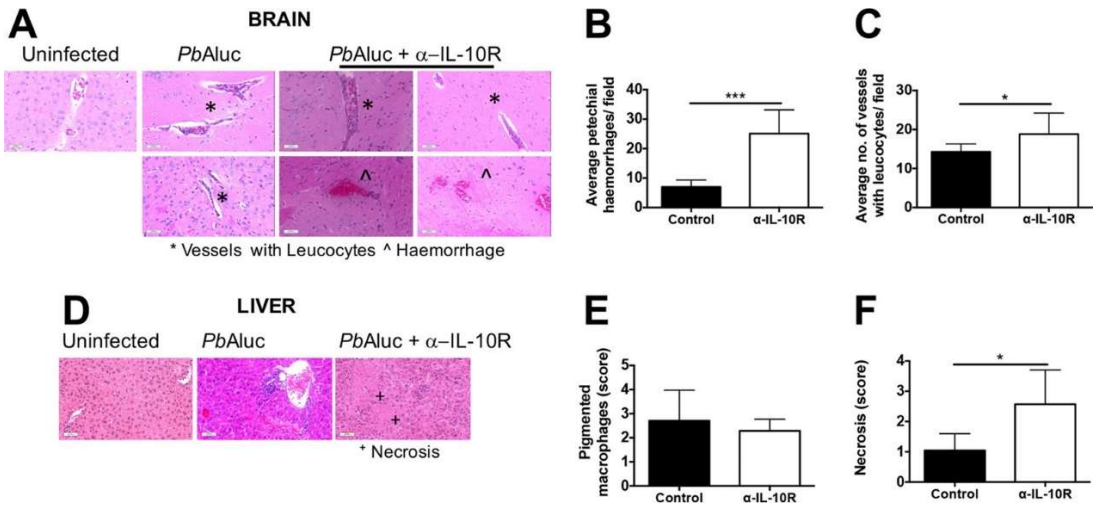

Figure 4.3: ECM after IL-10R blockade in *Pb* ANKA-infected BALB/c mice is associated with brain pathology.

(A) Histological examination of H&E-stained brain sections from uninfected and day 7 *Pb* ANKA *luc* pRBC-infected mice (*n* 7 per group). Asterisks indicate areas of vessels with leukocytes, while circumflexes signify hemorrhages. Magnification, 20. Graphs show the quantification of the number of petechial hemorrhages (B) and vessels with leukocytes (C). (D) Similar to panel A but with liver sections. Graphs show the scoring of pigmented macrophages (E) and necrosis (F). In panels B, C, E, and F, the data shown are the mean the standard deviation. *, *P* 0.05; ***, *P* 0.0001 (Mann-Whitney U test).

ECM is a result of T-cell-mediated inflammation in C57BL/6 mice. The development of ECM in *Pb* ANKA-infected anti-IL-10R antibody-treated BALB/c mice was indicative of an amplified inflammatory response. As an indicator of systemic inflammation, serum IFNγ concentrations (Figure 4.4A) were significantly higher in anti-IL-10R antibody-treated mice than in control and uninfected mice on day 7 postinfection. Consistent with the blockade of IL-10R signalling, serum IL-10 concentrations (Figure 4.4B) were also significantly higher in anti-IL-10R antibody-treated mice than in control and uninfected mice. The levels of splenic activation were also evaluated on day 6 postinfection. The flow cytometry gating strategies used are shown in Figure 4.5 A, B, and F in the supplemental material. There was a trend toward larger proportions of splenic $CD4^+$ and $CD8^+$ T cells expressing CD62L and CD11a and producing IFNγ in the anti-IL-10R antibody- treated mice than in the control and uninfected mice (see Figure 4.5 B-I). Considering splenic leukocyte counts, a statistically significant difference between the control and anti-IL-10R antibody-treated groups was reached for the total numbers of $CD4^+$ T cells expressing CD11a , and $CD4^+$ and $CD8^+$ T cells producing IFNγ (Figure 4.4C to H). Taken together, the results show that the development of ECM in *Pb* ANKA-infected anti-IL-10R antibody-treated BALB/c mice correlates with higher levels of systemic inflammation and T cell activation.

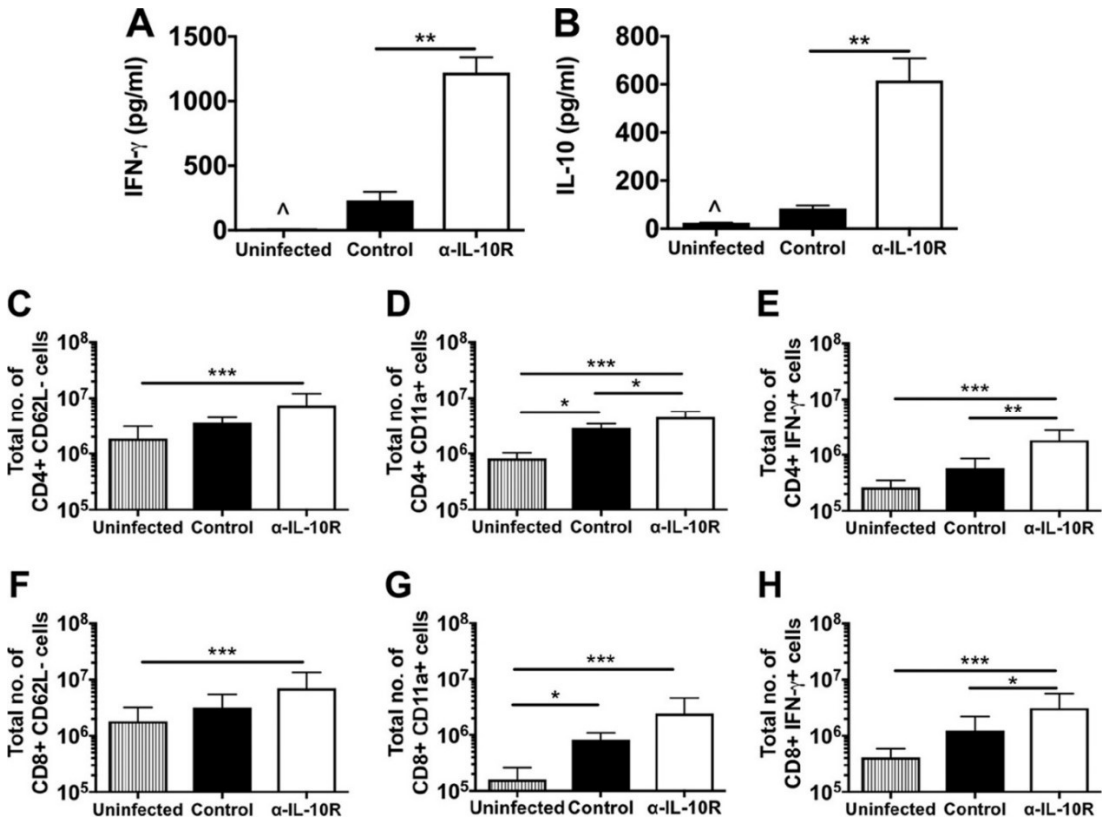

Figure 4.4: Enhanced effector responses after IL-10R blockade in *Pb* ANKA-infected BALB/c mice.

BALB/c mice were infected i.v. with 10^4 *Pb* ANKA *luc* pRBCs (A and B) or 10^4 *Pb* ANKA pRBCs (C to E) and either left untreated (control) or treated with anti-IL-10R antibodies. Serum IFNγ (A) and IL-10 (B) levels were determined with Quantikine kits from R&D Systems. For cellular analyses, splenocytes were prepared from uninfected or day 6 infected mice and stained for surface CD3, CD4, CD8, CD62L, and CD11a. The data shown are gated on CD3 T cells (see Figure 4.5). The absolute numbers (mean standard deviation) of CD4 CD62L cells (C), CD4 CD11a cells (D), CD8 CD62L cells (F), and CD8 CD11a cells (G) are shown. Splenocytes were also stimulated with PMA/ionomycin for 5 h in the presence of brefeldin A; this was followed by intracellular IFNγ staining. The absolute numbers (mean standard deviation) of CD4 IFNγ cells (E) and CD8 IFNγ cells (H) are shown. The results shown are pooled data from two similar experiments (three to five mice per group). The data shown are the mean the standard deviation. *, *P* 0.05; **, *P* 0.001; ***, *P* 0.0001 (Kruskal-Wallis test/Dunn's multiple comparisons test).

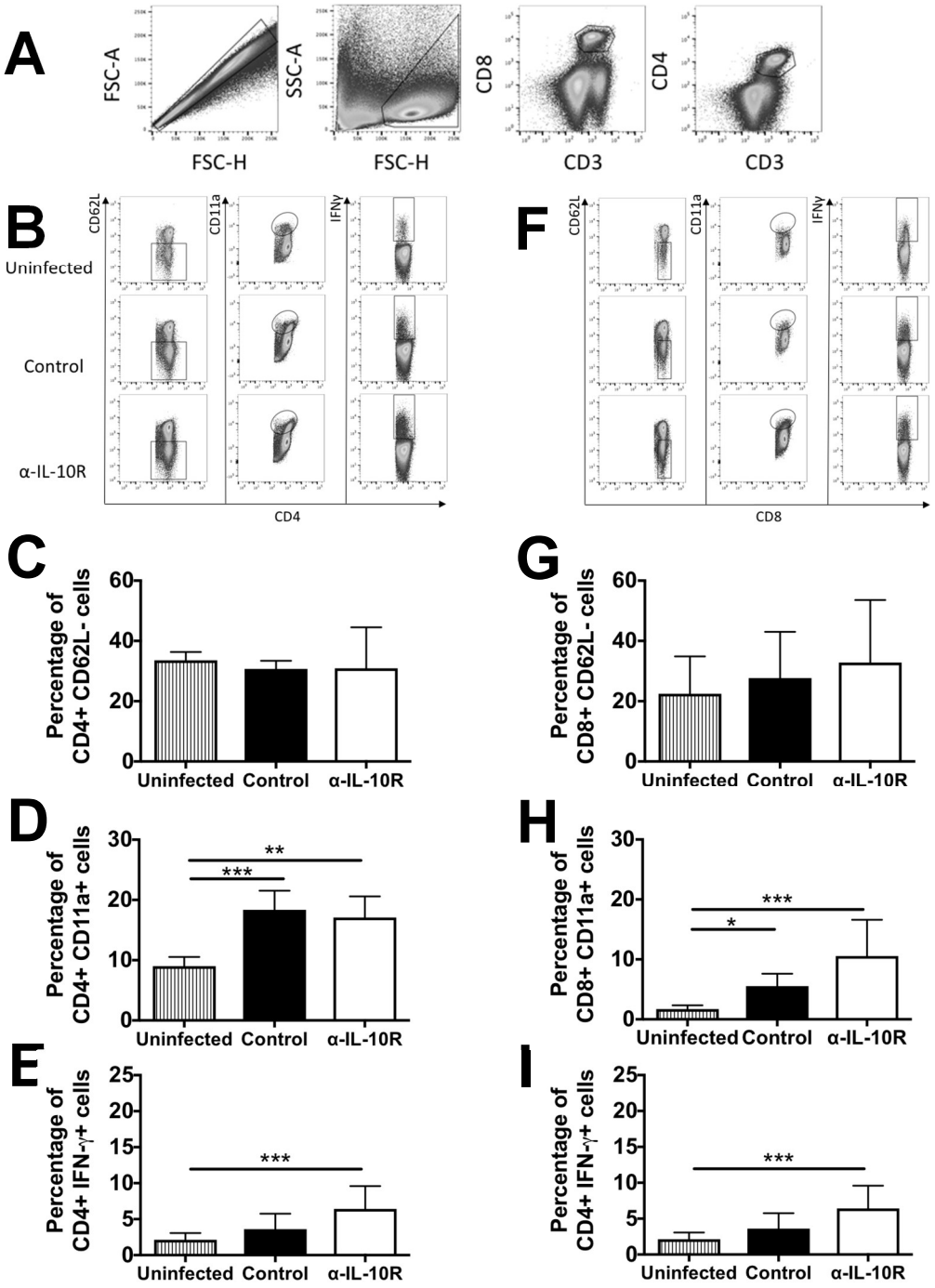

Figure 4.5: Flow cytometric analysis of splenocytes after IL-10R blockade in *Pb*A-infected BALB/c mice.

BALB/c mice were infected i.v. with 10^4 *Pb* ANKA pRBCs and either left untreated (control) or treated with anti-IL-10R antibodies. For cellular analyses, splenocytes were prepared from uninfected or day 6 infected mice and stained for surface CD3, CD4, CD8, CD62L, and CD11a. Gating strategies are shown (A, B and F) for $CD8^+$ and $CD4^+$ T cells. The absolute numbers (mean standard deviation) of CD4 CD62L cells (C), CD4 CD11a cells (D), CD8 CD62L cells (G), and CD8 CD11a cells (H) are shown. Splenocytes were also stimulated with PMA/ionomycin for 5 h in the presence of brefeldin A; this was followed by intracellular IFNγ staining (E and I). The results shown are pooled data from two similar experiments (three to five mice per group). The data shown are the mean and the standard deviation. *, *P* 0.05; **, *P* 0.001; ***, *P* 0.0001 (Kruskal-Wallis test followed by Dunn's multiple comparisons post test).

The data presented so far indicate that blockade of IL-10R signalling leads to full ECM susceptibility in otherwise resistant BALB/c mice, and this is associated with amplified T cell activation and higher serum IFNγ concentrations. These findings are consistent with the hypothesis that signalling through the IL-10R switches off T cell reactivity and thus inhibits the development of ECM. To ascertain whether T cell populations are the targets of IL-10R-mediated regulation, anti-IL-10R antibodies were combined with depletion of antibodies specific for $CD4^+$ or $CD8^+$ T cells *in vivo*. Depletion of either $CD4^+$ or $CD8^+$ T cells during *Pb* ANKA *luc* infection prevented the development of ECM in anti-IL-10R antibody-treated mice (Figure 4.5A and B). CD4 or CD8 T-cell-depleted mice developed severe anaemia and eventually died 2 to 3 weeks postinfection. The role of IFNγ in the development of ECM in anti-IL-10R antibody-treated *Pb* ANKA *luc*-infected BALB/c mice was also determined by combination with anti-IFNγ neutralizing antibodies throughout infection. Neutralization of IFNγ during *Pb* ANKA *luc* infection prevented the development of ECM in anti-IL-10R antibody-treated mice (Figure 4.5A and B). *Pb* ANKA *luc*-infected anti-IL-10R antibody-treated mice presented peripheral parasitemia levels similar to those of mice given anti-CD8 , -CD4 , or -IFNγ antibodies (Figure 4.5C). Interestingly, treatment with anti-CD8 , -CD4 , or -IFNγ antibodies led to significantly less parasite accumulation in the whole bodies (Figure 4.5D) and heads of infected animals (Figure 4.5E). These data demonstrated that while the parasite biomass is increased by IL-10R blockade, the effect is reversed in the absence of T cells or IFNγ.

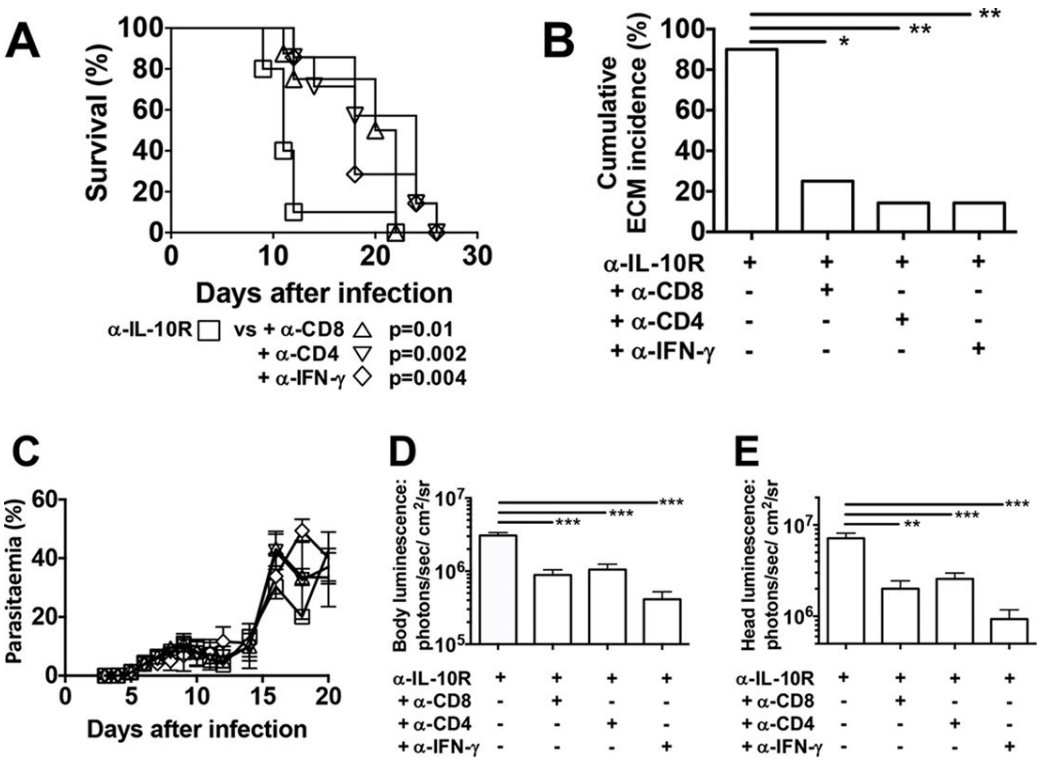

Figure 4.6: ECM after IL-10R blockade in *Pb* ANKA-infected BALB/c mice is dependent on T cells and IFNγ.

BALB/c mice were infected i.v. with 10^4 *Pb* ANKA *luc* pRBCs and treated with anti-IL-10R antibody. (A) Cumulative survival curves of IL-10R blockade alone (*n* 10), with anti-$CD8^+$ T cell depletion (*n* 8), with anti-$CD4^+$ T cell depletion (*n* 7), and with anti-IFNγ neutralization (*n* 7). *P* values (log rank [Mantel-Cox] test) are shown. (B) Cumulative incidence of mice developing ECM. *, *P* 0.05; **, *P* 0.001; ***, *P* 0.0001 (Fisher's exact test). Similar to Figure 4.1 and 4.2, mice that survived were euthanized because of high levels of parasitemia and anaemia. (C) Parasitemia levels, shown as the mean the standard deviation, of *Pb* ANKA *luc*-infected mice represented by the same symbols as in panel A. (D, E) Parasite accumulation in the whole body (D) and head (E) as measured by luciferase activity on day 7 postinfection. The data shown are the mean the standard deviation. **, *P* 0.001; ***, *P* 0.0001 (Kruskal-Wallis test/Dunn's multiple-comparison test). The data shown are representative of two independent experiments of at least seven animals per group.

Previous work by our group has investigated the role of CTLA-4 and PD-1 signalling during acute blood stage infection and shows that blockade of either of these pathways results in severe immune pathology[94]. As we have already shown that IL-10R signalling is critical for protection against immune pathology, I also investigated whether blockade of the IL-10R influenced CTLA-4 and PD-1 expression on activated $CD8^+$ and $CD4^+$ T cells (Figure 4.7 A and B respectively). Interestingly, I observed that blockade of IL-10R signalling during blood stage infection increased the frequency of CTLA-4^+PD-1^+ double positive $CD8^+$ and $CD4^+$ T cells. A significant increase was also seen in total CTLA-4^+ compared to controls; however, this was not seen with total PD-1 expressing T cells.

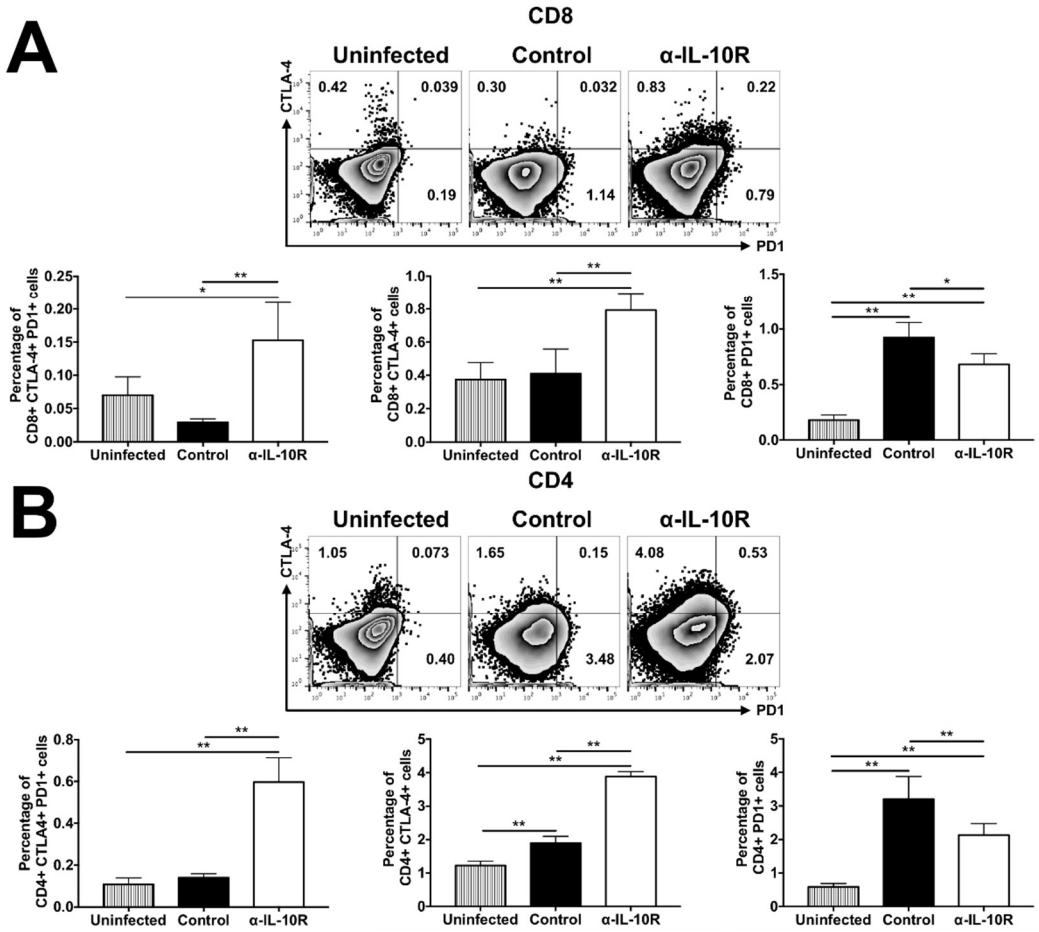

Figure 4.7. Blockade of IL-10R leads to increased CTLA-4, but not increased PD-1 expression during blood stage *Pb* infection

BALB/c mice were infected i.v. with 10^4 *Pb* ANKA pRBCs and either left untreated (control) or treated with anti-IL-10R antibodies. For cellular analyses, splenocytes were prepared from uninfected or day 6 infected mice and stained for surface CD3, CD4, CD8, CD62L, CD11a and PD-1 and intracellular CTLA-4. Proportions of CTLA-4$^+$PD-1$^+$, CTLA-4$^+$ and PD-1$^+$ populations are shown for CD8$^+$ (A) and CD4$^+$ (B) T cells. The results shown are pooled data from two similar experiments (three to five mice per group). The data shown are the mean and the standard deviation. *, *P* 0.05; **, *P* 0.001; ***, *P* 0.0001 (Kruskal-Wallis test followed by Dunn's multiple comparisons post test).

4.4 Discussion

Our findings provide an increased understanding of the regulatory pathways that impact the outcome of infection with an ECM-inducing rodent malaria strain that mimics the pathological processes associated with CM due to *P. falciparum* in humans. We have shown that blocking IL-10R facilitates the development of acute immune pathology in normally ECM-resistant BALB/c mice with pathological features compatible with ECM in susceptible C57BL/6 mice. Neuropathological signs were associated with heavy parasite loads, the development of IFNγ secreting CD4 and $CD8^+$ T cells in the spleen, and an influx of $CD8^+$ T cells into the brains of IL-10R-treated mice. Thus, IL-10R signalling plays a vital role in the prevention of immune-mediated neuropathology during *Pb* ANKA infection of ECM-resistant BALB/c mice.

The outcomes reported in this study expand those reported in our previous work, where blockade of CTLA-4 or PD-1/PD-L1 inhibitory pathways in *Pb* ANKA- infected BALB/c mice also rendered the animals susceptible to ECM[94]. Both studies show that depletion of T cells and neutralization of IFNγ abrogated the effects of regulatory pathway blockade, validating the notion that ECM has similar aetiologies in both BALB/c mice and susceptible C57BL/6 mice. Both studies further corroborate that $CD8^+$ T cells and IFNγ are the critical effectors of ECM. While damage to brain vessels has implicated perforin and granzyme B secretion in *Pb* ANKA-infected C57BL/6 mice[90–92], the roles of these molecules in BALB/c mice warrant further investigation. While it appears that the CTLA-4, PD-1/PD-L1, and IL-10-R pathways independently regulate host resistance to *Pb* ANKA infection of BALB/c mice, we have shown that the CTLA-4 and/or PD-1/PD-L1 axes are influenced by the blockade of IL-10R.

Signalling through CTLA-4 and IL-10 provides two distinct mechanisms for T cell inhibition however, there is evidence that in the absence of one, the other works to compensate to provide correct T cell responses. With *Pb* blood stage infection, blockade of CTLA-4 leads to fatal cerebral malaria in normally refractory mice as well as a significant increase in IL-10 production by T cells after re-stimulation[94]. Similarly, the Jacobs group investigated whether blockade of CTLA-4 during non-lethal or lethal *Py* infection influenced the outcome of disease [163]. Using a non-lethal strain, they

found a reduced peak parasitaemia with CTLA-4 blockade. A protective increase in serum IFNγ production was accompanied by a significant increase in IL-4 and IL-10. In comparison, infection with a lethal *Py* strain concurrently with CTLA-4 blockade led to decreased survival with pathology due to increased IFNγ and TNFα. Interestingly, there was also a significant increase in IL-4 and a noticeable, but non-significant increase in IL-10. This suggests that CTLA-4 blockade induces overproduction of IL-10 during infection which may contribute to preventing pathology in non-lethal *Py* infection, but is not sufficient to protect against pathology with lethal infection. Tang and colleagues used constitutive expression of CTLA-4Ig to specifically investigate Treg cells and their functional relationship with CTLA-4 [252]. They found that even in the absence of CTLA-4, Treg cells could still suppress proliferation of WT T cells, indicating no loss in suppressive capacity. CTLA-4$^{-/-}$ Treg cells produced 5-fold more IL-10 than WT controls however, further blockade of IL-10 in addition to CTLA-4 did not abrogate normal suppressive function of WT T cells *in vitro*. This observation differs from findings by Read et al. who investigated CTLA-4 blockade of Treg cells *in vivo* using CTLA-4 blocking antibodies [253]. Using a model of colitis, they found that blockade of CTLA-4 did not alter Treg ability to prevent colitis when transferred with WT CD4^{+}CD45RB^{high} cells into BALB/c.RAG2 KO mice. When they blocked the IL-10R receptor as well as CTLA-4 this protective suppression was completely abrogated. This suggests that blockade of CTLA-4 induces alternative suppressive pathways as WT Treg cells protect from colitis through pathways independent of IL-10 [254]. Although CTLA-4 is constitutively expressed on Treg cells, it is a crucial co-receptor in conventional T cell activation. Paterson et al. used a conditional knock out mouse model of CTLA-4 to investigate adult T cell function in the absence of CTLA-4 [255]. After knocking out CTLA-4 with tamoxifen administration they implanted a tumour using MC38 tumour cells and investigated T cell responses. As well as an increase in IL-10, LAG3 and PD-1 in Treg cells, there was a significant increase in IL-10 production by conventional CD4 T cells and CD8 T cells. Interestingly, the absence of CTLA-4 did not lead to reduced tumour size, possibly due to the increase in Treg numbers and compensatory inhibitory mechanisms.

Although there appears to be an agreement that blockade of CTLA-4 leads to an increase in IL-10 in mouse models of infection and inflammation, studies differ in the method and duration of CTLA-4 abrogation. It would appear however, that short-term, targeted CTLA-4 blockade increases compensatory mechanisms but not to a level that suppresses increased T cell activation. With long-term blockade there may be

time for these mechanisms, including IL-10 signalling, to reach levels that restore more of a balance between T cell activation and inhibition.

While our depletion experiments suggest that the pathological effects of IL-10R blockade result from the regulation of T cell responses, additional studies are required to ascertain the roles of IL-10R expression and IL-10R blockade in other immune cells. DCs and monocytes have been shown to produce IL-10 during malaria infections[256–258]. Similarly, B cells have also been reported to produce IL-10 in *Pb* ANKA-infected C57BL/6 mice[259]. Recently, tissue-resident CD169 macrophages were shown to produce high levels of IL-10 during *Pb* ANKA infection in BALB/c mice and to restrict inflammatory responses[260]. Concerning T cells, protection against ECM may also be due to balanced IFNγ /IL-10 secretion in activated T cells versus regulatory T cells Tregs. The failure of IL-10 to counterbalance IFNγ release during IL-10R blockade may be attributed to a failure in the IL-10 signalling pathway in both activated T cells and Tregs with consequent release of IFNγ. This assumption on Tregs is backed up by recent findings of a loss of FoxP3 expression in Treg cells with increased pro-inflammatory cytokine release during *P. chabaudi* AS infection in IL-10R-treated DBA/2 mice[261]. Failure of the IL-10R signalling pathway in Tregs has also been associated with loss of FoxP3 expression and inflammatory cytokine release in a murine model of inflammatory bowel disease[262,263]. Furthermore, in the murine model of hepatitis C virus infection, IL-10R blockade steers the inflammatory response toward a type 1 IFNγ-mediated T cell response[264].

IL-10 production is also increased during *Pb* ANKA infection of ECM- susceptible C57BL/6 mice[265,266]. It is likely that IL-10 performs a similar regulatory role in C57BL/6 mice, although its failure to provide protection against ECM remains unclear. It is possible that an over exuberant inflammatory response supersedes the physiological levels of regulation facilitated by IL-10R signalling. Alternatively, down- stream IL-10R signalling is impaired on target cells.

Although the kinetics and precise interactions between the effector and regulatory pathways remain undefined in this model of ECM, our studies reveal the importance of maintaining a balance between effector and regulatory immune responses for

preventing ECM. Disproportionate pro-inflammatory responses consistently lead to immuno- pathology, although there is reasonable control of parasitemia. Equally, poor antiparasite immune responses generated concurrently with strong regulatory responses permit parasitemia with harmful consequences, as demonstrated in this *Pb* ANKA/BALB/c model of severe malaria.

5 | Identification of Novel Pre-erythrocytic Malaria Antibody Epitopes Using High-Density Peptide Microarray Techniques

5.1 Introduction

There is strong evidence that during liver stage infection, high titres of parasite-specific antibodies are capable of neutralising sporozoites and subsequently preventing patent disease[79,267,268]. Passive transfer of antibodies from immunised animals to naïve animals has been shown to be protective in mouse models of malaria against *Pb* and *Py* sporozoites and in monkey models against *Pv* and *Pk* sporozoites[171,269]. Monoclonal antibodies specific to *Pb* sporozoites are capable of neutralising sporozoites *in vitro* [85] as well as *in vivo* [84]. This can also be seen with monoclonal antibodies towards *Pf* CSP that can neutralise *Pf* sporozoites and prevent hepatocyte invasion of splenectomised chimpanzees[270]. In experiments done by Oliveira and colleagues, BALB/c and C57BL/6 mice that were deficient in β_2-microglobulin and therefore had no activation of cytotoxic T cells through Class I MHC were used. They found that immunisation of these mice with irradiated *Pb* or *Py* sporozoites still elicited sterile protection and this was mediated through $CD4^+$ T cell activation and antibodies that neutralised extracellular sporozoites[79]. Further support for antibody protection in pre-erythrocytic malaria can be seen in endemic settings where the presence of memory B cells specific to *Pf* CSP have been identified[271] and in a study by John et al. the presence of antibodies against CSP and liver stage antigen type-1 (LSA-1) in Kenyan children was associated with a decreased risk of clinical malaria[272]. These studies show that CSP is a highly immunodominant surface protein and other studies have shown that the target of antibodies is the region of tandem repeats[268,273,274]. Currently, RTS, S is the most advanced malaria vaccine that utilises this property of CSP, including both antibody and T cell epitopes. Surprisingly, although preliminary research was very promising for the RTS, S vaccine and immunisation produces high antibody titres, phase III trials have shown it to have lower long-term efficacy than hoped[275–279]. Despite the understanding that antibody responses are known to be protective, there is a paucity in known immunogenic antibody antigens other than CSP.

The ability to identify immunologically relevant epitopes requires either the identification of monoclonal functional antibodies, accurate prediction of antibody binding to putative epitope sequences, the parallel synthesis of many potential epitopes for simultaneous analysis or a combination of these strategies. The

immunodominant protein CSP was identified through hybridoma generation of protective monoclonal antibodies[84], which is now considered a long and costly strategy for identifying novel antigens. It is limited by the breadth of the immune response that can be investigated in one set of experiments. The popular development of reverse vaccinology techniques since the beginning of the 'genome era' has allowed for the analysis of epitopes on a whole genome, transcriptome or proteome scale. Taking advantage of this, work done by the Fernan Aguero group used a high-density peptide microarray to design the largest investigation of fine antibody specificities for a human infection[117]. Using the annotated *T. cruzi* CL-Brener genome, they identified 457 proteins which were synthesised as peptides 15 amino acids in length with an overlap of 14 amino acids with the previous peptide in the sequence, resulting in over 175,000 peptides. Sera from *T. cruzi* infected patients was incubated with the microarray and after analysis, more than 120 novel antibody antigenic determinants were identified. This study highlights how the use of novel technology now allows for the simultaneous investigation of hundreds of thousands of potential epitopes towards improved diagnostics, therapeutics and vaccines. Although experiments of this kind are still expensive and microarray slides cannot be used many times for multiple experiments, it is significantly cheaper than experimentally investigating the same number of potential epitopes using any other technique and ultimately requires significantly less serum. Unfortunately, probing a peptide microarray with serum only assists in the identification of linear epitopes. This means that discontinuous epitopes cannot be discovered, leaving potentially up to 90% of antigenic determinants not investigated. Although whole protein microarrays can be done, the synthesis of physiologically correct proteins raises further problems that peptide microarrays do not have.

Significant development has occurred in the technological ability to map epitopes experimentally. Currently, peptide microarrays offer the most high throughput approach to linear epitope identification, allowing tens or hundreds of thousands of peptides to be probed simultaneously. For this study, I designed a microarray that allows for the investigation of the entire sporozoite and liver stage *Pb* ANKA proteome. As CSP is a highly immunodominant protein, I also used a novel immunisation schedule that specifically boosts all non-CSP antigens through the use of a transgenic *Pb* strain that expresses *Pf* CSP rather than *Pb* CSP (*Pb*[*Pf*CSP])[280]. *Pb* CSP and *Pf* CSP are homologous proteins that are both expressed on the surface of the sporozoite but they only share a similarity in protein sequence of 47.6% (Figure

5.1). Therefore, a boosting immunisation with Pb(PfCSP) does not expose the host immune system to the majority of the PbCSP sequence. This means that all other Pb proteins are available for boosting immune responses; however, PbCSP is not. In this way, non-CSP proteins can be preferentially targeted with an immunisation schedule using two separate immunisations.

```
# Length: 403
# Identity:   151/403 (37.5%)
# Similarity:  192/403 (47.6%)
# Gaps:        69/403 (17.1%)
# Score: 627.0
#
#
#=======================================

PfCSP       1 MMRKLAILSVSSFLFVEALFQEYQCYGSSSNTRVLNELNYDNAGTN-LYN     49
              |:|..||.|:|.|.|.:|...|....|....|.||||.|:....| ||:
PbCSP       1 -MKKCTILVVASLLLVNSLLPGYGQNKSIQAQRNLNELCYNEGNDNKLYH     49

PfCSP      50 ELEMNYYGKQENWYSLKKNSRSLGENDDG--NNEDNEKLRKPKHKKLKQP     97
              .|.    .|....|:...:|.|.:..:|  |.:.|||:.  ::.||||
PbCSP      50 VLN----SKNGKIYNRNTVNRLLADAPEGKKNEKKNEKIE--RNNKLKQ-     92

PfCSP      98 ADGNPDPNANPNVDPNANPNVDPNANPNVDPNANPNANPNANPNANPNAN    147
                  |.|..|||..|..|||..|..|||..|..|||..|
PbCSP      93 ----PPPPPNPNDPPPPNPNDPPPPNPNDPPPPNPNDPP-----------    127

PfCSP     148 PNANPNANPNANPNANPNANPNANPNANPNANPNANPNANPNANPNANPN    197
                        .||||....||||..|.||||..|.||||..|.||||..
PbCSP     128 -----------PPNANDPPPPNANDPAPPNANDPAPPNANDPAPPNANDP    166

PfCSP     198 VDPNANPNANPNANPNANPNANPNANPNANPNANPNANPNANPNANPNAN    247
              ..||||....||.|..|.||||....||.|..|.|..|.|..|...|...
PbCSP     167 APPNANDPPPPNPNDPAPPNANDPPPPNPNDPAPPQGNNNPQPQPRPQPQ    216

PfCSP     248 PNANPNANPNANPNANPNANPNANPNKNNQGNGQGHNMPNDPNRNVDENA    297
              |...|...|...|...|...|....|.||
PbCSP     217 PQPQPQPQPQPQPQPRPQPQPQPGGNNNN----------------------    245

PfCSP     298 NANSAVKNNNNEE---PSDKHIKEYLNKIQNSLSTEWSPCSVTCGNGIQV    344
                    ||||||::   ||.:.|.|::.:|::|::.|||.|:||||:||:|
PbCSP     246 ------KNNNNDDSYIPSAEKILEFVKQIRDSITEEWSQCNVTCGSGIRV    289

PfCSP     345 RIKPGSANKPKDELDYANDIEKKICKMEKCSSVFNVVNSSIGLIMVLSFL    394
              |.:.|| ||..::|. ..||:.:||||:||||:||:|::|:|.:::|..:
PbCSP     290 RKRKGS-NKKAEDLT-LEDIDTEICKMDKCSSIFNIVSNSLGFVILLVLV    337

PfCSP     395 FLN    397
              |.|
PbCSP     338 FFN    340
```

Figure 5.1. Alignment of *Pb* and *Pf* CSP protein sequences.

Protein alignment of the protein sequences for *Pf* CSP and *Pb* CSP was performed using the European Molecular Biology Open Sequence Suite (EMBOSS) Needle protein alignment tool[281].

5.2 Methods

5.2.1 Mosquito and mouse conditions

C57BL/6 mice between 5-8 weeks were bred in-house at London School of Hygiene and Tropical Medicine (LSHTM) or by Charles River Laboratories (UK). They were housed in filter-topped cages up to 6 per cage with absorbent bedding, nesting material and enrichment. Their diet consisted of autoclaved water and food pellets. Procedures were performed under license from the United Kingdom Home Office under the Animals (Scientific Procedures) Act 1986 and approved by the Animal Care and Ethical Review Committee.

Pb ANKA infected *Anopheles stephensi* mosquitoes grown at LSHTM and the Max Planck Institute for Infection Biology, Berlin were kept at 22°C with 80% humidity and fed on 10% glucose solution (10% D-Glucose [Sigma-Aldrich] in distilled water). *Pb*(*Pf*CSP) infected *Anopheles stephensi* mosquitoes were grown at the Max Planck Institute for Infection Biology, Berlin and were also kept at 22°C with 80% humidity and fed on 10% glucose solution (10% D-Glucose in distilled water). In order to generate infectious *Pb* sporozoites, blood stage parasites were first collected from infected C57BL/6 mice via cardiac puncture into 1.5ml Eppendorf tubes (Sigma) with heparin (Sigma) and kept on ice. Blood was diluted 1:2 in freezing media made from 7.5% Glycerol (Sigma) in RPMI complete (RPMI 1640 [Gibco] with 10% FCS [Gibco], 2% L-Glutamine [Gibco] and 1% Penicillin and Streptomycin [Gibco]) and kept at -80C. When required, blood stage parasites were thawed and 200µl was injected i.v. into a naïve C57BL/6 mouse. After three days, blood was collected from the infected mouse via cardiac puncture and 100,000 infected RBCs were passaged into two naïve C57BL/6 mice. 4 days after passage, mice were given a terminal dose (100-150µl) of anaesthesia consisting of 50% PBS, 33% ketamine (Ketamidor, 100mg/ml [National Veterinary Services Limited]) and 17% xylazine (Rompun, 2% w/v [National Veterinary Services Limited]) i.p. and placed on a cage of mosquitoes (70 mosquitoes per mouse) for a 30 minute blood feed. 18-20 days after blood feed, mosquitoes were judged to be positive for sporozoites in the salivary glands.

5.2.2 Whole sporozoite immunisation

Female *Anopheles stephensi* salivary glands were dissected from infected mosquitoes in RPMI complete and *Pb* ANKA sporozoites were isolated through homogenisation and centrifugation. Glands were homogenised using autoclaved plastic pestles in Eppendorf tubes and centrifuged at 10,000 rpm for 3 minutes. The pellet was re-suspended in 200µl of RPMI complete and *Pb* ANKA sporozoites were counted on a C-chip haemocytometer (Digital bio). For immunisations, *Pb* ANKA sporozoites were diluted to 50,000/ml in RPMI complete. To attenuate by irradiation for immunisation, the suspension was exposed to gamma radiation at $1.2x10^4$ centigray (cGY) for 20.5 minutes. C57BL/6 mice were immunised by an i.v. injection of 0.2ml attenuated *Pb* ANKA sporozoites per mouse. 14 days after the final immunisation, blood was collected via tail vein puncture in heparin. 28 days after the final immunisation blood was also collected via cardiac puncture. After blood collection at both time points, blood was centrifuged at 1,000 x g for 10 minutes and serum was taken by pipette. Serum was stored at -80°C until needed.

5.2.3 Immunofluorescence Assay (IFA)

Pb ANKA sporozoites were air dried on microscope slides in spots of 20µl with 5,000 sporozoites per spot and kept at -20 until required. When needed, slides were fixed by dipping in cold acetone for 1 minute and rehydrated in 20µl of PBS at room temperature for 20 minutes. Spots were blocked by removing the PBS and adding 20µl of RPMI complete followed by a 1 hour incubation in a humid chamber at 37°C. After incubation 20ul of serum was added to each spot in a serial dilution in RPMI complete followed by a further 1 hour incubation at 37C in a humid chamber. Spots were washed three times with RPMI complete before adding 20ul of AlexaFluor 546/488 goat anti-mouse IgG (Sigma) diluted 1:2,000 in RPMI complete. Slides were incubated at 37C for 1 hour in the dark before a final three washes with PBS and mounting of the slide using Vectashield (Fisher Scientific) and a coverslip sealed with nail varnish.

5.2.4 Hepatocyte Invasion Assay

Huh7 cells were cultured in RPMI complete (RPMI [Gibco] with 10% FCS [Gibco], 2% L-Glutamine [Gibco] and 1% Penicillin and Streptomycin [Gibco]) at 37°C with 5% CO_2. 24 hours before sporozoite invasion, cells were seeded into Labtek wells (ThermoFisher Scientific) at 30,000 cells per well. On the day of infection salivary glands were dissected from *Pb* infected female *Anopheles stephensi* mosquitoes. Glands were homogenised and sporozoites were isolated by centrifugation. After counting, 5,000 to 10,000 sporozoites were added per experimental Labtek well. Slides were centrifuged and incubated for 2 hours at 37°C with 5% CO_2 to allow for invasion before being washed 3 times with RPMI complete. Slides were incubated for a further 48 hours to allow for EEF development. To stain, cells were first fixed with 4% paraformaldehyde (PFA) and permeabalised with 0.3% Triton X-100 (Sigma). As our *Pb* ANKA strain constitutively expresses GFP, EEFs were stained with chicken antibodies specific to green fluorescent protein (GFP) at 1:300 dilution, followed by goat anti-chicken IgG Alexa Fluor 488 fluorescent antibodies (ThermoFisher Scientific) at 1:1,000 dilution. Nuclei were stained with DAPI (ThermoFisher Scientific). Cells were coated in Vectashield under a sealed coverslip. Imaging was performed on a Zeiss LSM510 confocal microscope.

5.2.5 Cell Traversal Assay

HepG2 cells were cultured in RPMI complete at 37°C with 5% CO_2. 24 hours before sporozoite invasion, cells were seeded into 96 well plates (ThermoFisher Scientific) at 10,000 cells per well. Sporozoites were diluted to 5,000 per sample and serum was added at a dilution of 1:5. Sporozoites were kept on ice with serum for 40 minutes. Fluorescent rhodamine B isothiocyanate high molecular weight dextran (Sigma) was added and 50µl was added per well to HepG2 cells. Sporozoites were sedimented by centrifugation for 10 mins at 2,200 rpm with no brake and cells were incubated at 37°C for 3 hours. After incubation wells were washed three times with PBS. 50µl of Trypsin was added per well and incubated for 10 minutes at 37°C. Trypsin was diluted with 150µl of medium and centrifuged at 1500rpm for 2 minutes followed by removing the medium and replacing it with 200µl FACS buffer (PBS with 1% BSA). Cells were run on a Guava Easycyte flow cytometer (Millipore)

5.2.6 Microarray

A list of the proteins of sporozoite and liver stages of *Pb* ANKA were determined using previously published experimental data available from PlasmoDB, resulting in 2977 proteins in total. Sequences for all proteins were divided into 15 amino acid oligomers with an 11 amino acid overlap with the previous sequence. This produced a total of 519,319 peptides that were randomly organised over the microarray slide. Microarray slides were synthesised by the company Schafer-N. This was done using maskless photolithography, whereby a digital micro-mirror device focuses 365nm light onto a derivatised glass slide with high resolution. An amino acid spacer was bound to the slide surface, followed by the synthesis of *Pb* ANKA peptides using 3′-nitrophenylpropyloxycarbonyl (NPPOC) photoprotected amino acids. In this way, light directed by the DMD removed the NPPOC block from specific peptides and allowed for the addition of the next amino acid in the sequence, each with a 9-fluorenylmethoxycarbonyl (Fmoc) group block. Once all amino acids for the layer were added, the Fmoc groups were removed and replaced with NPPOC blocks. This was repeated until all peptides were synthesised. Slides were probed with immunised mouse serum (25µl/ml), followed by secondary fluorescent antibody Cy3 sheep anti-mouse IgG (Fab)2 (Sigma) (1 µg/ml). Fluorescence was measured using an InnoScan900 microarray scanner (Innopsys) with an excitation wavelength of 532nm.

5.2.7 Enzyme Linked Immunosorbent Assay (ELISA)

Antigens were diluted to 20µg/ml in coating buffer (for 1 litre, 1.59g Na_2CO_3 and 2.93g $NaHCO_3$ dissolved in 1 litre of distilled water) and added to a 96 well Maxisorp ELISA plate (NUNC) at 50µl per well. Plates were left at 4°C overnight for antigen adsorption. The following day, plates were washed three times in a PBS/Tween wash solution (PBS with 0.05% Tween 20) and 150µl of blocking solution (3% BSA [Gibco] in PBS) was added per well. Plates were incubated at 37°C for 1 hour and washed a further three times with PBS with 0.5% BSA. Serum samples were diluted 1:200 in PBS and 50µl was added per well and incubated at 37°C for 1 hour followed by a further three washes with PBS with 0.5% BSA. Horseradish peroxidase conjugated sheep anti-mouse IgG (Sigma) was diluted 1:6,000 in PBS/0.5%BSA and 50µl was

added per well with a further 1 hour incubation at 37°C. After a final five washes with PBS with 0.5% BSA, OPD (Sigma) was made up according to instructions and 100ul was added per well. After 15 minutes the reaction was stopped by the addition of 25ul of 2M sulphuric acid. Plates were read at 492nm on an ELISA plate reader using Revelation software.

5.3 Results

CSP is a highly immunodominant protein on the surface of the malaria parasite, but antibodies against CSP do not contribute to 100% of the pre-erythrocytic stage-specific antibody response. In order to fully understand non-CSP antibody responses, I adopted a novel vaccination schedule to preferentially boost antibody responses to non-CSP *Pb* antigens (Figure 5.2). To do this, C57BL/6 and BALB/c mice were vaccinated with two different *Pb* strains. A primary vaccination consisted of *Pb* γ-radiation attenuated sporozoites, which was followed two weeks later by a secondary vaccination using *Pb*(*Pf*CSP) γ-radiation attenuated sporozoites. The rationale for such a schedule is that mice are exposed to all non-CSP antigens twice, providing a prime-boost strategy; however, *Pb* CSP is only encountered once as the second vaccination only exposes the immune system to *Pf* CSP. Serum was collected 14 days and 28 days after the final vaccination so that I could investigate short term and persisting antibody responses. As this is a novel vaccination regimen, I performed some preliminary experiments to confirm, firstly, that vaccinated mouse sera recognised *Pb* sporozoites and both *Pb* and *Pf* CSP and, secondly, that such a vaccination regimen elicited functional responses to *Pb* sporozoites.

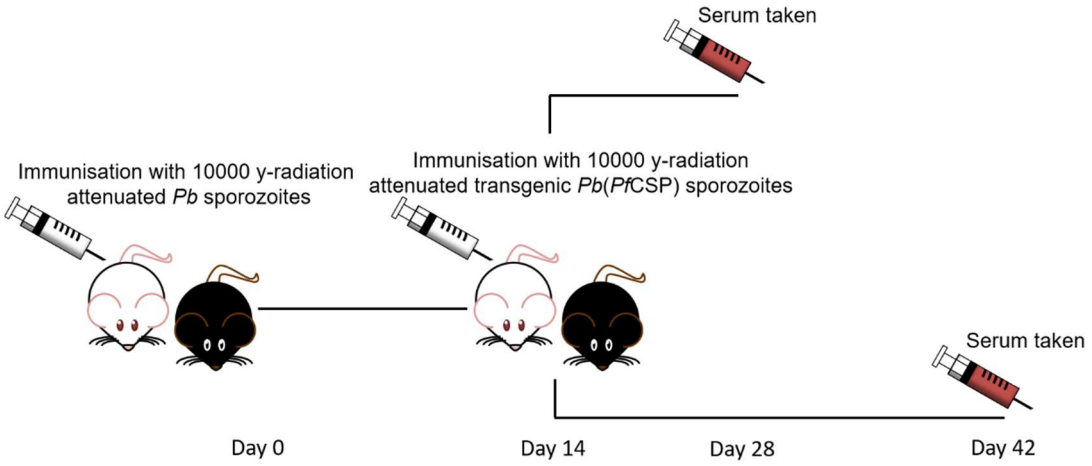

Figure 5.2. Vaccination and serum collection.

C57BL/6 and BALB/c mice were given a primary vaccination of 10,000 γ-radiation attenuated *Pb* ANKA sporozoites i.v. followed by a second vaccination 14 days later with 10,000 γ-radiation attenuated *Pb*(*Pf*CSP) sporozoites i.v. Blood was collected by tail bleed at 14 days and cardiac puncture at 28 days after the final vaccination. Serum was isolated by centrifugation and stored for further analyses. This vaccination was performed twice with 5-7 mice per strain.

In order to investigate whether antibodies generated using my novel immunisation schedule could recognise WT *Pb* ANKA sporozoites, I performed an IFA to determine *Pb* ANKA sporozoite recognition (Figure 5.3A) and to compare antibody titers between experimental groups (Figure 5.3B). Air dried *Pb* sporozoites were incubated with serum collected from immunised mice to allow for antibody binding. This was followed by washing with a fluorescent anti-mouse secondary antibody to visualise antibody-specific binding to *Pb* sporozoites. As serum was collected by tail bleed at 14 days and cardiac puncture at 28 days, there was much more material available to investigate serum responses at 28 days. As the microarray would be performed using serum collected at 28 days and material from collections on 14 and 28 days were to be used for ELISA experiments, I decided to perform IFA's for 28 days only to save material. Interestingly, BALB/c serum was consistent in its higher antibody titer compared to C57BL/6 serum. As expected, antibody titers of *Pb*(*Pf*CSP)+WT were similar to 1x WT for both BALB/c and C57BL/6. The majority of surface protein on the sporozoite surface is CSP and therefore, as *Pb*(*Pf*CSP)+WT immunisation only exposes mice to *Pb* CSP once, their antibody responses should be equivalent to 1x WT.

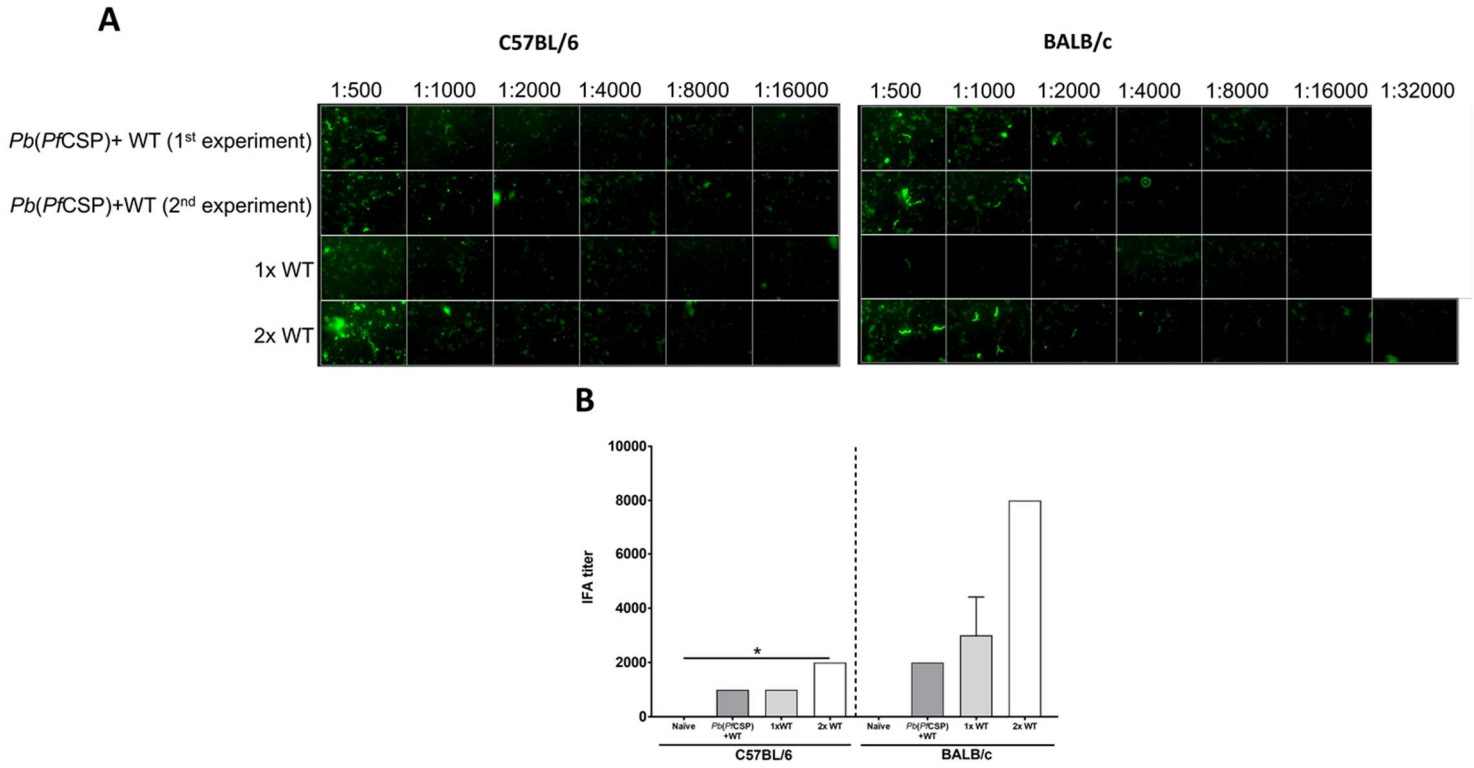

Figure 5.3. IFA of vaccinated C57BL/6 and BALB/c serum to confirm antibody recognition of *Pb* ANKA sporozoites.

Serum from C57BL/6 and BALB/c mice was collected 28 days after vaccination. Vaccination schedules consisted of 10,000 γ-radiation attenuated sporozoites i.v. using WT *Pb* ANKA or transgenic *Pb*(*Pf*CSP) sporozoites. 1 vaccination with WT was compared with 2 WT vaccinations and a novel strategy of *Pb*(*Pf*CSP)+WT. Boost vaccinations were given 14 days after the primary vaccination. *Pb* ANKA sporozoites were isolated from infected female *Anopheles stephensi* mosquito salivary glands, diluted to 100,000 per ml and air dried on glass slides. Slides were incubated with serial dilutions of serum and probed with anti-mouse FITC antibodies (A and B) to identify the endpoint titer of sporozoite-specific antibody (C). Representative results from IFA shown in A and B and pooled results from two experiments shown in C. Statistics were performed using Kruskal-Wallis non-parametric t test followed by Dunn's multiple comparisons test.

To confirm successful antibody recognition of *Pb* CSP I performed ELISA experiments using known immunogenic peptides from the repeat region of *Pb* ANKA CSP (Figure 5.4). As all mice were exposed to *Pb* CSP only once, I compared antigen recognition of the novel schedule with a single and prime-boost vaccination schedules using only *Pb* ANKA WT sporozoites. For BALB/c responses, *Pb*(*Pf*CSP)+WT was very similar to 1x WT vaccination as expected, with greater antigen binding at 28 days (Figure 5.4B) compared to 14 days (Figure 5.4A). Interestingly, C57BL/6 appeared to have higher responses with *Pb*(*Pf*CSP)+WT compared to 1x WT vaccination. Both mouse strains showed greater antigen recognition if serum was collected 28 days after vaccination in *Pb*(*Pf*CSP)+WT and 1x WT groups, but not for 2x WT. This is to be expected due to the nature of antibody responses to primary and secondary antigen exposure. In other models of immunisation, a primary vaccination initiates specific IgM antibodies as well as some IgG antibody responses that peak at around 3-4 weeks. This high titre rapidly wanes to baseline; however, upon secondary stimulation high titres of high affinity IgG antibodies are rapidly produced, peaking after only a few days. Also unlike primary responses, these higher antibody titres are much more long-lasting. Therefore, after a single exposure I would expect antibody titers to be increasing between 1 and 28 days post vaccination. In contrast, after a boosting secondary response I would expect antibody titres to already be peaking before 14 days and for titres to still be high at 28 days. Overall, these results show that all vaccination schedules successfully elicit antibody responses to *Pb* ANKA CSP peptide.

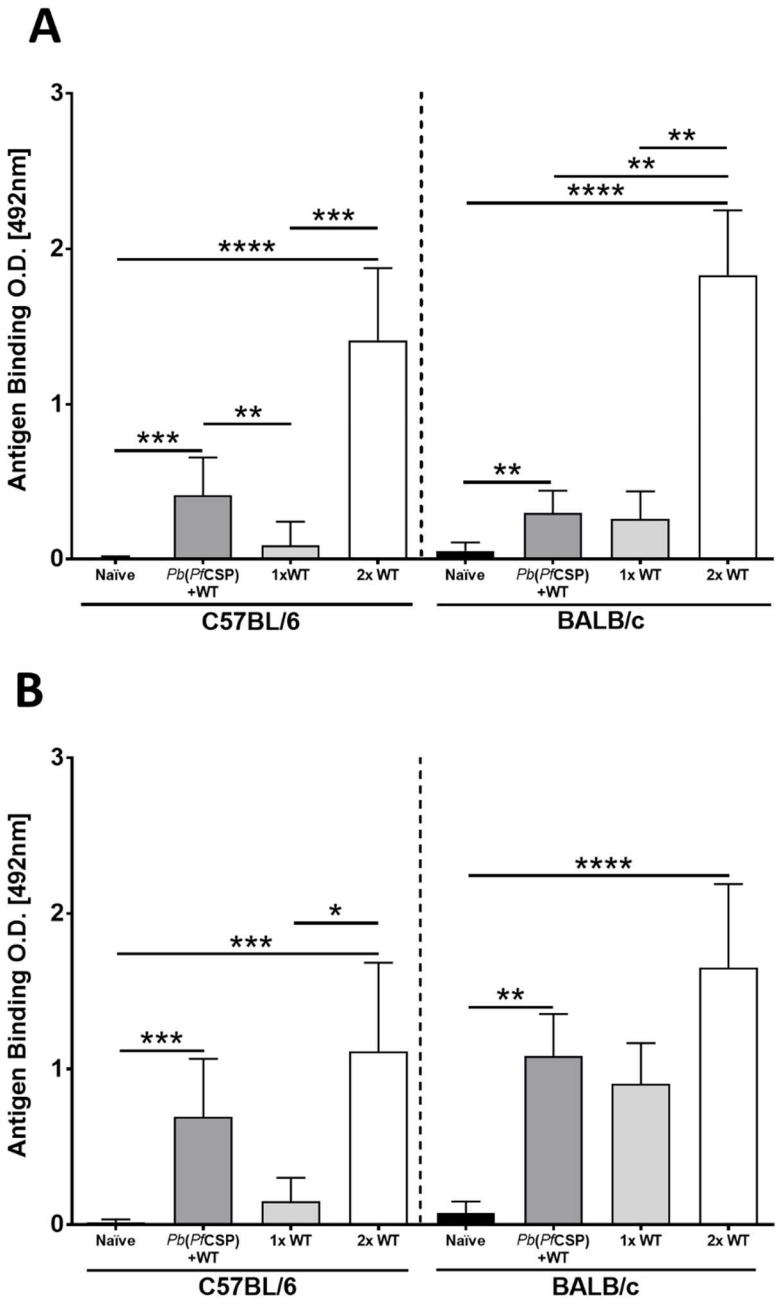

Figure 5.4. Use of a novel vaccination strategy successfully induces antibody responses to *Pb* CSP peptide antigen.

Serum from C57BL/6 and BALB/c mice was collected 14 and 28 days after vaccination. Vaccination schedules consisted of 10,000 γ-radiation attenuated *Pb* ANKA sporozoites i.v. using WT *Pb* ANKA or transgenic *Pb*(*Pf*CSP) sporozoites. 1 vaccination with WT was compared with 2 WT vaccinations and a novel strategy of *Pb*(*Pf*CSP)+WT. Boost vaccinations were given 14 days after the primary vaccination. Antibody responses at 14 days (A) and 28 days (B) after the final vaccination were measured against the *Pb* $CSP_{94\text{-}108}$ peptide PPPPNPNDPPPPNPN by ELISA. Pooled data from two experiments with 5-10 mice per group. Statistics were performed using Kruskal-Wallis non-parametric t test followed by Dunn's multiple comparisons test.

To confirm that vaccinating with our transgenic *Pb*(*Pf*CSP) sporozoites was also successful, I performed similar ELISA experiments to measure antibody recognition of *Pf* recombinant CSP (Figure 5.5). As WT vaccinations did not expose mice to *Pf* antigens, I hypothesised that antibody recognition of *Pf* CSP would only occur in mice vaccinated with *Pb*(*Pf*CSP). As expected, antibody responses for *Pf* CSP were present in the *Pb*(*Pf*CSP)+WT group, but not in mice vaccinated only with WT *Pb*. This persisted between 14 days (Figure 5.5A) and 28 days (Figure 5.5B) after the boost vaccination. The kinetics of antibody responses resembled the *Pb*(*Pf*CSP)+WT and 1x WT groups in experiments performed for figure 5.3 as they increased in both mouse strains if serum was collected on day 28. This would suggest that the responses are characteristic of a single exposure, which is as expected. Another similarity between experiments performed for figures 5.3 and 5.5 is that there was a trend towards BALB/c having higher antibody responses to antigen. This could be due to the fact that BALB/c mice are more resistant to *Pb* infection than C57BL/6 mice[165]. As ELISA experiments for figure 5.4 were performed with recombinant protein generated using *E. coli*, there is a possibility that antibody responses were for bacterial antigens rather than recombinant protein. To confirm antibody responses were towards CSP alone, I performed an ELISA comparing antibody recognition of the well characterised *Pf* Merozoite Surface Protein 1 19kDa region of the C-terminal (MSP1-19)[282–285] and *Pf* CSP recombinant protein (Supplementary Figure 5.S1). As MSP1 is a blood stage protein it is not expressed by liver stage malaria parasites, therefore any responses would be towards *E.Coli* bacterial antigen. As expected, there was no antibody recognition of antigen in the MSP1-19 condition, confirming successful purification of *Pf* CSP product. Together, figure 5.3 and figure 5.4 show that vaccination with *Pb*(*Pf*CSP)+WT *Pb* elicits antibody responses to both *Pb* and *Pf* CSP antigen with the kinetics of a single exposure. As antibody responses were consistently higher in serum collected 28 days after the final vaccination, I chose to continue with these sera for future experiments. In addition, as serum collected at 14 days was taken by tail bleed and serum collected at 28 days was by cardiac puncture, I had much more material from the 28 day collection.

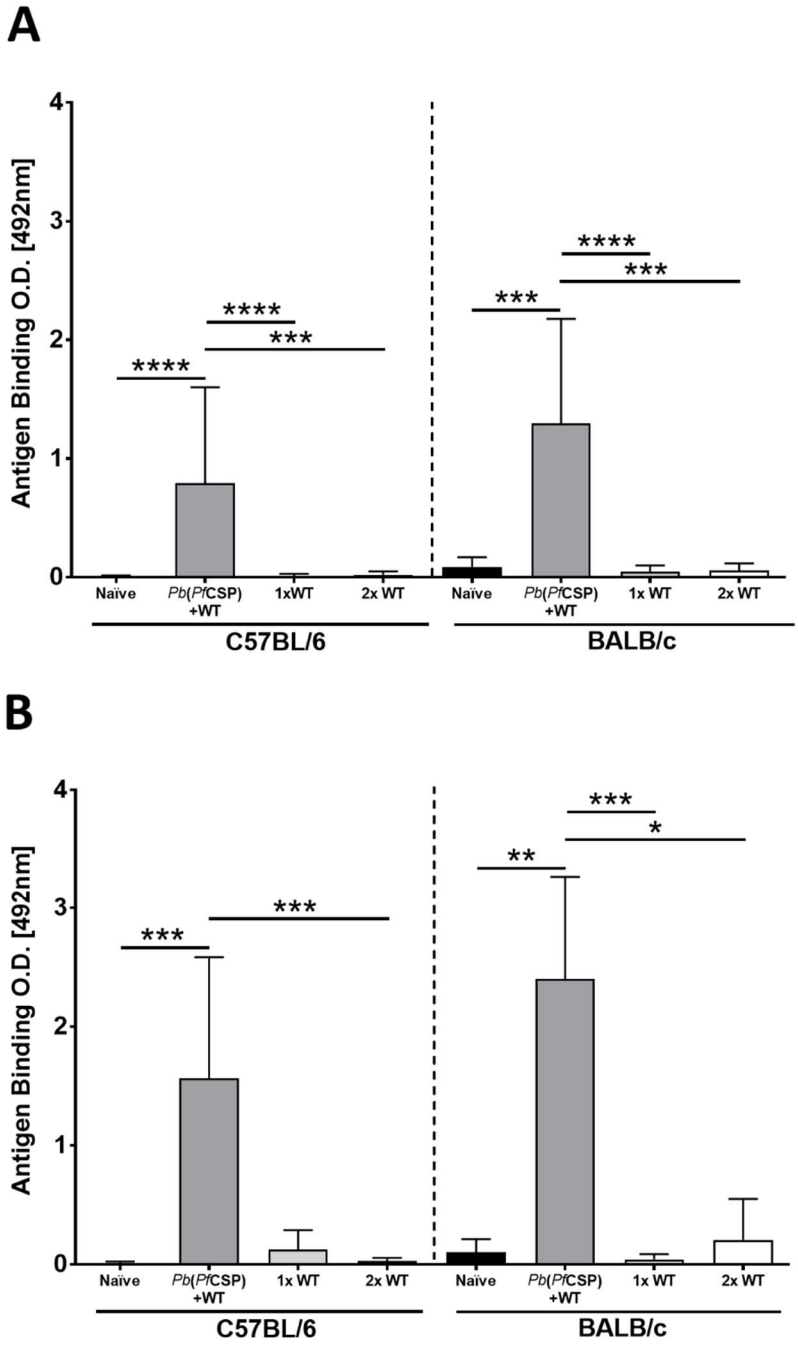

Figure 5.5. Use of a novel vaccination strategy successfully induces antibody responses to *Pf* recombinant CSP.

Serum from C57BL/6 and BALB/c mice was collected 14 and 28 days after vaccination. Vaccination schedules consisted of 10,000 γ-radiation attenuated sporozoites i.v. using WT *Pb* ANKA or transgenic *Pb*(*Pf*CSP) sporozoites. 1 vaccination with WT was compared with 2 WT vaccinations and a novel strategy of *Pb*(*Pf*CSP) followed by WT. Boost vaccinations were given 14 days after the primary vaccination. Antibody responses at 14 days (A) and 28 days (B) after the final vaccination were measured against recombinant *Pf* CSP by ELISA. Pooled data from two experiments with 5-10 mice per group. Statistics were performed using Kruskal-Wallis non-parametric t test followed by Dunn's multiple comparisons test.

The previous experiments show that my novel immunisation schedule generates immune responses to both vaccinations with kinetics that were expected and that serum from these immunisations correctly recognises *Pb* ANKA sporozoites. My next question was whether the binding of these antibodies resulted in functional neutralisation of sporozoites to the extent that cell traversal across the liver and EEF development within hepatocytes was reduced. *In vitro* techniques have been used extensively to investigate this[286] and I employed some of these strategies to answer my question. In order to investigate the neutralising effects of my pooled serum, *Pb* ANKA sporozoites were incubated with serum from each group diluted 1:5 for 40 minutes on ice before adding them to a culture of immortalised Huh7 cells for 2 hours. Although Huh7 cells are originally of human origin, *Pb* ANKA sporozoites have been shown to be relatively promiscuous in their ability to invade several hepatocyte cell lines[287]. After exposure, cells were washed and incubated for 48 hours before immunofluorescent staining to allow for counting of EEFs (Figure 5.6A). As can be seen in figure 5.6B, all immunisation schedules decreased the invasion rate compared to naïve controls but this was only statistically significant for 2x WT *Pb* ANKA immunisations and *Pb*(*Pf*CSP)+WT *Pb* ANKA. Interestingly, the reduction in invasion rate between both imunisation schedules is very similar, suggesting that the functional responses of antibodies generated is the same. As the only difference is the absence of exposure to *Pb* ANKA CSP boosting in one immunisation schedule, this suggests that the repertoire of non-CSP-specific antibodies may contribute to a similar neutralising effect.

An as yet not fully explained phenomenon of sporozoite invasion of the liver is that sporozoites traverse multiple hepatocytes before finally beginning development into an EEF in a final hepatocyte[288]. This is a non-phagocytic movement of sporozoites through hepatocytes, which results in damage of the cell membrane of the traversed cell[289]. As this is a typical feature of sporozoite invasion of the liver and antibody neutralisation inhibits the development of EEFs, I also investigated by flow cytometry the amount of hepatocytes that are traversed by sporozoites after exposure to pooled serum from each of my immunisation groups (Figure 5.7). This was done by exposing HepG2 hepatocyte cells to sporozoites in the presence of high molecular weight fluorescent dextran. As cell membranes are disrupted by cell traversal, dextran enters the hepatocyte and allows it to be detected by flow cytometry. Similar to my results

showing EEF development, immunisation led to a reduction in cell traversal in all groups apart from C57BL/6 serum from a single *Pb* ANKA immunisation. It is also interesting that the reduction of cell traversal is also comparative between two *Pb* ANKA immunisations and *Pb*(*Pf*CSP) followed by *Pb* ANKA, perhaps for reasons similar to those for the reduction in EEF development.

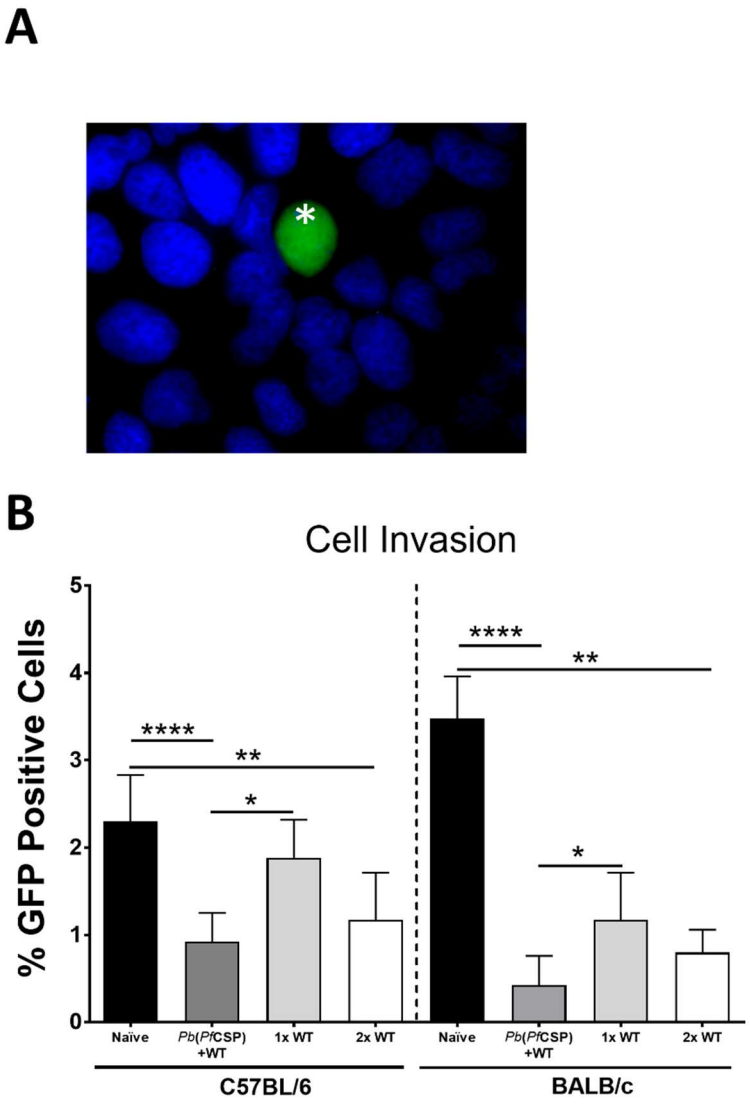

Figure 5.6. Immunisation with all schedules results in a reduction of EEFs in hepatocytes in vitro.

Serum from C57BL/6 and BALB/c mice was collected 28 days after vaccination. Vaccination schedules consisted of 10,000 γ-radiation attenuated sporozoites i.v. using WT *Pb* ANKA or transgenic *Pb*(*Pf*CSP) sporozoites. 1 vaccination with WT was compared with 2 WT vaccinations and a novel strategy of *Pb*(*Pf*CSP) followed by WT. Boost vaccinations were given 14 days after the primary vaccination. *Pb* ANKA sporozoites were isolated from infected female *Anopheles stephensi* mosquito salivary glands and incubated with pooled serum from each schedule or naïve for 40 minutes on ice. Sporozoites were cultured on Huh7 hepatocytes for 2 hours before being washed. After 48 hours of incubation, cells were permeabalised and stained FITC green for EEFs (*) and blue for nuclei (A). EEFs in an area of 0.8 cm^2 per well were counted for each condition and calculated as an invasion rate (%) as the number of EEFs as a percentage of the control with no serum (B). Results shown from two experiments with pooled serum in triplicate. Statistics performed using Kruskal-Wallis non-parametric t test followed by Dunn's multiple comparisons post-test.

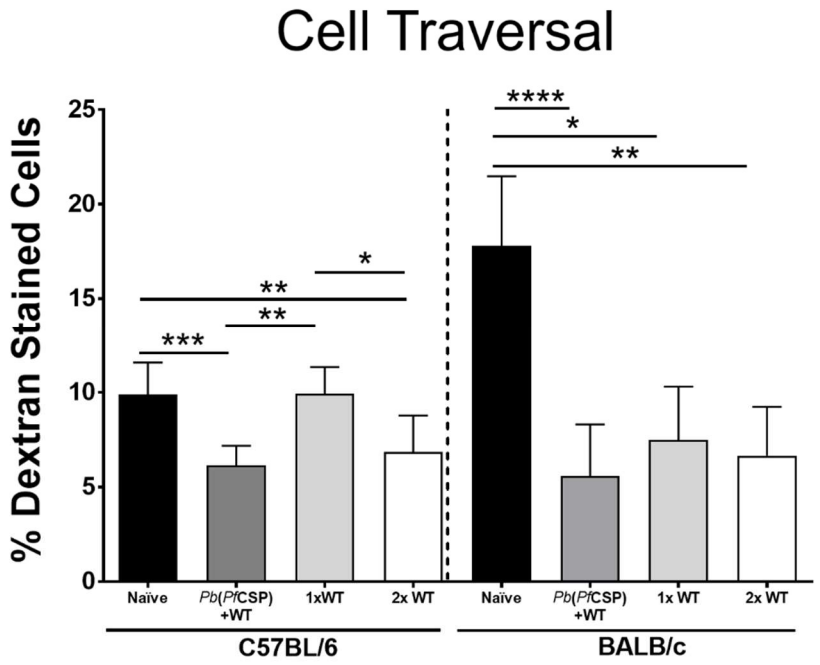

Figure 5.7. Cell traversal of *Pb* ANKA sporozoites through hepatocytes is reduced after exposure to serum from immunised mice.

Serum from C57BL/6 and BALB/c mice was collected 28 days after vaccination. Vaccination schedules consisted of 10,000 γ-radiation attenuated sporozoites i.v. using WT *Pb* ANKA or transgenic *Pb*(*Pf*CSP) sporozoites. 1 vaccination with WT was compared with 2 WT vaccinations and a novel strategy of *Pb*(*Pf*CSP) followed by WT. Boost vaccinations were given 14 days after the primary vaccination. *Pb* ANKA sporozoites were isolated from infected female *Anopheles stephensi* mosquito salivary glands and incubated with serum from each schedule or naïve for 40 minutes on ice. Sporozoites were cultured on Huh7 hepatocytes for 3 hours in the presence of fluorescent high molecular weight dextran. Hepatocytes that had been damaged by cell traversal were identified using flow cytometry. Results shown for two experiments with n=7 per group per experiment. Statistics performed using Kruskal-Wallis non-parametric t test followed by Dunn's multiple comparisons post-test.

The promising results shown so far confirm that my novel immunisation schedule successfully generates immune responses for immunisation with γ-radiation attenuated *Pb*(*Pf*CSP) and *Pb* ANKA. Additionally, these immunisations generate antibodies that recognise *Pb* ANKA sporozoites and are capable of functionally inhibiting cell traversal and EEF development. From these results I was confident that serum from these immunisations would be suitable for further investigation into non-CSP antibody antigens using microarray technology. I first generated a list of proteins

that are expressed in the sporozoite and liver stages of *Pb* ANKA development using the PlasmoDB online database. This resulted in 2977 genes needed to be synthesised as peptides 15 amino acids in length on the microarray chip. As antibody epitopes do not consist of more than 15 linear amino acids, the sequences that were synthesised allowed for an overlap of 11 amino acids from the previous oligomer. This allows for a 'sliding window' and if there is a true antibody epitope, antibodies would be expected to have affinities to more than one peptide, suggesting a region of antigenicity. This resulted in a total of 519,139 peptides being synthesized on a single chip for each immunisation condition. This was done as outlined in figure 5.8. First, alanine amino acids that have a photosensitive block are covalently bound to the microarray slide. Using photolithography, light directed at certain points on the slide removes the block and allows for the second amino acid to be added to some of the chains. This is repeated with each of the 21 amino acids until all peptides are a 2 amino acid chain. This process is repeated until all peptides are synthesized. The microarray slide is probed with the serum of interest and bound antibodies are determined using species specific secondary fluorescent antibodies. A fluorescent output for each peptide is detected and subsequently this can be visualized graphically.

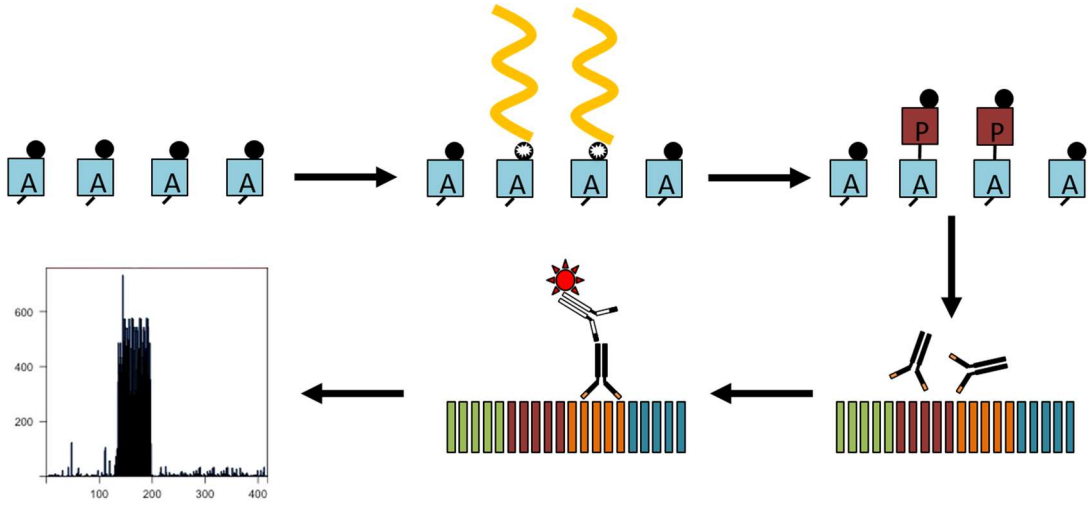

Figure 5.8. Schematic of the process of microarray chip synthesis and analysis.

First Alanine (A) amino acids are covalently bound to the microarray slide. Each A amino acid has a block that prevents the condensation reaction between amino acids, therefore preventing any unwanted polymerisation. Light is directed at the microarray chip, which degrades the block at certain points on the slide. This allows for a second amino acid to be added, leading to polymerisation at only specific points on the slide. This is repeated for each amino acid as required until all peptides are synthesised. The slide is probed with serum of interest, allowing for antibody binding to specific peptides. The slide is washed and any antibody binding is recognised by a secondary fluorescent antibody-specific for the species of origin for the serum of interest. Once fluorescence is measured, signals for each peptide can be put together to show potential regions of antigenicity for each protein included in the microarray.

In order to reduce any non-specific binding in the microarray experiment the microarray slides were first incubated with pooled naïve serum and for both experiments there was no positive detection of antibody binding to peptides (data not shown). After probing with serum from mice immunised with γ-radiation attenuated *Pb*(*Pf*CSP)+WT Pb ANKA or from mice immunised twice with *Pb* ANKA, most peptides elicited negligible antibody responses (Figure 5.9). It is probably not surprising that the majority of positive responses to epitopes are very low (Figure 5.9) due to the efficiency with which sporozoites can evade the immune response. With peptides that did elicit an antibody signal, there is a clear difference in the magnitude of responses between the two strains of mice. Pooled serum from immunised BALB/c mice show higher signals for more peptides compared to C57BL/6. This supports previous results shown here that BALB/c responses were consistently higher for ELISA and functional experiments.

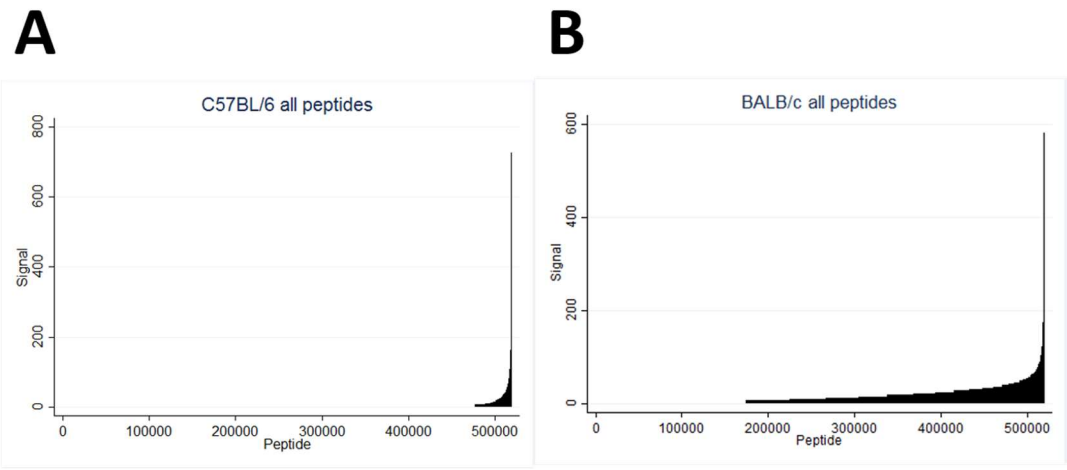

Figure 5.9. Representative output of microarray for C57BL/6 and BALB/c mice after *Pb*(*Pf*CSP) followed by *Pb* ANKA immunisation.

Serum from C57BL/6 and BALB/c mice was collected 28 days after final vaccination. Vaccination schedules consisted of 10,000 γ-radiation attenuated sporozoites i.v. using *Pb*(*Pf*CSP) followed by *Pb* ANKA. Boost vaccinations were given 14 days after the primary vaccination. Pooled serum was used to probe a microarray consisting of 519,139 peptides, all 15 amino acids in length, which covered the *Pb* ANKA sporozoite and liver stage proteome. Each sequential peptide had an 11 amino acid overlap with the previous peptide sequence. The microarray output was measured by a fluorescent signal produced from secondary mouse-specific antibodies. Graphs show the total output for each peptide for each strain with peptides ordered from the lowest signal to the highest. Data is representative for two experiments using pooled serum from 5-10 mice per group.

The use of pooled serum from mice immunised twice with γ-radiation attenuated *Pb* ANKA sporozoites was to validate the microarray technique. Using this immunisation schedule I hypothesised that there would be clear antibody responses to previously validated sporozoite and liver stage antigens. Microarray results for two such antigens are shown in figure 5.10. As expected, antibody responses were observed for the repeat region of *Pb* CSP; however, in addition to this antibody responses are also seen for the previously validated antigen CelTOS[290].

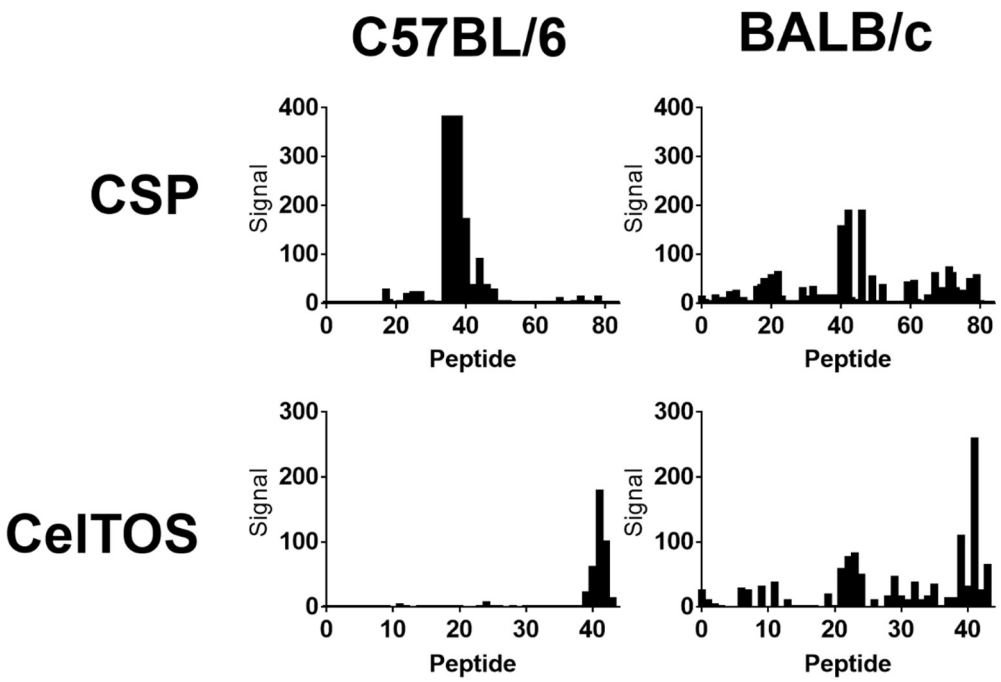

Figure 5.10. Validated antigens are recognised by antigens from mice immunised twice with Pb ANKA sporozoites using microarray technique.

Serum from C57BL/6 and BALB/c mice was collected 28 days after vaccination. Vaccination schedules consisted of two immunisations with 10,000 γ-radiation attenuated *Pb* ANKA sporozoites i.v. Boost vaccinations were given 14 days after the primary vaccination. Pooled serum was used to probe a microarray consisting of 519,139 peptides, all 15 amino acids in length, which covered the *Pb* ANKA sporozoite and liver stage proteome. Each sequential peptide had an 11 amino acid overlap with the previous peptide sequence. The microarray output was measured by a fluorescent signal produced from secondary mouse-specific antibodies. Graphs show the output for both mouse strains for two proteins that have previously been validated as antigens that generate functional antibody responses against *Plasmodium* sporozoites. Experiments were performed using pooled serum from 5-10 mice per group.

With these results it was possible to continue analysis of the microarray data to investigate any novel non-CSP antigens. Firstly though, the data was smoothed for each protein. This process uses one or more rules that are applied to the data in order to remove antibody signals that are less likely to be towards true epitopes. Some peptides elicited strong antibody responses; however, their flanking peptides did not. Although a true epitope could be in a single peptide, antibody responses to flanking peptides provides greater evidence that there is a region of antigenicity. As not all peptides could be further investigated, rules were applied to the data to preferentially rank peptides that were more likely to be epitopes. This approach has previously been used by the Nielsen group, who used similar rules to smooth data from a peptide microarray for *T. cruzi*[117].

In order to perform the smoothing, 4 rules were implemented. Firstly, a running median score was calculated for each peptide and its flanking peptides. If the middle peptide scores a high signal but its flanking peptides do not, the median score reflects this:

Signal	Peptide	Outcome
0	A	
21	B	0
0	C	

If; however, the flanking peptides have a signal but the central peptide does not, it can be assumed that these signals are not from the same antigenic region. If this is the case, the value returned is for the lowest signal score:

Signal	Peptide	Outcome
150	A	
0	B	0
89	C	

An important consideration in analysing the microarray data is that all peptides were analysed only once on the microarray. Therefore signals returned for repeat sequences are not for multiple peptides but from a single peptide on the microarray. If this is the case, the peptide before the repeat region and the peptide after the repeat region are considered and the median value is returned for the whole repeat region:

Signal	Peptide	Outcome
0	A	
212	B	30
212	B	30
212	B	30
212	B	30
30	C	

Another possibility is that a peptide is flanked by two peptides of the same sequence (i.e. the same peptide that was analysed only once). In this instance, a median score is calculated using other peptides that differ in sequence by the central peptide by 1 amino acid:

Signal	Peptide	Outcome
0	A	
204	B	0
0	A	

Signal	Peptide	New Outcome
204	B	
87	B^1	87
21	B^2	
48	B^3	

After applying these rules an additional filter was added to further increase the chance of identifying true regions of antigenicity. Amino acids have individual characteristics due to their varying structure and molecular formula, one important characteristic being their electrostatic charge. It is known that peptide sequences that have a high proportion of charged amino acids, even if they have a very low complexity, can show high antibody binding purely due to their charged nature[291]. As a result of this, it is possible that certain peptides would be given a high signal due to this single feature rather than due to an induced immune response from the immunisation schedule. In order to account for this, any sequence that had more that 50% aspartic acid (D) or glutamic acid (E) was not considered for further ranking. In addition, any sequence that had more than 3 consecutive D or E amino acids would also not be considered. Filtering for these two amino acids in particular was because these are both charged, hydrophilic amino acids that consistently appeared in high percentages of the top ranking peptides by their original signal. Although there is a possibility that antibody responses to these peptides are functional only a small number of peptides could be

further analysed and therefore filtering was used to increase the chances of finding novel, functional peptides. An example of the results after smoothing is shown in figure 5.11 using *Pb* ANKA CSP.

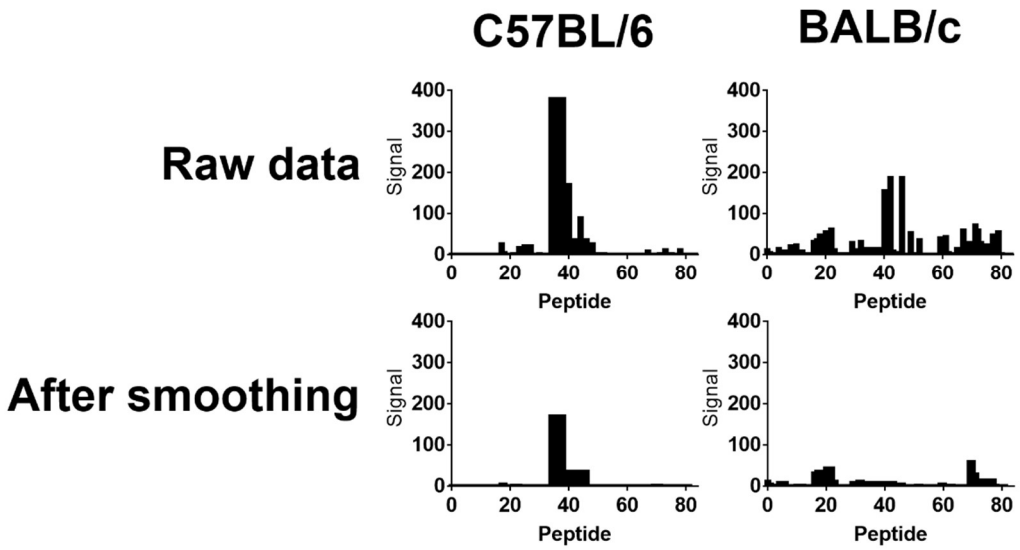

Figure 5.11. Example of smoothing raw microarray output

Serum from C57BL/6 and BALB/c mice was collected 28 days after vaccination. Vaccination schedules consisted of two immunisations with 10,000 γ-radiation attenuated *Pb* ANKA sporozoites i.v. Boost vaccinations were given 14 days after the primary vaccination. Pooled serum was used to probe a microarray consisting of 519,139 peptides, all 15 amino acids in length, which covered the *Pb* ANKA sporozoite and liver stage proteome. Each sequential peptide had an 11 amino acid overlap with the previous peptide sequence. The microarray output was measured by a fluorescent signal produced from secondary mouse-specific antibodies. Graphs show the original output for both mouse strains for *Pb* ANKA CSP before and after smoothing. Experiments were performed with pooled serum from 5-10 mice per group.

The microarray experiment was performed twice with pooled serum from two independent immunisation experiments. Previous research has been performed using the same microarray technique to show the experimental reproducibility when using the same serum samples[117]. I analysed the results from both experiments to determine the biological reproducibility and the strain specificity of antibody responses to *Plasmodium* sporozoite immunisation (Figure 5.12). By plotting the signal for C57BL/6 antibody results against BALB/c, I investigated the agreement between both strains for each experiment (Figure 5.12A-B). Using Pearson's correlation coefficient (PCC), there was a positive but weak correlation for experiment

1 (PCC=0.4949) and a moderate positive correlation for experiment 2 (PCC=0.5410). In addition, I measured the correlation for each strain between both experiments (Figure 5.12C-D). A moderate positive correlation was observed for both C57BL/6 (PCC=0.5120) and BALB/c (PCC=0.5208). It is promising that there is consistent positive correlation for these analyses; however, correlation is relatively low. This could be due to biological differences during immunisation e.g. viability of sporozoites at immunisation, or it could be a result of noise due to the large amount of peptides that were analysed, the majority of which will not induce functional antibody responses and therefore may have a more stochastic antibody-mediated response.

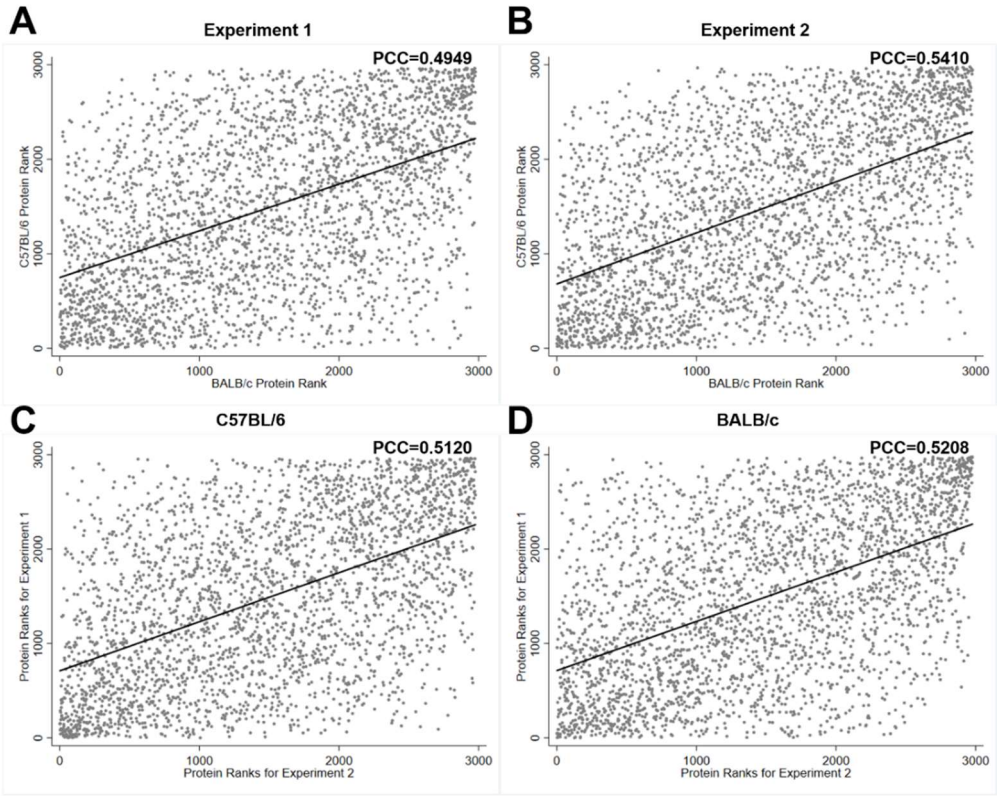

Figure 5.12. Correlation between C57BL/6 and BALB/c antibody responses to immunisation

Serum from C57BL/6 and BALB/c mice was collected 28 days after final vaccination. Vaccination schedules consisted of 10,000 γ-radiation attenuated sporozoites i.v. using *Pb*(*Pf*CSP) followed by *Pb* ANKA. Boost vaccinations were given 14 days after the primary vaccination. Pooled serum was used to probe a microarray consisting of 519,139 peptides, all 15 amino acids in length, which covered the *Pb* ANKA sporozoite and liver stage proteome. Each sequential peptide had an 11 amino acid overlap with the previous peptide sequence. The microarray output was measured by a fluorescent signal produced from secondary mouse-specific antibodies. Graphs show correlation between both mouse strains for experiment 1 and experiment 2 using pooled serum from 5-10 mice per group as well as correlation for each strain between experiments. Statistics performed using Pearson's Correlation Coefficient (PCC).

A small percentage of the total number of peptides generated strong signals in each microarray experiment. Using the protein rank after smoothing was applied to the data, the 15 top proteins were chosen for further analysis in order to maximise chances of identifying a true immunogenic region in a manageable number of candidate proteins. These proteins were considered to be the best candidates for novel antibody epitopes against *Pb* ANKA sporozoite and liver stages. As these antigens are under current investigation, they are presented here as numbered antigens 1-15. The decision was made based on the proteins that ranked highest in both experiments for both C57BL/6 and BALB/c. All proteins had published evidence of expression during the sporozoite and/or liver stages that was available from the PlasmoDB database. 65% of the top proteins showed evidence of a signal sequence when sequences were put through SignalP software (Center for Biological Sequence analysis [CBS]) and all proteins showed no homology with mouse (*mus musculus*) or human (*homo sapien*) proteomes. The top peptide for each protein was synthesized for ELISA investigation, with 2 peptides synthesized for antigen 3 due to the presence of two distinct regions of putative antigenicity. ELISA results are shown in figure 5.13; however, the majority of measured responses were not significantly different from naïve serum responses. Interestingly, antibody responses from immunised C57BL/6 mice against all peptides was not different from the naïve control but in contrast, BALB/c immunised responses were much more likely to be increased compared to naïve controls. Unfortunately, only two peptides showed a statistical increase in antibody responses by ELISA in immunised sera compared to naïve sera (one peptide for Antigen 3 and the peptide for Antigen 11).

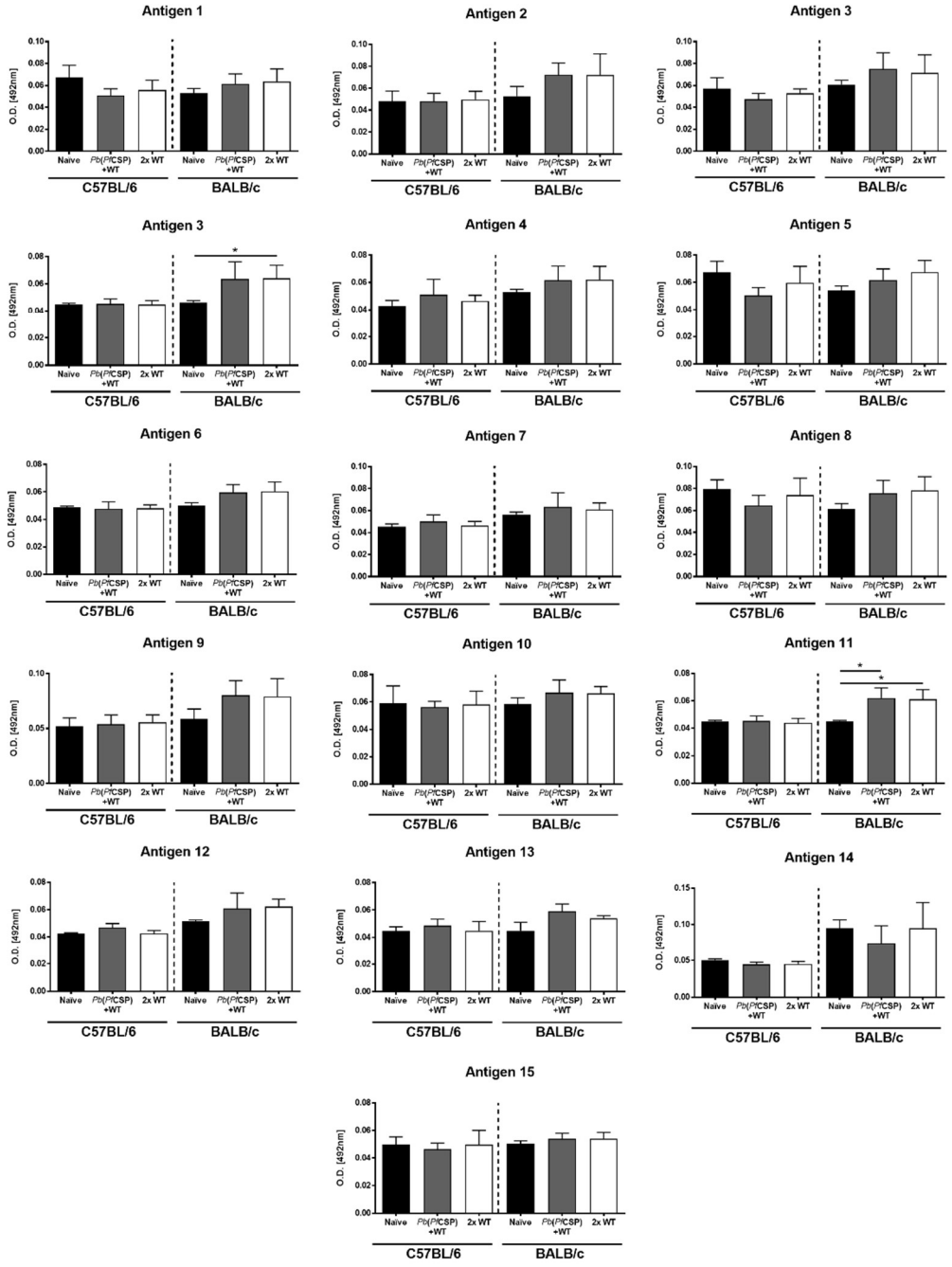

Figure 5.13. ELISA investigation of *Pb* ANKA putative antibody epitopes identified by microarray.

Serum from C57BL/6 and BALB/c mice was collected 28 days after final vaccination. Vaccination schedules consisted of 10,000 γ-radiation attenuated sporozoites i.v. using a novel strategy of *Pb*(*Pf*CSP)+WT *Pb* ANKA. Boost vaccinations were given 14 days after the primary vaccination. Antibody responses were measured against 15 putative epitopes of 15 amino acids in length by ELISA. Putative epitopes were identified by microarray. Pooled data from two experiments with pooled serum from 7 mice per group. Statistics were performed using Kruskal-Wallis non-parametric t test followed by Dunn's multiple comparisons test.

5.4 Discussion

The generation of long-lived, specific antibody responses against infection is an attractive avenue of investigation for vaccinology. This is due to the efficacy with which antibodies can recognise and respond to free antigen and the ease with which B cells can be stimulated relative to the induction of T cell responses. With regard to malaria, the parasite spends most of its life in the vertebrate host inside host cells. Therefore, there are only two opportunities for antibodies to neutralise the parasite. These are early during infection when sporozoites are locating to the liver and infecting hepatocytes and during blood stage infection when merozoites rupture their host RBC and move freely through the blood system before infecting a new RBC. Antibody responses towards the blood stage merozoites have been researched to a greater extent than liver stages, particularly due to the amount of antigen available during blood stage infection to induce antibody responses. A difficulty with inducing antibody responses to the sporozoite is that there is a relatively short window of minutes before the parasite has sequestered in the liver; however, it has been shown that antibodies are capable of functionally neutralising sporozoite invasion[79]. Another difficulty is that the sporozoite surface is coated with a high density of CSP. This would not necessarily be a problem if antibody responses to CSP alone were sufficient to protect from malaria infection in humans. Early investigations of antibody responses to CSP were very promising in mice, offering complete protection when administered[268] and later shown to be protective with CSP immunisation[292]. This has led to the first malaria vaccine RTS, S, which uses epitopes from CSP to stimulate B and T cell responses. Unfortunately, Phase 3 trials show that the efficacy of this vaccine is lower than what was expected after non-human animal investigations. It is promising that antibodies from RTS, S vaccinations do have a protective impact on malaria infection[293]; however, responses to CSP alone appear to not be sufficient in a non-laboratory setting. Therefore, knowing that antibodies against liver stage infection can be protective but responses against CSP alone does not confer particularly good efficacy as a vaccine, there appears to be a clear question of whether there are more immunogenic antigens that could be used and whether they would facilitate a CSP vaccine. As part of this investigation, I attempted to answer the first part of this question through the use of a novel immunisation schedule in a mouse model.

In order to investigate novel non-CSP antibody antigens I first designed a novel immunisation schedule to promote antibody responses to non-CSP proteins. CSP is a highly immunodominant protein on the sporozoite and as such, it can dampen antibody responses to other immunogenic antigens. To avoid this, immunisations were performed using a transgenic *Pb* ANKA strain that expressed *Pf* CSP rather than *Pb* ANKA CSP. An initial immunisation with WT, followed by a booster immunisation with the transgenic *Pb* ANKA strain would preferentially boost non-CSP antibody responses. As this is a new schedule it was crucial that I validated it by investigating antibody recognition of known antigens and functional responses. As expected, I observed antibody recognition of *Pb* ANKA CSP and *Pf* CSP after both immunisations (Figures 5.3 and 5.4 respectively) and further showed that serum from immunised mice recognised *Pb* ANKA sporozoites (Figure 5.5). In these experiments BALB/c serum consistently gave higher antibody responses compared to C57BL/6 serum. As BALB/c mice are more resistant to *Pb* ANKA infection, being refractory to ECM, these results are probably due to an immunological variance between the two mouse strains.

Further to purely recognising *Pb* ANKA CSP and *Pf* CSP, it was crucial that my immunisations elicited functional antibody responses. It is particularly interesting that antibody neutralisation of sporozoites, preventing EEF development in vitro, was similar between my immunisation schedule and 2x WT *Pb* ANKA immunisations for both BALB/c and C57BL/6 serum (Figure 5.6). Also, this appeared to be the case for my investigation into the inhibition of cell traversal (Figure 5.7). This might suggest that the comparable neutralisation was due to additional non-CSP-specific antibodies.

The use of microarray technology has previously been used to investigate novel antibody antigenic determinants for infectious disease[117,294,295]. This offers a versatile, high-density technology for the simultaneous investigation of hundreds of thousands of antigenic candidates for vaccine, diagnostic and therapeutic discovery. By using this technology I was able to investigate 519,139 peptides that covered the entire sporozoite and liver stage proteome. As expected, there was clear antibody recognition of CSP and another previously validated liver stage antigen CelTOS (Figure 5.10), but this quantity of data raises problems with analysis in order to accurately identify true antibody epitopes. In order to address this problem I incorporated a smoothing strategy, similar to the one used by Carmona et al.[117] and

described in detail earlier in this chapter. This increased the probability that the highest ranked peptides were part of a region of antigenicity and had sequences of higher complexity. Unfortunately, due to the nature of the results obtained for all peptides, it was not possible to determine a threshold using finite mixture model statistics. Because of this, 15 proteins that consistently ranked highly in both experiments between both mouse strains were chosen for further investigation and validation. It is interesting that several of the chosen peptides from these proteins did not show a significant antibody response with the same pooled mouse sera when ELISA was performed. This could be due to several factors including the limit of detection for ELISA and microarray techniques, differences in peptide presentation to antibody as peptide adsorption on the ELISA plate is stochastic, or perhaps as a result of differences in peptide synthesis. From all the ELISA results, two antigens appear to be the most promising candidates for further investigation as they showed increased antibody responses with immunisation in both the novel and 2x *Pb* ANKA immunisation schedules. For these two proteins further investigation would be particularly interesting. Synthesis of these proteins would allow for further study via protein immunisation of mice. Showing that protein immunisation using these candidates leads to functional inhibition of sporozoite invasion in vitro and protection in vivo would provide very exciting and supportive evidence for non-CSP antibody vaccine targets.

5.5 Conclusion

Research towards novel vaccines against liver stage malaria requires the investigation of novel antigenic determinants. Antibodies have been shown to be protective against liver stage malaria; however, there is a paucity of information regarding non-CSP antibody targets that could be used for future vaccines. In this study, I have used a novel immunisation schedule to promote non-CSP antibody responses and investigated them using high throughput microarray technology. Results show promising candidates that should be investigated further towards confirmation of their eligibility for vaccine research.

5.6 Supplementary Data

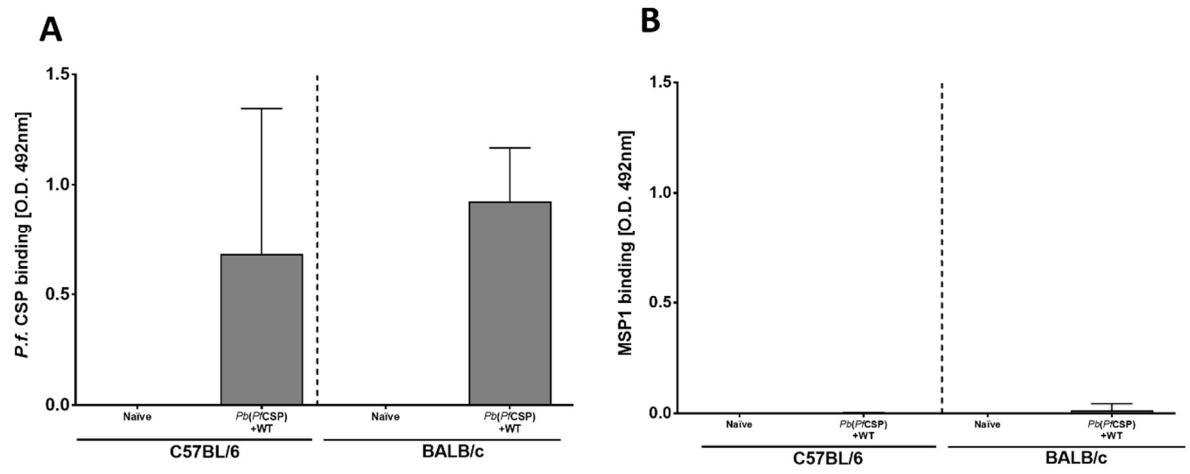

Figure 5.S1. Antibody recognition of recombinant *Pf* CSP is not due to the generation of *E. coli*-specific antibody

Serum from C57BL/6 and BALB/c mice was collected 28 days after vaccination. Vaccination schedules consisted of 10,000 γ-radiation attenuated sporozoites i.v. using transgenic *Pb*(*Pf*CSP) followed by WT *Pb* ANKA. Boost vaccinations were given 14 days after the primary vaccination. Antibody responses were measured against recombinant *Pf* CSP (A) and MSP1-19 (B) by ELISA. Data from two experiments with 5-10 mice per group. Statistics were performed using Mann-Whitney t test.

6 | Discussion

6.1 Summary and significance of findings

The majority of the work presented in this thesis investigates how $CD8^+$ T cell responses are regulated during malaria infection. In **chapter 2** I used antibody-mediated blockade to investigate co-inhibitory regulatory molecules CTLA-4 and PD-1 and their respective signalling pathways during exposure to pre-erythrocytic infection in a mouse model of malaria. By immunising C57BL/6 mice with a non-protective single dose of γ-radiation attenuated *Pb* ANKA sporozoites, I attempted to discern the possibility that CTLA-4, PD-1/PD-L1 and PD-1/PD-L2 signalling negatively regulate $CD8^+$ T cell activation upon attenuated sporozoite exposure, therefore preventing sterile immunity. Antibody-mediated blockade of CTLA-4 resulted in a significant increase in antigen experienced $CD8^+$ T cells that produced IFNγ upon stimulation with *Pb* sporozoite antigens as measured by flow cytometry, whereas blockade of PD-L1 or PD-L2 did not. On a functional level, blockade of CTLA-4 with a single γ-radiation attenuated *Pb* ANKA sporozoite immunisation elicited sterile protection against *Pb* ANKA sporozoite challenge; however, this was not the case with blockade of PD-L1 as challenge resulted in patent parasitaemia in all mice. Protection via CTLA-4 blockade with *Pb* ANKA sporozoite immunisation was due to $CD4^+$ and $CD8^+$ T cells and the cytokine IFNγ as depletion of any of these abrogated protection from challenge. The level of protection with CTLA-4 blockade concurrently with a non-protective *Pb* ANKA immunisation appears to wane over time. When challenged 45 days after immunisation and blockade, the majority of mice succumb to patent infection; however, there is a reduction in parasitaemia and a delay in patency compared to controls. Taken together, this is a novel investigation into the mechanisms of $CD8^+$ T cell regulation during pre-erythrocytic malaria, an area of research that is currently lacking. Further to this, it is a proof of principle that a non-protective pre-erythrocytic sporozoite vaccine can be significantly increased in efficacy through concurrent immune modulation.

In **chapter 3** I continued my investigation of $CD8^+$ T cell regulation during pre-erythrocytic malaria infection, this time by focusing on two cytokines that are known to have immunoregulatory functions. The roles of IL-27 and IL-10 have not been investigated with regard to their regulation of $CD8^+$ T cell responses to whole sporozoite exposure in a mouse model. Using knock-out mice that do not express the

wsx-1 gene and therefore are deficient in the IL-27R, I gave a non-protective immunisation with γ-radiation attenuated *Pb* ANKA sporozoites. Compared to C57BL/6 controls, WSX-1$^{-/-}$ mice did indeed show a trend towards more antigen experienced sporozoite-specific CD8 T^{+} cells upon exposure to antigen; however, this only achieved significance with S20 peptide re-stimulation and significance was lost if re-stimulation was delayed until 45 days after immunisation. Despite the trend, challenge of WSX-1$^{-/-}$ mice with *Pb* ANKA 14 or 45 days after immunisation resulted in very similar fold reductions in parasite liver load to C57BL/6 controls that are not protected from ECM. In the previous chapter, a reduction of over 3 log was required before protection could be seen with CTLA-4 blockade concurrently with a single *Pb* ANKA sporozoite immunisation. In order to investigate IL-10 signalling, I used antibody blockade similarly to chapter 2. Using this method my results showed that blockade of IL-10R with a non-protective *Pb* ANKA sporozoite immunisation did not lead to an increase in sporozoite antigen-specific CD8^{+} T cells. Additionally, it does not lead to any decrease in parasite liver load upon challenge with *Pb* ANKA sporozoites. Although IL-27R and IL-10R signalling do not appear to negatively regulate CD8^{+} T cell activation with *Pb* sporozoite exposure in my mouse model, it does highlight that CD8^{+} T cell regulatory mechanisms are different between pre-erythrocytic and blood stage infection and should be thought of as such.

Continuing with regulation but moving into blood stage malaria infection, **chapter 4** investigates the role of IL-10R regulatory signalling in resistance to acute immune pathology. Antibody blockade of IL-10R in normally ECM resistant BALB/c mice resulted in an increase in leukocyte and CD8^{+} T cell infiltration into the brain, increased brain haemorrhage and increased IFNγ and CD8^{+} T cell activation. From these results, it appears that IL-10R signalling can indeed regulate pathogenic CD8^{+} T cell responses in an ECM resistant mouse model of blood stage malaria infection. It is understood that there are subtle variations in how the adaptive immune system responds to blood stage malaria infection through previous work on various mouse models[93]. As human malaria blood stage infection can also lead to a multitude of varying pathogenic or non-pathogenic outcomes, it is important for us to better understand the specificities of these varying responses. Chapter 4 contributes to our understanding of how inhibitory pathways can significantly influence CD8^{+} T cell activation to the extent that, in certain conditions a single pathway can completely protect from immune-mediated pathology.

My final data chapter is not concerned with T cell regulation, rather it focuses on the antibody response to pre-erythrocytic malaria in a mouse model. There is a paucity in information concerning what antigens (other than CSP) in the pre-erythrocytic stage generate functional antibody responses that may contribute to protection. In **chapter 5** I used a novel immunisation schedule in a mouse model to maximise the potential for identifying non-CSP epitopes. Immunising once with γ-radiation attenuated transgenic *Pb* ANKA that expresses *Pf* CSP rather than *Pb* ANKA CSP and boosting with WT *Pb* ANKA meant that all non-CSP antigens were boosted, whereas CSP was not. As microarray technology now allows for incredibly high-density peptide microarrays, this was used to simultaneously investigate all potential antibody antigenic determinants in *Pb* ANKA pre-erythrocytic infection of BALB/c and C57BL/6 mice. Due to the incredible amount of data generated and the low to absent antibody binding to the majority of peptides, a threshold for positive and negative antibody responses was not identified. Instead, by ranking peptides and adopting a smoothing strategy to remove peptides not from an antigenic region, a selection of top candidates could be investigated. As expected, previously validated antibody antigens were ranked very highly. Additionally, there were several antigens that warranted further investigation due to their rank as well as other properties such as the presence of a signal region. Performing ELISA with a selection of putative epitopes resulted in only two candidates having a significant antibody response in immunised sera compared to control sera. Due to the moderate agreement in antibody responses between both microarray experiments, these peptides were expected to generate an increased antibody response in ELISA. The discrepancy between these two techniques could be due to differences between them such as synthesis of peptides, the way in which peptides were presented to antibody or the sensitivity of each technique. Regardless, these results provide evidence for two novel putative antibody epitopes that warrants further investigation into their functionality and potential as vaccine candidates.

6.2 Opportunities for further research

My investigations into the regulation of $CD8^+$ T cells during pre-erythrocytic malaria infection in chapters 2 and 3 have aimed to increase our understanding of an as yet poorly researched facet of malaria infection. Antibody-mediated blockade of CTLA-4 with a non-protective γ-radiation attenuated *Pb* ANKA sporozoite immunisation elicited sterile immunity in C57BL/6 mice. This is a proof of concept that immune

regulation of T cell activation can influence protective T cell responses to whole sporozoite immunisation. Therefore, broadening our understanding of this could contribute to better malaria vaccine design. It is interesting that blockade of PD-L1 with immunisation did not lead to an increase in $CD8^+$ T cell activation or protection from sporozoite challenge. A potential avenue of research in this regard could be blockade of PD-L1 with blockade of another regulatory molecule. Previous research in blood stage malaria has shown that concurrent blockade of PD-L1 and LAG3 leads to an improvement in parasitaemia control with non-lethal infection of outbred Swiss Webster or C576L/6 with *Py* or *P. chabaudi* respectively[105]. The synergistic nature of PD-1 and LAG3 blockade has already been described in an investigation into immune responses to tumours in a mouse model by Woo et al.[296]. More evidence from cancer studies has shown that PD-1 blockade and OX40 activation can also lead to a synergistic protection against a mouse model of ovarian cancer, which is dependent on T cell activation[297]. Therefore, there are also opportunities for investigating concurrent blockade of co-inhibitory molecules and excitation of co-stimulatory molecules with regard to $CD8^+$ T cell regulation during whole sporozoite immunisation.

In chapter 3 I did not observe any decrease in parasite liver load if a challenge of *Pb* ANKA sporozoites was given following a non-protective γ-radiation attenuated *Pb* ANKA sporozoite immunisation in the absence of IL-27R or IL-10R signalling. This is in itself quite interesting as both pathways have been implicated in T cell regulation in blood stage infection and pathology. To continue this line of research it may be interesting to investigate other regulatory cytokines such as TGFβ, which has also been investigated with regard to regulation during blood stage malaria[298,299]. TGFβ negatively regulates $CD8^+$ as well as $CD4^+$ T cell responses[300]; however, its role in regulation of $CD8^+$ T cells during pre-erythrocytic infection is as yet unknown.

A particularly interesting avenue of future research regarding my work in chapter 4 would be towards a greater understanding of the protective capacity of antigens identified using high-density peptide microarrays. My work has resulted in at least two proteins that are expressed during the pre-erythrocytic stage of *Pb* that are recognised by antibodies in both a microarray and ELISA using C57BL/6 and BALB/c sera from mice immunised with γ-radiation attenuated *Pb*(*Pf*CSP) followed by *Pb* ANKA sporozoites. In order to better understand the functional capacity of antibodies

that recognise these antigens, it would be interesting to synthesise these proteins for use in a protein immunisation experiment. In this way, there is the exciting possibility that immunisation with these novel antigens could elicit a level of functional protective immunity. This would give further evidence to support the investigation of these antigens with regard to their potential as malaria vaccine candidates. Additionally, it would allow for the investigation of any elicited protection in two mouse models of malaria infection, BALB/c and C57BL/6. If indeed there does appear to be a functional protection from antibodies generated towards these antigens, another important investigation would be to identify epitopes. As regions of antigenicity have been identified using high-density peptide microarrays as discussed in chapter 4, the salient epitope sequences could be identified using Alanine scans. In this way, replacing amino acids within the regions of antigenicity with the unreactive Alanine in a sequential manner could result in the true epitopes that generate functional antibodies.

The work presented in this thesis offers some insight into how $CD8^+$ T cells are regulated during exposure to a non-protective attenuated *Pb* ANKA sporozoite immunisation in a mouse model of ECM. Further to this, the regulation of $CD8^+$ T cells during blood stage infection and its relation to immune-mediated pathology has also been investigated. These studies attempt to increase our understanding of $CD8^+$ T cell regulation in mouse models of malaria; however, this understanding is far from complete. Further investigation is particularly important to allow for, among other things, better vaccine design. My final data chapter also contributes to research towards better malaria vaccines through its investigation of non-CSP antibody antigenic determinants in mouse models. Although this offers some promising results, further work is required in order to fully understand whether the candidates identified might also contribute towards better future malaria vaccine design.

Bibliography

1. Health Organization, W. World Malaria Report 2016. at <http://apps.who.int/iris/bitstream/10665/252038/1/9789241511711-eng.pdf?ua=1>

2. Gallup, J. L. & Sachs, J. D. The Economic Burden of Malaria. (2001).

3. Leighton, C. *et al.* ECONOMIC IMPACTS OF MALARIA IN KENYA AND NIGERIA in collaboration with Vector Biology Control Project, Medical Services Corporation International KENYA RESEARCH TEAM. (1993).

4. Sachs, J. & Malaney, P. The economic and social burden of malaria. *Nature* **415,** 680–685 (2002).

5. Nur, E. T. The impact of malaria on labour use and efficiency in the Sudan. *Soc. Sci. Med.* **37,** 1115–9 (1993).

6. Rodríguez-Morales, A. J. *et al.* Venezuela's failure in malaria control. *Lancet* **384,** 663–664 (2014).

7. Health Organization, W. World Malaria Report 2015.

8. Mendis, K., Sina, B. J., Marchesini, P. & Carter, R. The neglected burden of Plasmodium vivax malaria. *Am. J. Trop. Med. Hyg.* **64,** 97–106

9. Cox-Singh, J. *et al.* Plasmodium knowlesi malaria in humans is widely distributed and potentially life threatening. *Clin. Infect. Dis.* **46,** 165–71 (2008).

10. Noedl, H. *et al.* Evidence of artemisinin-resistant malaria in western Cambodia. *N. Engl. J. Med.* **359,** 2619–20 (2008).

11. Peters, W. Chemotherapy and drug resistance in malaria. 2nd edition. Vols 1 and 2continued. *Chemotherapy and drug resistance in malaria. 2nd edition. Vols 1 and 2continued.* (1987).

12. Dondorp, A. M. *et al.* Artemisinin resistance in Plasmodium falciparum malaria. *N. Engl. J. Med.* **361,** 455–67 (2009).

13. Rosner, D. & Markowitz, G. Persistent pollutants: A brief history of the discovery of the widespread toxicity of chlorinated hydrocarbons. *Environ. Res.* **120,** 126–133 (2013).

14. Alonso, P. L. *et al.* The effect of insecticide-treated bed nets on mortality of Gambian children. *Lancet* **337,** 1499–502 (1991).

15. Frischknecht, F. *et al.* Imaging movement of malaria parasites during transmission by Anopheles mosquitoes. *Cell. Microbiol.* **6,** 687–694 (2004).

16. Rosenberg, R., Wirtz, R. A., Schneider, I. & Burge, R. An estimation of the number of malaria sporozoites ejected by a feeding mosquito. *Trans. R. Soc. Trop. Med. Hyg.* **84,** 209–12

17. Vanderberg, J. P. Plasmodium berghei: quantitation of sporozoites injected by mosquitoes feeding on a rodent host. *Exp. Parasitol.* **42,** 169–81 (1977).

18. Medica, D. L. & Sinnis, P. Quantitative dynamics of Plasmodium yoelii sporozoite transmission by infected anopheline mosquitoes. *Infect. Immun.* **73,** 4363–9 (2005).

19. Vanderberg, J. P. & Frevert, U. Intravital microscopy demonstrating antibody-mediated immobilisation of Plasmodium berghei sporozoites injected into skin

by mosquitoes. *Int. J. Parasitol.* **34,** 991–6 (2004).

20. Amino, R. *et al.* Quantitative imaging of Plasmodium transmission from mosquito to mammal. *Nat. Med.* **12,** 220–4 (2006).

21. Langer, R. C. *et al.* Micronemal transport of Plasmodium ookinete chitinases to the electron-dense area of the apical complex for extracellular secretion. *Infect. Immun.* **68,** 6461–5 (2000).

22. Münter, S. *et al.* Plasmodium Sporozoite Motility Is Modulated by the Turnover of Discrete Adhesion Sites. *Cell Host Microbe* **6,** 551–562 (2009).

23. Sheth, K. & Bankey, P. The liver as an immune organ. *Curr. Opin. Crit. Care* **7,** 99–104 (2001).

24. Shin, S. C., Vanderberg, J. P. & Terzakis, J. A. Direct infection of hepatocytes by sporozoites of Plasmodium berghei. *J. Protozool.* **29,** 448–54 (1982).

25. Stewart, M. J. & Vanderberg, J. P. Malaria sporozoites release circumsporozoite protein from their apical end and translocate it along their surface. *J. Protozool.* **38,** 411–21

26. Lyon, M., Deakin, J. A. & Gallagher, J. T. Liver heparan sulfate structure. A novel molecular design. *J. Biol. Chem.* **269,** 11208–15 (1994).

27. Cerami, C. *et al.* The basolateral domain of the hepatocyte plasma membrane bears receptors for the circumsporozoite protein of plasmodium falciparum sporozoites. *Cell* **70,** 1021–1033 (2014).

28. Francia, M. E. & Striepen, B. Cell division in apicomplexan parasites. *Nat. Rev. Microbiol.* **12,** 125–136 (2014).

29. Keeley, A. & Soldati, D. The glideosome: a molecular machine powering motility and host-cell invasion by Apicomplexa. *Trends Cell Biol.* **14,** 528–32 (2004).

30. Smalley, M. E. & Sinden, R. E. Plasmodium falciparum gametocytes: their longevity and infectivity. *Parasitology* **74,** 1–8 (1977).

31. Bousema, T. *et al.* Revisiting the circulation time of Plasmodium falciparum gametocytes: molecular detection methods to estimate the duration of gametocyte carriage and the effect of gametocytocidal drugs. *Malar. J.* **9,** 136 (2010).

32. Billker, O., Shaw, M. K., Margos, G. & Sinden, R. E. The roles of temperature, pH and mosquito factors as triggers of male and female gametogenesis of Plasmodium berghei in vitro. *Parasitology* 1–7 (1997). at <http://www.ncbi.nlm.nih.gov/pubmed/9280891>

33. Garcia, G. E., Wirtz, R. A., Barr, J. R., Woolfitt, A. & Rosenberg, R. Xanthurenic acid induces gametogenesis in Plasmodium, the malaria parasite. *J. Biol. Chem.* **273,** 12003–5 (1998).

34. Kawamoto, F., Alejo-Blanco, R., Fleck, S. L. & Sinden, R. E. Plasmodium berghei: Ionic regulation and the induction of gametogenesis. *Exp. Parasitol.* **72,** 33–42 (1991).

35. Sidjanski, S. P., Vanderberg, J. P. & Sinnis, P. Anopheles stephensi salivary glands bear receptors for region I of the circumsporozoite protein of Plasmodium falciparum. *Mol. Biochem. Parasitol.* **90,** 33–41 (1997).

36. Bousema, T. & Drakeley, C. Epidemiology and infectivity of Plasmodium falciparum and Plasmodium vivax gametocytes in relation to malaria control and elimination. *Clin. Microbiol. Rev.* **24,** 377–410 (2011).

37. Cotter, C. *et al.* The changing epidemiology of malaria elimination: new strategies for new challenges. *Lancet* **382,** 900–11 (2013).

38. Tulloch, J., David, B., Newman, R. D. & Meek, S. Artemisinin-resistant malaria in the Asia-Pacific region. *Lancet* **381,** e16-7 (2013).

39. Ranson, H. *et al.* Pyrethroid resistance in African anopheline mosquitoes: what are the implications for malaria control? *Trends Parasitol.* **27,** 91–98 (2014).

40. Nussenzweig, R. S., Vanderberg, J., Most, H. & Orton, C. Protective immunity produced by the injection of x-irradiated sporozoites of plasmodium berghei. *Nature* **216,** 160–162 (1967).

41. Romero, P. *et al.* Cloned cytotoxic T cells recognize an epitope in the circumsporozoite protein and protect against malaria. *Nature* **341,** 323–6 (1989).

42. Weiss, W. R. & Jiang, C. G. Protective CD8+ T lymphocytes in Primates Immunized with Malaria Sporozoites. *PLoS One* **7,** e31247 (2012).

43. Clyde, D. F., McCarthy, V. C., Miller, R. M. & Hornick, R. B. Specificity of protection of man immunized against sporozoite-induced falciparum malaria. *Am. J. Med. Sci.* **266,** 398–403 (1973).

44. Hoffman, S. L. *et al.* Protection of Humans against Malaria by Immunization with Radiation-Attenuated *Plasmodium falciparum* Sporozoites. *J. Infect. Dis.* **185,** 1155–1164 (2002).

45. Epstein, J. E. *et al.* Live attenuated malaria vaccine designed to protect through hepatic $CD8^+$ T cell immunity. *Science* **334,** 475–80 (2011).

46. Mellouk, S., Lunel, F., Sedegah, M., Beaudoin, R.-L. & Druilhe, P. Protection against malaria induced by irradiated sporozoites. *The Lancet* **335,** (1990).

47. Hall, N. *et al.* Sequence of Plasmodium falciparum chromosomes 1, 3–9 and 13. *Nature* **419,** 527–531 (2002).

48. Gardner, M. J. *et al.* Sequence of Plasmodium falciparum chromosomes 2, 10, 11 and 14. *Nature* **419,** 531–534 (2002).

49. Hyman, R. W. *et al.* Sequence of Plasmodium falciparum chromosome 12. *Nature* **419,** 534–7 (2002).

50. Hall, N. *et al.* A comprehensive survey of the Plasmodium life cycle by genomic, transcriptomic, and proteomic analyses. *Science* **307,** 82–6 (2005).

51. Mueller, A.-K., Labaied, M., Kappe, S. H. I. & Matuschewski, K. Genetically modified Plasmodium parasites as a protective experimental malaria vaccine. *Nature* **433,** 164–7 (2005).

52. van Dijk, M. R. *et al.* Genetically attenuated, P36p-deficient malarial sporozoites induce protective immunity and apoptosis of infected liver cells. *Proc. Natl. Acad. Sci. U. S. A.* **102,** 12194–9 (2005).

53. Vaughan, A. M. *et al.* Type II fatty acid synthesis is essential only for malaria parasite late liver stage development. *Cell. Microbiol.* **11,** 506–20 (2009).

54. Mikolajczak, S. A. *et al.* A Next-generation Genetically Attenuated Plasmodium falciparum Parasite Created by Triple Gene Deletion. *Mol. Ther.* **22,** 1707–15 (2014).

55. Belnoue, E. *et al.* Vaccination with live Plasmodium yoelii blood stage parasites under chloroquine cover induces cross-stage immunity against malaria liver stage. *J. Immunol.* **181,** 8552–8 (2008).

56. Ewer, K. J. *et al.* Protective CD8+ T-cell immunity to human malaria induced by chimpanzee adenovirus-MVA immunisation. *Nat. Commun.* **4,** 2836 (2013).

57. Schofield, L. *et al.* Gamma interferon, CD8+ T cells and antibodies required for immunity to malaria sporozoites. *Nature* **330,** 664–6

58. Weiss, W. R., Sedegah, M., Beaudoin, R. L., Miller, L. H. & Good, M. F. CD8+ T cells (cytotoxic/suppressors) are required for protection in mice immunized with malaria sporozoites. *Proc. Natl. Acad. Sci. U. S. A.* **85,** 573–6 (1988).

59. Schmidt, N. W., Butler, N. S., Badovinac, V. P. & Harty, J. T. Extreme CD8 T Cell Requirements for Anti-Malarial Liver-Stage Immunity following Immunization with Radiation Attenuated Sporozoites. *PLoS Pathog.* **6,** e1000998 (2010).

60. Seguin, M. C. *et al.* Induction of nitric oxide synthase protects against malaria in mice exposed to irradiated Plasmodium berghei infected mosquitoes: involvement of interferon gamma and CD8+ T cells. *J. Exp. Med.* **180,** 353–8 (1994).

61. Rodrigues, M. M. *et al.* CD8+ cytolytic T cell clones derived against the Plasmodium yoelii circumsporozoite protein protect against malaria. *Int. Immunol.* **3,** 579–85 (1991).

62. Van Braeckel-Budimir, N. & Harty, J. T. CD8 T-cell-mediated protection against liver-stage malaria: lessons from a mouse model. *Front. Microbiol.* **5,** 272 (2014).

63. Schmidt, N. W. *et al.* Memory CD8 T cell responses exceeding a large but definable threshold provide long-term immunity to malaria. *Proc. Natl. Acad. Sci. U. S. A.* **105,** 14017–22 (2008).

64. Butler, N. S., Schmidt, N. W. & Harty, J. T. Differential effector pathways regulate memory CD8 T cell immunity against Plasmodium berghei versus P. yoelii sporozoites. *J. Immunol.* **184,** 2528–38 (2010).

65. Arun Kumar, K. *et al.* The circumsporozoite protein is an immunodominant protective antigen in irradiated sporozoites. *Nature* **444,** 937–940 (2006).

66. Hafalla, J. C. R. *et al.* Identification of Targets of CD8+ T Cell Responses to Malaria Liver Stages by Genome-wide Epitope Profiling. *PLoS Pathog.* **9,** (2013).

67. Robinson, M. W., Harmon, C. & O'Farrelly, C. Liver immunology and its role in inflammation and homeostasis. *Cell. Mol. Immunol.* **13,** 267–276 (2016).

68. Bamboat, Z. M. *et al.* Human Liver Dendritic Cells Promote T Cell Hyporesponsiveness. *J. Immunol.* **182,** 1901–1911 (2009).

69. Knolle, P. A. *et al.* IL-10 down-regulates T cell activation by antigen-

presenting liver sinusoidal endothelial cells through decreased antigen uptake via the mannose receptor and lowered surface expression of accessory molecules. *Clin. Exp. Immunol.* **114,** 427–33 (1998).

70. Wei, H.-X. *et al.* CD4+CD25+ Foxp3+ Regulatory T Cells Protect against T Cell-Mediated Fulminant Hepatitis in a TGF-β-Dependent Manner in Mice. *J. Immunol.* **181,** (2008).

71. Fernandez-Ruiz, D. *et al.* Liver-Resident Memory CD8+ T Cells Form a Front-Line Defense against Malaria Liver-Stage Infection. *Immunity* **45,** 889–902 (2016).

72. Takahashi, T. *et al.* Immunologic self-tolerance maintained by CD25(+)CD4(+) regulatory T cells constitutively expressing cytotoxic T lymphocyte-associated antigen 4. *J. Exp. Med.* **192,** 303–10 (2000).

73. Friedline, R. H. *et al.* CD4 $^{+}$ regulatory T cells require CTLA-4 for the maintenance of systemic tolerance. *J. Exp. Med.* **206,** 421–434 (2009).

74. Carambia, A. *et al.* Inhibition of inflammatory CD4 T cell activity by murine liver sinusoidal endothelial cells. *J. Hepatol.* **58,** 112–118 (2013).

75. Kaczmarek, J. *et al.* Liver Sinusoidal Endothelial Cell-Mediated CD8 T Cell Priming Depends on Co-Inhibitory Signal Integration over Time. *PLoS One* **9,** e99574 (2014).

76. Schurich, A. *et al.* Dynamic Regulation of CD8 T Cell Tolerance Induction by Liver Sinusoidal Endothelial Cells. *J. Immunol.* **184,** 4107–4114 (2010).

77. Knolle, P. A. & Wohlleber, D. Immunological functions of liver sinusoidal endothelial cells. *Cell. Mol. Immunol.* **13,** 347–353 (2016).

78. Carvalho, L. H. *et al.* IL-4-secreting CD4+ T cells are crucial to the development of CD8+ T-cell responses against malaria liver stages. *Nat. Med.* **8,** 166–170 (2002).

79. Oliveira, G. A. *et al.* Class II-restricted protective immunity induced by malaria sporozoites. *Infect. Immun.* **76,** 1200–1206 (2008).

80. John, C. C. *et al.* Correlation of high levels of antibodies to multiple pre-erythrocytic Plasmodium falciparum antigens and protection from infection. *Am. J. Trop. Med. Hyg.* **73,** 222–8 (2005).

81. Stewart, M. J., Nawrot, R. J., Schulman, S. & Vanderberg, J. P. Plasmodium berghei Sporozoite Invasion Is Blocked In Vitro by Sporozoite-Immobilizing Antibodies. *Infect. Immun.* **51,** 859–864 (1986).

82. Hollingdale, M. R., Zavala, F., Nussenzweig, R. S. & Nussenzweig, V. Antibodies to the Protective Antigen of Plasmodium bergbei Sporozoites Prevent Entry into Cultured Cells'. *J Immunol J. Immunol. Commun.* **128,** 1929–1930 (1982).

83. Keitany, G. J. *et al.* Immunization of mice with live-attenuated late liver stage-arresting Plasmodium yoelii parasites generates protective antibody responses to preerythrocytic stages of malaria. *Infect. Immun.* **82,** 5143–53 (2014).

84. Potocnjak, P., Yoshida, N., Nussenzweig, R. S. & Nussenzweig, V. Monovalent fragments (Fab) of monoclonal antibodies to a sporozoite surface antigen (Pb44) protect mice against malarial infection. *J. Exp. Med.* **151,**

1504–13 (1980).

85. Yoshida, N., Nussenzweig, R. S., Potocnjak, P., Nussenzweig, V. & Aikawa, M. Hybridoma produces protective antibodies directed against the sporozoite stage of malaria parasite. *Science* **207,** 71–3 (1980).

86. Finley, R. W., Mackey, L. J. & Lambert, P. H. Virulent P. berghei malaria: prolonged survival and decreased cerebral pathology in cell-dependent nude mice. *J. Immunol.* **129,** 2213–8 (1982).

87. Van Der Heyde, C. *et al.* Participation of lymphocyte subpopulations in Participation of Lymphocyte Subpopulations in the Pathogenesis of Experimental Murine Cerebral Malaria'. *J Immunol J. Immunol. by guest* **157,** 1620–1624 (1996).

88. Mice lacking MHC class II molecules. *Cell* **66,** 1051–1066 (1991).

89. Villegas-Mendez, A. *et al.* IFN-γ-producing CD4+ T cells promote experimental cerebral malaria by modulating CD8+ T cell accumulation within the brain. *J. Immunol.* **189,** 968–79 (2012).

90. Poh, C. M., Howland, S. W., Grotenbreg, G. M. & Renia, L. Damage to the Blood-Brain Barrier during Experimental Cerebral Malaria Results from Synergistic Effects of CD8+ T Cells with Different Specificities. *Infect. Immun.* **82,** 4854–4864 (2014).

91. Haque, A. *et al.* Granzyme B expression by CD8+ T cells is required for the development of experimental cerebral malaria. *J. Immunol.* **186,** 6148–56 (2011).

92. Nitcheu, J. *et al.* Perforin-dependent brain-infiltrating cytotoxic CD8+ T lymphocytes mediate experimental cerebral malaria pathogenesis. *J. Immunol.* **170,** 2221–8 (2003).

93. Sanni, L. A., Fonseca, L. F. & Langhorne, J. in *Malaria Methods and Protocols* **72,** 57–76 (Humana Press, 2002).

94. Hafalla, J. C. R. *et al.* The CTLA-4 and PD-1/PD-l1 inhibitory pathways independently regulate host resistance to Plasmodium-induced acute immune pathology. *PLoS Pathog.* **8,** (2012).

95. Kossodo, S. *et al.* Interleukin-10 modulates susceptibility in experimental cerebral malaria. *Immunology* **91,** 536–40 (1997).

96. Van Braeckel-Budimir, N., Kurup, S. P. & Harty, J. T. Regulatory issues in immunity to liver and blood-stage malaria. *Curr. Opin. Immunol.* **42,** 91–97 (2016).

97. Perez-Mazliah, D. & Langhorne, J. CD4 T-cell subsets in malaria: TH1/TH2 revisited. *Front. Immunol.* **5,** 671 (2014).

98. Dups, J. N., Pepper, M. & Cockburn, I. A. Antibody and B cell responses to Plasmodium sporozoites. *Front. Microbiol.* **5,** (2014).

99. Jagannathan, P. *et al.* IFNγ/IL-10 co-producing cells dominate the CD4 response to malaria in highly exposed children. *PLoS Pathog.* **10,** e1003864 (2014).

100. Keswani, T. & Bhattacharyya, A. Differential role of T regulatory and Th17 in Swiss mice infected with Plasmodium berghei ANKA and Plasmodium yoelii. *Exp. Parasitol.* **141,** 82–92 (2014).

101. Koch, O. *et al.* Investigation of malaria susceptibility determinants in the IFNG/IL26/IL22 genomic region. *Genes Immun.* **6,** 312–8 (2005).

102. Findlay, E. G. *et al.* Essential role for IL-27 receptor signaling in prevention of Th1-mediated immunopathology during malaria infection. *J. Immunol.* **185,** 2482–92 (2010).

103. Finney, O. C., Riley, E. M. & Walther, M. Regulatory T cells in malaria – friend or foe? *Trends Immunol.* **31,** 63–70 (2010).

104. Abel, S. *et al.* Strong Impact of CD4+Foxp3+ Regulatory T Cells and Limited Effect of T Cell-Derived IL-10 on Pathogen Clearance during Plasmodium yoelii Infection. *J. Immunol.* **188,** (2012).

105. Butler, N. S. *et al.* Therapeutic blockade of PD-L1 and LAG-3 rapidly clears established blood-stage Plasmodium infection. *Nat. Immunol.* **13,** 188–95 (2011).

106. Jacobs, T., Graefe, S. E. B., Niknafs, S., Gaworski, I. & Fleischer, B. Murine malaria is exacerbated by CTLA-4 blockade. *J. Immunol.* **169,** 2323–9 (2002).

107. COHEN, S., McGREGOR, I. A. & CARRINGTON, S. Gamma-globulin and acquired immunity to human malaria. *Nature* **192,** 733–7 (1961).

108. S, C., IA, M. & S, C. Gamma-globulin and acquired immunity to human malaria. *Nature* **192,** 733–737 (1961).

109. Boyle, M. J. *et al.* Human Antibodies Fix Complement to Inhibit Plasmodium falciparum Invasion of Erythrocytes and Are Associated with Protection against Malaria. *Immunity* **42,** 580–590 (2015).

110. Duncan, C. J. A., Hill, A. V. S. & Ellis, R. D. Can growth inhibition assays (GIA) predict blood-stage malaria vaccine efficacy? *Hum. Vaccin. Immunother.* **8,** 706–714 (2012).

111. Bouharoun-Tayoun, H., Attanath, P., Sabchareon, A., Chongsuphajaisiddhi, T. & Druilhe, P. Antibodies that protect humans against Plasmodium falciparum blood stages do not on their own inhibit parasite growth and invasion in vitro, but act in cooperation with monocytes. *J. Exp. Med.* **172,** 1633–41 (1990).

112. Osier, F. H. *et al.* Opsonic phagocytosis of Plasmodium falciparummerozoites: mechanism in human immunity and a correlate of protection against malaria. *BMC Med.* **12,** 108 (2014).

113. Joos, C. *et al.* Clinical Protection from Falciparum Malaria Correlates with Neutrophil Respiratory Bursts Induced by Merozoites Opsonized with Human Serum Antibodies. *PLoS One* **5,** e9871 (2010).

114. Merrifield, R. B. Solid Phase Peptide Synthesis. I. The Synthesis of a Tetrapeptide. *J. Am. Chem. Soc.* **85,** 2149–2154 (1963).

115. Lam, K. S. *et al.* A new type of synthetic peptide library for identifying ligand-binding activity. *Nature* **354,** 82–84 (1991).

116. Furka, A., Sebestyén, F., Asgedom, M. & Dibó, G. General method for rapid synthesis of multicomponent peptide mixtures. *Int. J. Pept. Protein Res.* **37,** 487–93 (1991).

117. Carmona, S. J. *et al.* Towards High-throughput Immunomics for Infectious

Diseases: Use of Next-generation Peptide Microarrays for Rapid Discovery and Mapping of Antigenic Determinants. *Mol. Cell. Proteomics* **14,** 1871–84 (2015).

118. Hansen, L. B. *et al.* Identification and Mapping of Linear Antibody Epitopes in Human Serum Albumin Using High-Density Peptide Arrays. *PLoS One* **8,** e68902 (2013).

119. Dunachie, S., Hill, A. V. S. & Fletcher, H. A. Profiling the host response to malaria vaccination and malaria challenge. *Vaccine* **33,** 5316–20 (2015).

120. Chen, D. H., Tigelaar, R. E. & Weinbaum, F. I. Immunity to sporozoite-induced malaria infeciton in mice. I. The effect of immunization of T and B cell-deficient mice. *J. Immunol.* **118,** 1322–7 (1977).

121. Weiss, W. R., Sedegaht, M., Beaudoint, R. L., Miller, L. H. & Good, M. F. CD8+ T cells (cytotoxic/suppressors) are required for protection in mice immunized with malaria sporozoites. *Immunology* **85,** 573–576 (1988).

122. Schmidt, N. W. *et al.* Memory CD8 T cell responses exceeding a large but definable threshold provide long-term immunity to malaria. *Proc. Natl. Acad. Sci. U. S. A.* **105,** 14017–22 (2008).

123. Brockstedt, D. G. *et al.* Listeria-based cancer vaccines that segregate immunogenicity from toxicity. *Proc. Natl. Acad. Sci. U. S. A.* **101,** 13832–7 (2004).

124. Reyes-Sandoval, A. *et al.* CD8+ T effector memory cells protect against liver-stage malaria. *J. Immunol.* **187,** 1347–1357 (2011).

125. Clyde, D. F. Immunization of man against falciparum and vivax malaria by use of attenuated sporozoites. *Am. J. Trop. Med. Hyg.* **24,** 397–401 (1975).

126. Wellde, B. T. & Sadun, E. H. Resistance produced in rats and mice by exposure to irradiated Plasmodium berghei. *Exp. Parasitol.* **21,** 310–24 (1967).

127. Waterhouse, P. *et al.* Lymphoproliferative disorders with early lethality in mice deficient in Ctla-4. *Science* **270,** 985–988 (1995).

128. Tivol, E. A. *et al.* Loss of CTLA-4 leads to massive lymphoproliferation and fatal multiorgan tissue destruction, revealing a critical negative regulatory role of CTLA-4. *Immunity* **3,** 541–547 (1995).

129. Walker, L. S. K. & Abbas, A. K. The enemy within: keeping self-reactive T cells at bay in the periphery. *Nat. Rev. Immunol.* **2,** 11–9 (2002).

130. Schneider, H., Cai, Y.-C., Prasad, K. V. S., Shoelson, S. E. & Rudd, C. E. T cell antigen CD28 binds to the GRB-2/SOS complex, regulators of p21ras. *Eur. J. Immunol.* **25,** 1044–1050 (1995).

131. K V Prasad, Y. C. C. M. R. B. D. L. C. S. E. S. C. E. R. T-cell antigen CD28 interacts with the lipid kinase phosphatidylinositol 3-kinase by a cytoplasmic Tyr(P)-Met-Xaa-Met motif. *Proceedings of the National Academy of Sciences of the United States of America* **91,** 2834 (1994).

132. King, P. D. *et al.* Analysis of CD28 cytoplasmic tail tyrosine residues as regulators and substrates for the protein tyrosine kinases, EMT and LCK. *J. Immunol. (Baltimore, Md. 1950)* **158,** 580–590 (1997).

133. Holdorf, A. D. *et al.* Proline residues in CD28 and the Src homology (SH)3

domain of Lck are required for T cell costimulation. *J. Exp. Med.* **190,** 375–84 (1999).

134. Iezzi, G., Karjalainen, K. & Lanzavecchia, A. The duration of antigenic stimulation determines the fate of naive and effector T cells. *Immunity* **8,** 89–95 (1998).

135. Gett, A. V & Hodgkin, P. D. A cellular calculus for signal integration by T cells. *Nat. Immunol.* **1,** 239–44 (2000).

136. Egen, J. G. & Allison, J. P. Cytotoxic T lymphocyte antigen-4 accumulation in the immunological synapse is regulated by TCR signal strength. *Immunity* **16,** 23–35 (2002).

137. Agata, Y. *et al.* Expression of the PD-1 antigen on the surface of stimulated mouse T and B lymphocytes. *Int. Immunol.* **8,** 765–72 (1996).

138. Qureshi, O. S. *et al.* Constitutive clathrin-mediated endocytosis of CTLA-4 persists during T cell activation. *J. Biol. Chem.* **287,** 9429–9440 (2012).

139. Collins, A. V. *et al.* The interaction properties of costimulatory molecules revisited. *Immunity* **17,** 201–210 (2002).

140. Marengère, L. E. *et al.* Regulation of T cell receptor signaling by tyrosine phosphatase SYP association with CTLA-4. *Science* **272,** 1170–3 (1996).

141. Oderup, C., Cederbom, L., Makowska, A., Cilio, C. M. & Ivars, F. Cytotoxic T lymphocyte antigen-4-dependent down-modulation of costimulatory molecules on dendritic cells in CD4+ CD25+ regulatory T-cell-mediated suppression. *Immunology* **118,** 240–249 (2006).

142. Qureshi, O. S. *et al.* Trans-endocytosis of CD80 and CD86: a molecular basis for the cell-extrinsic function of CTLA-4. *Science (80-.).* **332,** 600–3 (2011).

143. Barber, D. L. *et al.* Restoring function in exhausted CD8 T cells during chronic viral infection. *Nature* **439,** 682–687 (2006).

144. Chen, L. Co-inhibitory molecules of the B7-CD28 family in the control of T-cell immunity. *Nat. Rev. Immunol.* **4,** 336–347 (2004).

145. Yokosuka, T. *et al.* Programmed cell death 1 forms negative costimulatory microclusters that directly inhibit T cell receptor signaling by recruiting phosphatase SHP2. *J. Exp. Med.* **209,** 1201–1217 (2012).

146. Yokosuka, T. *et al.* Spatiotemporal Basis of CTLA-4 Costimulatory Molecule-Mediated Negative Regulation of T Cell Activation. *Immunity* **33,** 326–339 (2010).

147. Sheppard, K. A. *et al.* PD-1 inhibits T-cell receptor induced phosphorylation of the ZAP70/CD3?? signalosome and downstream signaling to PKC?? *FEBS Lett.* **574,** 37–41 (2004).

148. Parry, R. V *et al.* CTLA-4 and PD-1 receptors inhibit T-cell activation by distinct mechanisms. *Mol. Cell. Biol.* **25,** 9543–53 (2005).

149. Anderson, K. M., Czinn, S. J., Redline, R. W. & Blanchard, T. G. Induction of CTLA-4-mediated anergy contributes to persistent colonization in the murine model of gastric Helicobacter pylori infection. *J. Immunol.* **176,** 5306–13 (2006).

150. Zubairi, S., Sanos, S. L., Hill, S. & Kaye, P. M. Immunotherapy with OX40L-

Fc or anti-CTLA-4 enhances local tissue responses and killing of Leishmania donovani. *Eur. J. Immunol.* **34,** 1433–1440 (2004).

151. Graefe, S. E. B., Jacobs, T., W??chter, U., Br??ker, B. M. & Fleischer, B. CTLA-4 regulates the murine immune response to Trypanosoma cruzi infection. *Parasite Immunol.* **26,** 19–28 (2004).

152. Ha, S.-J. *et al.* Enhancing therapeutic vaccination by blocking PD-1-mediated inhibitory signals during chronic infection. *J. Exp. Med.* **205,** 543–555 (2008).

153. Pedicord, V. a, Montalvo, W., Leiner, I. M. & Allison, J. P. Single dose of anti – CTLA-4 enhances CD8 + T-cell memory formation , function , and maintenance. *Pnas* **108,** 266–271 (2011).

154. Pentcheva-Hoang, T., Simpson, T. R., Montalvo-Ortiz, W. & Allison, J. P. Cytotoxic T Lymphocyte Antigen-4 (CTLA-4) Blockade Enhances Anti-Tumor Immunity by Stimulating Melanoma-Specific T Cell Motility. *Cancer Immunol. Res.* **4,** 970–980 (2014).

155. Keler, T. *et al.* Activity and safety of CTLA-4 blockade combined with vaccines in cynomolgus macaques. *J. Immunol.* **171,** 6251–6259 (2003).

156. Hodi, F. S. *et al.* Biologic activity of cytotoxic T lymphocyte-associated antigen 4 antibody blockade in previously vaccinated metastatic melanoma and ovarian carcinoma patients. *Proc. Natl. Acad. Sci. U. S. A.* **100,** 4712–4717 (2003).

157. Curran, M. A., Montalvo, W., Yagita, H. & Allison, J. P. PD-1 and CTLA-4 combination blockade expands infiltrating T cells and reduces regulatory T and myeloid cells within B16 melanoma tumors. *Proc. Natl. Acad. Sci. U. S. A.* **107,** 4275–80 (2010).

158. Linch, S. N. *et al.* Combination OX40 agonism/CTLA-4 blockade with HER2 vaccination reverses T-cell anergy and promotes survival in tumor-bearing mice. *Proc. Natl. Acad. Sci. U. S. A.* **113,** E319-27 (2016).

159. Butler, N. S. *et al.* Therapeutic blockade of PD-L1 and LAG-3 rapidly clears established blood-stage Plasmodium infection. *Nat. Immunol.* **13,** 188–95 (2011).

160. Mackroth, M. S., Abel, A., Steeg, C., Schulze zur Wiesch, J. & Jacobs, T. Acute Malaria Induces PD1+CTLA4+ Effector T Cells with Cell-Extrinsic Suppressor Function. *PLOS Pathog.* **12,** e1005909 (2016).

161. Doe, H. T. *et al.* Expression of PD-1/LAG-3 and cytokine production by CD4 $^{+}$ T cells during infection with *Plasmodium* parasites. *Microbiol. Immunol.* **60,** 121–131 (2016).

162. Chandele, A., Mukerjee, P., Das, G., Ahmed, R. & Chauhan, V. S. Phenotypic and functional profiling of malaria-induced CD8 and CD4 T cells during blood-stage infection with Plasmodium yoelii. *Immunology* **132,** 273–86 (2011).

163. Lepenies, B. *et al.* CTLA-4 blockade differentially influences the outcome of non-lethal and lethal Plasmodium yoelii infections. *Microbes Infect.* **9,** 687–94 (2007).

164. Sampson, W. R., Patsiouras, H. & Ede, N. J. The synthesis of 'difficult' peptides using 2-hydroxy-4-methoxybenzyl or pseudoproline amino acid building blocks: a comparative study. *J. Pept. Sci.* **5,** 403–409 (1999).

165. Bopp, S. E. R. *et al.* Genome Wide Analysis of Inbred Mouse Lines Identifies a Locus Containing Ppar-γ as Contributing to Enhanced Malaria Survival. *PLoS One* **5,** e10903 (2010).

166. Krummel, M. F. & Allison, J. P. CD28 and CTLA-4 have opposing effects on the response of T cells to stimulation. *J. Exp. Med.* **182,** 459–65 (1995).

167. Brian de Souza, J. & Riley, E. M. Cerebral malaria: the contribution of studies in animal models to our understanding of immunopathogenesis. *Microbes Infect.* **4,** 291–300 (2002).

168. Rai, D., Pham, N.-L. L., Harty, J. T. & Badovinac, V. P. Tracking the Total CD8 T Cell Response to Infection Reveals Substantial Discordance in Magnitude and Kinetics between Inbred and Outbred Hosts. *J. Immunol.* **183,** 7672–7681 (2009).

169. Ando, K., Guidotti, L. G., Cerny, A., Ishikawa, T. & Chisari, F. V. CTL access to tissue antigen is restricted in vivo. *J. Immunol.* **153,** 482–8 (1994).

170. Kruse, N. *et al.* Priming of CD4+ T cells by liver sinusoidal endothelial cells induces CD25low forkhead box protein 3− regulatory T cells suppressing autoimmune hepatitis. *Hepatology* **50,** 1904–1913 (2009).

171. Doolan, D. L. & Hoffman, S. L. The complexity of protective immunity against liver-stage malaria. *J. Immunol.* **165,** 1453–62 (2000).

172. Seder, R. A. *et al.* Protection Against Malaria by Intravenous Immunization with a Nonreplicating Sporozoite Vaccine. *Science (80-.).* **341,** 1359–1365 (2013).

173. Kimura, D. *et al.* Interleukin-27-Producing CD4+ T Cells Regulate Protective Immunity during Malaria Parasite Infection. *Immunity* **44,** 672–682 (2016).

174. Villegas-Mendez, A. *et al.* Parasite-Specific CD4+ IFN-γ+ IL-10+ T Cells Distribute within Both Lymphoid and Nonlymphoid Compartments and Are Controlled Systemically by Interleukin-27 and ICOS during Blood-Stage Malaria Infection. *Infect. Immun.* **84,** 34–46 (2015).

175. Rahiman, F., Yusoff, M. & Majid, A. Interleukin-27 exhibited anti-inflammatory activity during Plasmodium berghei infection in mice. *Trop. Biomed.* **30,** 663–680 (2013).

176. Villegas-Mendez, A. *et al.* WSX-1 Signalling Inhibits CD4+ T Cell Migration to the Liver during Malaria Infection by Repressing Chemokine-Independent Pathways. *PLoS One* **8,** e78486 (2013).

177. Villarino, A. V *et al.* Positive and negative regulation of the IL-27 receptor during lymphoid cell activation. *J. Immunol.* **174,** 7684–91 (2005).

178. Mendon?a, V. R. de & Barral-Netto, M. Immunoregulation in human malaria: the challenge of understanding asymptomatic infection. *Mem?rias do Inst. Oswaldo Cruz* **110,** 945–955 (2015).

179. Couper, K. N. *et al.* IL-10 from CD4+CD25−Foxp3−CD127− Adaptive Regulatory T Cells Modulates Parasite Clearance and Pathology during Malaria Infection. *PLoS Pathog.* **4,** e1000004 (2008).

180. Oppmann, B. *et al.* Novel p19 protein engages IL-12p40 to form a cytokine, IL-23, with biological activities similar as well as distinct from IL-12. *Immunity* **13,** 715–25 (2000).

181. Niedbala, W. *et al.* IL-35 is a novel cytokine with therapeutic effects against collagen-induced arthritis through the expansion of regulatory T cells and suppression of Th17 cells. *Eur. J. Immunol.* **37,** 3021–9 (2007).

182. Pflanz, S. *et al.* IL-27, a Heterodimeric Cytokine Composed of EBI3 and p28 Protein, Induces Proliferation of Naive CD4+ T Cells. *Immunity* **16,** 779–790 (2002).

183. Yoshida, H. & Hunter, C. A. The Immunobiology of Interleukin-27. *Annu. Rev. Immunol.* **33,** 417–443 (2015).

184. Curran, M. A. *et al.* Systemic 4-1BB activation induces a novel T cell phenotype driven by high expression of Eomesodermin. *J. Exp. Med.* **210,** (2013).

185. Dibra, D., Cutrera, J. J. & Li, S. Coordination between TLR9 signaling in macrophages and CD3 signaling in T cells induces robust expression of IL-30. *J. Immunol.* **188,** 3709–15 (2012).

186. van Seventer, J. M., Nagai, T. & van Seventer, G. A. Interferon-β differentially regulates expression of the IL-12 family members p35, p40, p19 and EBI3 in activated human dendritic cells. *J. Neuroimmunol.* **133,** 60–71 (2002).

187. Remoli, M. E. *et al.* IFN-β modulates the response to TLR stimulation in human DC: Involvement of IFN regulatory factor-1 (IRF-1) in IL-27 gene expression. *Eur. J. Immunol.* **37,** 3499–3508 (2007).

188. Molle, C. *et al.* IL-27 synthesis induced by TLR ligation critically depends on IFN regulatory factor 3. *J. Immunol.* **178,** 7607–15 (2007).

189. Liu, J., Guan, X. & Ma, X. Regulation of IL-27 p28 gene expression in macrophages through MyD88- and interferon-γ–mediated pathways. *J. Exp. Med.* **204,** (2007).

190. Pirhonen, J., Sirén, J., Julkunen, I. & Matikainen, S. IFN-alpha regulates Toll-like receptor-mediated IL-27 gene expression in human macrophages. *J. Leukoc. Biol.* **82,** 1185–92 (2007).

191. Pflanz, S. *et al.* WSX-1 and glycoprotein 130 constitute a signal-transducing receptor for IL-27. *J. Immunol.* **172,** 2225–31 (2004).

192. Hu, S., Wong, C. K. & Lam, C. W. K. Activation of eosinophils by IL-12 family cytokine IL-27: Implications of the pleiotropic roles of IL-27 in allergic responses. *Immunobiology* **216,** 54–65 (2011).

193. Li, J. P. *et al.* Interleukin-27 as a Negative Regulator of Human Neutrophil Function. *Scand. J. Immunol.* **72,** 284–292 (2010).

194. Yoshimoto, T., Yoshimoto, T., Yasuda, K., Mizuguchi, J. & Nakanishi, K. IL-27 suppresses Th2 cell development and Th2 cytokines production from polarized Th2 cells: a novel therapeutic way for Th2-mediated allergic inflammation. *J. Immunol.* **179,** 4415–23 (2007).

195. Morishima, N. *et al.* Augmentation of effector CD8+ T cell generation with enhanced granzyme B expression by IL-27. *J. Immunol.* **175,** 1686–93 (2005).

196. Batten, M. *et al.* Cutting edge: IL-27 is a potent inducer of IL-10 but not FoxP3 in murine T cells. *J. Immunol.* **180,** 2752–6 (2008).

197. Villarino, A. V *et al.* IL-27 limits IL-2 production during Th1 differentiation. *J.*

Immunol. **176,** 237–47 (2006).

198. Owaki, T. *et al.* IL-27 suppresses CD28-mediated [correction of medicated] IL-2 production through suppressor of cytokine signaling 3. *J. Immunol.* **176,** 2773–80 (2006).

199. Hall, A. *et al.* The Cytokines Interleukin 27 and Interferon-? Promote Distinct Treg Cell Populations Required to Limit Infection-Induced Pathology. *Immunity* **37,** 511–523 (2012).

200. Zeng, H., Zhang, R., Jin, B. & Chen, L. Type 1 regulatory T cells: a new mechanism of peripheral immune tolerance. *Cell. Mol. Immunol.* **12,** 566–571 (2015).

201. Nieuwenhuis, E. E. S. *et al.* Disruption of T helper 2-immune responses in Epstein-Barr virus-induced gene 3-deficient mice. *Proc. Natl. Acad. Sci. U. S. A.* **99,** 16951–6 (2002).

202. de Sauvage, F. J. *et al.* Development of Th1-type immune responses requires the typeI cytokine receptor TCCR. *Nature* **407,** 916–920 (2000).

203. Yoshida, H. *et al.* WSX-1 Is Required for the Initiation of Th1 Responses and Resistance to L. major Infection. *Immunity* **15,** 569–578 (2001).

204. Villarino, A. *et al.* The IL-27R (WSX-1) is required to suppress T cell hyperactivity during infection. *Immunity* **19,** 645–55 (2003).

205. Torrado, E. *et al.* Interleukin 27R regulates CD4+ T cell phenotype and impacts protective immunity during Mycobacterium tuberculosis infection. *J. Exp. Med.* **212,** 1449–63 (2015).

206. Hamano, S. *et al.* WSX-1 is required for resistance to Trypanosoma cruzi infection by regulation of proinflammatory cytokine production. *Immunity* **19,** 657–67 (2003).

207. Yang, A. S. & Lattime, E. C. Tumor-induced Interleukin 10 Suppresses the Ability of Splenic Dendritic Cells to Stimulate CD4 and CD8 T-Cell Responses. *Cancer Res.* **63,** (2003).

208. Anderson, C. F., Oukka, M., Kuchroo, V. J. & Sacks, D. CD4 $^{+}$ CD25 $^{?}$ Foxp3 $^{?}$ Th1 cells are the source of IL-10?mediated immune suppression in chronic cutaneous leishmaniasis. *J. Exp. Med.* **204,** 285–297 (2007).

209. Abrahamsohn, I. A. & Coffman, R. L. Trypanosoma cruzi:IL-10, TNF, IFN-?, and IL-12 Regulate Innate and Acquired Immunity to Infection. *Exp. Parasitol.* **84,** 231–244 (1996).

210. Hunter, C. A. *et al.* IL-10 is required to prevent immune hyperactivity during infection with Trypanosoma cruzi. *J. Immunol.* **158,** 3311–6 (1997).

211. Deckert, M. *et al.* Endogenous Interleukin-10 Is Required for Prevention of a Hyperinflammatory Intracerebral Immune Response in Listeria monocytogenes Meningoencephalitis. *Infect. Immun.* **69,** 4561–4571 (2001).

212. Sun, J., Madan, R., Karp, C. L. & Braciale, T. J. Effector T cells control lung inflammation during acute influenza virus infection by producing IL-10. *Nat. Med.* **15,** 277–284 (2009).

213. Oakley, O. R., Garvy, B. A., Humphreys, S., Qureshi, M. H. & Pomeroy, C. Increased weight loss with reduced viral replication in interleukin-10 knock-out mice infected with murine cytomegalovirus. *Clin. Exp. Immunol.* **151,**

155–164 (2007).

214. Linke, A. *et al.* Plasmodium chabaudi chabaudi:Differential Susceptibility of Gene-Targeted Mice Deficient in IL-10 to an Erythrocytic-Stage Infection. *Exp. Parasitol.* **84,** 253–263 (1996).

215. Wolk, K., Kunz, S., Asadullah, K. & Sabat, R. Cutting edge: immune cells as sources and targets of the IL-10 family members? *J. Immunol.* **168,** 5397–402 (2002).

216. Moore, K. W., de Waal Malefyt, R., Coffman, R. L. & O'Garra, A. I NTERLEUKIN -10 AND THE I NTERLEUKIN -10 R ECEPTOR. *Annu. Rev. Immunol.* **19,** 683–765 (2001).

217. Schandené, L. *et al.* B7/CD28-dependent IL-5 production by human resting T cells is inhibited by IL-10. *J. Immunol.* **152,** (1994).

218. Joss, A., Akdis, M., Faith, A., Blaser, K. & Akdis, C. A. IL-10 directly acts on T cells by specifically altering the CD28 co-stimulation pathway. *Eur. J. Immunol.* **30,** 1683–90 (2000).

219. De Souza, J. B., Williamson, K. H., Otani, T. & Playfair, J. H. Early gamma interferon responses in lethal and nonlethal murine blood-stage malaria. *Infect. Immun.* **65,** 1593–8 (1997).

220. van der Heyde, H. C., Pepper, B., Batchelder, J., Cigel, F. & Weidanz, W. P. The time course of selected malarial infections in cytokine-deficient mice. *Exp. Parasitol.* **85,** 206–13 (1997).

221. Pombo, D. J. *et al.* Immunity to malaria after administration of ultra-low doses of red cells infected with Plasmodium falciparum. *Lancet (London, England)* **360,** 610–7 (2002).

222. Schmidt, N. W., Butler, N. S., Badovinac, V. P. & Harty, J. T. Extreme CD8 T Cell Requirements for Anti-Malarial Liver-Stage Immunity following Immunization with Radiation Attenuated Sporozoites. *PLoS Pathog.* **6,** e1000998 (2010).

223. Matsui, M. *et al.* Adjuvant Activities of Novel Cytokines, Interleukin-23 (IL-23) and IL-27, for Induction of Hepatitis C Virus-Specific Cytotoxic T Lymphocytes in HLA-A*0201 Transgenic Mice. *J. Virol.* **78,** 9093–9104 (2004).

224. Pennock, N. D., Gapin, L. & Kedl, R. M. IL-27 is required for shaping the magnitude, affinity distribution, and memory of T cells responding to subunit immunization. *Proc. Natl. Acad. Sci. U. S. A.* **111,** 16472–7 (2014).

225. Couper, K. N., Blount, D. G. & Riley, E. M. IL-10: the master regulator of immunity to infection. *J. Immunol.* **180,** 5771–7 (2008).

226. Yoeli, M., Vanderberg, J., Nawrot, R. & Most, H. Studies on sporozoite-induced infections of rodent malaria. II. Anopheles stephensi as an experimental vector of Plasmodium berghei. *Am. J. Trop. Med. Hyg.* **14,** 927–30 (1965).

227. Yoeli, M., Vanderberg, J., Upmanis, R. S. & Most, H. Primary tissue phase of Plasmodium berghei in different experimental hosts. *Nature* **208,** 903 (1965).

228. Landau, I. & Killick-Kendrick, R. Rodent plasmodia of the République Centrafricaine: the sporogony and tissue stages of Plasmodium chabaudi and

P. berghei yoelii. *Trans. R. Soc. Trop. Med. Hyg.* **60,** 633–49 (1966).

229. Wéry, M. Studies on the sporogony of rodent malaria parasites. *Ann. Soc. Belges Med. Trop. Parasitol. Mycol.* **48,** 11–137 (1968).

230. Espinosa, D. A., Yadava, A., Angov, E., Maurizio, P. L. & Zavala, F. Development of a chimeric Plasmodium berghei expressing the repeat region of P. vivax CSP for in vivo evaluation of vaccine efficacy. doi:10.1128/IAI.00461-13

231. Gwyer Findlay, E. *et al.* IL-27 Receptor Signaling Regulates Memory CD4+ T Cell Populations and Suppresses Rapid Inflammatory Responses during Secondary Malaria Infection. *Infect. Immun.* **82,** 10–20 (2014).

232. Ahmed, R. & Gray, D. Immunological Memory and Protective Immunity: Understanding Their Relation. *Science (80-.).* **272,** (1996).

233. Claser, C. *et al.* Host Resistance to Plasmodium-Induced Acute Immune Pathology Is Regulated by Interleukin-10 Receptor Signaling. *Infect. Immun.* **85,** e00941-16 (2017).

234. Engwerda, C., Belnoue, E., Grüner, A. C. & Rénia, L. Experimental models of cerebral malaria. *Curr. Top. Microbiol. Immunol.* **297,** 103–43 (2005).

235. van der Heyde, H. C., Nolan, J., Combes, V., Gramaglia, I. & Grau, G. E. A unified hypothesis for the genesis of cerebral malaria: sequestration, inflammation and hemostasis leading to microcirculatory dysfunction. *Trends Parasitol.* **22,** 503–508 (2006).

236. Hearn, J., Rayment, N., Landon, D. N., Katz, D. R. & de Souza, J. B. Immunopathology of cerebral malaria: morphological evidence of parasite sequestration in murine brain microvasculature. *Infect. Immun.* **68,** 5364–76 (2000).

237. Haldar, K., Murphy, S. C., Milner, D. A. & Taylor, T. E. Malaria: Mechanisms of Erythrocytic Infection and Pathological Correlates of Severe Disease. *Annu. Rev. Pathol. Mech. Dis.* **2,** 217–249 (2007).

238. BRIAN de SOUZA, J., HAFALLA, J. C. R., RILEY, E. M. & COUPER, K. N. Cerebral malaria: why experimental murine models are required to understand the pathogenesis of disease. *Parasitology* **137,** 755 (2010).

239. deWalick, S. *et al.* Cutting Edge: Conventional Dendritic Cells Are the Critical APC Required for the Induction of Experimental Cerebral Malaria. *J. Immunol.* **178,** (2007).

240. Piva, L. *et al.* Cutting Edge: Clec9A+ Dendritic Cells Mediate the Development of Experimental Cerebral Malaria. *J. Immunol.* **189,** (2012).

241. Claser, C. *et al.* CD8+ T cells and IFN-γ mediate the time-dependent accumulation of infected red blood cells in deep organs during experimental cerebral malaria. *PLoS One* **6,** e18720 (2011).

242. Howland, S. W., Poh, C. M. & Rénia, L. Activated Brain Endothelial Cells Cross-Present Malaria Antigen. *PLoS Pathog.* **11,** e1004963 (2015).

243. Howland, S. W. *et al.* Brain microvessel cross-presentation is a hallmark of experimental cerebral malaria. *EMBO Mol. Med.* **5,** 984–99 (2013).

244. Ho, A. S. *et al.* A receptor for interleukin 10 is related to interferon receptors. *Proc. Natl. Acad. Sci. U. S. A.* **90,** 11267–71 (1993).

245. O'Farrell, A. M., Liu, Y., Moore, K. W. & Mui, A. L. IL-10 inhibits macrophage activation and proliferation by distinct signaling mechanisms: evidence for Stat3-dependent and -independent pathways. *EMBO J.* **17,** 1006–18 (1998).

246. Li, C., Sanni, L. A., Omer, F., Riley, E. & Langhorne, J. Pathology of Plasmodium chabaudi chabaudi infection and mortality in interleukin-10-deficient mice are ameliorated by anti-tumor necrosis factor alpha and exacerbated by anti-transforming growth factor beta antibodies. *Infect. Immun.* **71,** 4850–6 (2003).

247. Li, C., Corraliza, I. & Langhorne, J. A defect in interleukin-10 leads to enhanced malarial disease in Plasmodium chabaudi chabaudi infection in mice. *Infect. Immun.* **67,** 4435–42 (1999).

248. Couper, K. N. *et al.* IL-10 from CD4+CD25−Foxp3−CD127− Adaptive Regulatory T Cells Modulates Parasite Clearance and Pathology during Malaria Infection. *PLoS Pathog.* **4,** e1000004 (2008).

249. Gazzinelli, R. T. *et al.* In the absence of endogenous IL-10, mice acutely infected with Toxoplasma gondii succumb to a lethal immune response dependent on CD4+ T cells and accompanied by overproduction of IL-12, IFN-gamma and TNF-alpha. *J. Immunol.* **157,** 798–805 (1996).

250. Franke-Fayard, B. *et al.* A Plasmodium berghei reference line that constitutively expresses GFP at a high level throughout the complete life cycle. *Mol. Biochem. Parasitol.* **137,** 23–33 (2004).

251. Malleret, B. *et al.* A rapid and robust tri-color flow cytometry assay for monitoring malaria parasite development. *Sci. Rep.* **1,** 118 (2011).

252. Tang, Q. *et al.* Distinct roles of CTLA-4 and TGF-beta in CD4+CD25+ regulatory T cell function. *Eur. J. Immunol.* **34,** 2996–3005 (2004).

253. Read, S. *et al.* Blockade of CTLA-4 on CD4+CD25+ regulatory T cells abrogates their function in vivo. *J. Immunol.* **177,** 4376–83 (2006).

254. Asseman, C., Read, S. & Powrie, F. Colitogenic Th1 cells are present in the antigen-experienced T cell pool in normal mice: control by CD4+ regulatory T cells and IL-10. *J. Immunol.* **171,** 971–8 (2003).

255. Paterson, A. M. *et al.* Deletion of CTLA-4 on regulatory T cells during adulthood leads to resistance to autoimmunity. *J. Exp. Med.* **212,** 1603–21 (2015).

256. Perry, J. A., Olver, C. S., Burnett, R. C. & Avery, A. C. Cutting edge: the acquisition of TLR tolerance during malaria infection impacts T cell activation. *J. Immunol.* **174,** 5921–5 (2005).

257. Keller, C. C. *et al.* Acquisition of Hemozoin by Monocytes Down-Regulates Interleukin-12 p40 (IL-12p40) Transcripts and Circulating IL-12p70 through an IL-10-Dependent Mechanism: In Vivo and In Vitro Findings in Severe Malarial Anemia. *Infect. Immun.* **74,** 5249–5260 (2006).

258. Zheng, W. *et al.* Distinct host-related dendritic cell responses during the early stage of Plasmodium yoelii infection in susceptible and resistant mice. *Parasite Immunol.* **32,** 324–34 (2010).

259. Liu, Y. *et al.* Role of IL-10-producing regulatory B cells in control of cerebral malaria in Plasmodium berghei infected mice. *Eur. J. Immunol.* **43,** 2907–18 (2013).

260. Gupta, P. *et al.* Tissue-Resident CD169+ Macrophages Form a Crucial Front Line against Plasmodium Infection. *Cell Rep.* **16,** 1749–1761 (2016).

261. Wang, G.-G. *et al.* Plasmodium chabaudi AS: Distinct CD4+CD25+Foxp3+ regulatory T cell responses during infection in DBA/2 and BALB/c mice. *Parasitol. Int.* **62,** 24–31 (2013).

262. Murai, M. *et al.* Interleukin 10 acts on regulatory T cells to maintain expression of the transcription factor Foxp3 and suppressive function in mice with colitis. *Nat. Immunol.* **10,** 1178–84 (2009).

263. Shouval, D. S. *et al.* Interleukin-10 Receptor Signaling in Innate Immune Cells Regulates Mucosal Immune Tolerance and Anti-Inflammatory Macrophage Function. *Immunity* **40,** 706–719 (2014).

264. Rigopoulou, E. I., Abbott, W. G. H., Haigh, P. & Naoumov, N. V. Blocking of interleukin-10 receptor--a novel approach to stimulate T-helper cell type 1 responses to hepatitis C virus. *Clin. Immunol.* **117,** 57–64 (2005).

265. Hafalla, J. C. R. *et al.* Experimental Cerebral Malaria Develops Independently of Caspase Recruitment Domain-Containing Protein 9 Signaling. *Infect. Immun.* **80,** 1274–1279 (2012).

266. Kordes, M., Matuschewski, K. & Hafalla, J. C. R. Caspase-1 activation of interleukin-1β (IL-1β) and IL-18 is dispensable for induction of experimental cerebral malaria. *Infect. Immun.* **79,** 3633–41 (2011).

267. Arun Kumar, K. *et al.* The circumsporozoite protein is an immunodominant protective antigen in irradiated sporozoites. *Nature* **444,** 937–940 (2006).

268. Potocnjak, P., Yoshida, N., Nussenzweig, R. S. & Nussenzweig, V. Monovalent fragments (Fab) of monoclonal antibodies to a sporozoite surface antigen (Pb44) protect mice against malarial infection. *J. Exp. Med.* **151,** 1504–13 (1980).

269. Malaria vaccine development: a multi-immune response approach. *Malar. vaccine Dev. a multi-immune response approach.* (1996). at <https://www.cabdirect.org/cabdirect/abstract/19970801972>

270. Nardin, E. H. *et al.* Circumsporozoite proteins of human malaria parasites Plasmodium falciparum and Plasmodium vivax. *J. Exp. Med.* **156,** 20–30 (1982).

271. Wipasa, J. *et al.* Long-Lived Antibody and B Cell Memory Responses to the Human Malaria Parasites, Plasmodium falciparum and Plasmodium vivax. *PLoS Pathog.* **6,** e1000770 (2010).

272. John, C. C. *et al.* Antibodies to Pre-erythrocytic *Plasmodium falciparum* Antigens and Risk of Clinical Malaria in Kenyan Children. *J. Infect. Dis.* **197,** 519–526 (2008).

273. Zavala, F., Cochrane, A. H., Nardin, E. H., Nussenzweig, R. S. & Nussenzweig, V. Circumsporozoite proteins of malaria parasites contain a single immunodominant region with two or more identical epitopes. *J. Exp. Med.* **157,** 1947–57 (1983).

274. Zavala, F. *et al.* Rationale for development of a synthetic vaccine against Plasmodium falciparum malaria. *Science* **228,** 1436–40 (1985).

275. Alonso, P. L. *et al.* Efficacy of the RTS,S/AS02A vaccine against Plasmodium

falciparum infection and disease in young African children: randomised controlled trial. *Lancet* **364,** 1411–1420 (2004).

276. Efficacy and safety of RTS,S/AS01 malaria vaccine with or without a booster dose in infants and children in Africa: final results of a phase 3, individually randomised, controlled trial. *Lancet* **386,** 31–45 (2015).

277. Olotu, A. *et al.* Seven-Year Efficacy of RTS,S/AS01 Malaria Vaccine among Young African Children. *N. Engl. J. Med.* **374,** 2519–2529 (2016).

278. Bojang, K. A. *et al.* Efficacy of RTS,S/AS02 malaria vaccine against Plasmodium falciparum infection in semi-immune adult men in The Gambia: a randomised trial. *Lancet* **358,** 1927–1934 (2001).

279. White, M. T. *et al.* Immunogenicity of the RTS,S/AS01 malaria vaccine and implications for duration of vaccine efficacy: secondary analysis of data from a phase 3 randomised controlled trial. *Lancet Infect. Dis.* **15,** 1450–1458 (2015).

280. Tewari, R., Spaccapelo, R., Bistoni, F., Holder, A. A. & Crisanti, A. Function of region I and II adhesive motifs of Plasmodium falciparum circumsporozoite protein in sporozoite motility and infectivity. *J. Biol. Chem.* **277,** 47613–8 (2002).

281. Rice, P., Longden, I. & Bleasby, A. EMBOSS: the European Molecular Biology Open Software Suite. *Trends Genet.* **16,** 276–7 (2000).

282. Gilson, P. R. *et al.* MSP1 $_{19}$ miniproteins can serve as targets for invasion inhibitory antibodies in Plasmodium falciparum provided they contain the correct domains for cell surface trafficking. *Mol. Microbiol.* **68,** 124–138 (2008).

283. de Koning-Ward, T. F. *et al.* A New Rodent Model to Assess Blood Stage Immunity to the *Plasmodium falciparum* Antigen Merozoite Surface Protein 1 $_{19}$ Reveals a Protective Role for Invasion Inhibitory Antibodies. *J. Exp. Med.* **198,** 869–875 (2003).

284. O'Donnell, R. A., Saul, A., Cowman, A. F. & Crabb, B. S. Functional conservation of the malaria vaccine antigen MSP-119across distantly related Plasmodium species. *Nat. Med.* **6,** 91–95 (2000).

285. HOLDER, A. A. The carboxy-terminus of merozoite surface protein 1: structure, specific antibodies and immunity to malaria. *Parasitology* **136,** 1445 (2009).

286. Sinnis, P., De La Vega, P., Coppi, A., Krzych, U. & Mota, M. M. in *Methods in molecular biology (Clifton, N.J.)* **923,** 385–400 (2012).

287. Calvo-Calle, J. M., Moreno, A., Eling, W. M. & Nardin, E. H. In vitro development of infectious liver stages of P. yoelii and P. berghei malaria in human cell lines. *Exp. Parasitol.* **79,** 362–73 (1994).

288. Mota, M. M. *et al.* Migration of Plasmodium Sporozoites Through Cells Before Infection. *Science (80-.).* **291,** 141–144 (2001).

289. Tavares, J. *et al.* Role of host cell traversal by the malaria sporozoite during liver infection. *J. Exp. Med.* **210,** 905–915 (2013).

290. Espinosa, D. A. *et al.* The Plasmodium falciparum Cell-Traversal Protein for Ookinetes and Sporozoites as a Candidate for Preerythrocytic and

Transmission-Blocking Vaccines. *Infect. Immun.* **85,** e00498-16 (2017).

291. Peng, H.-P., Lee, K. H., Jian, J.-W. & Yang, A.-S. Origins of specificity and affinity in antibody-protein interactions. *Proc. Natl. Acad. Sci. U. S. A.* **111,** E2656-65 (2014).

292. Kastenmüller, K. *et al.* Full-length Plasmodium falciparum circumsporozoite protein administered with long-chain poly(I·C) or the Toll-like receptor 4 agonist glucopyranosyl lipid adjuvant-stable emulsion elicits potent antibody and CD4+ T cell immunity and protection in mice. *Infect. Immun.* **81,** 789–800 (2013).

293. Foquet, L. *et al.* Vaccine-induced monoclonal antibodies targeting circumsporozoite protein prevent Plasmodium falciparum infection. *J. Clin. Invest.* **124,** 140–4 (2014).

294. Doolan, D. L. *et al.* Profiling humoral immune responses to P. falciparum infection with protein microarrays. *Proteomics* **8,** 4680–4694 (2008).

295. Microarray profiling of antiviral antibodies for the development of diagnostics, vaccines, and therapeutics. *Clin. Immunol.* **111,** 196–201 (2004).

296. Woo, S.-R. *et al.* Immune inhibitory molecules LAG-3 and PD-1 synergistically regulate T-cell function to promote tumoral immune escape. *Cancer Res.* **72,** 917–27 (2012).

297. Guo, Z. *et al.* PD-1 Blockade and OX40 Triggering Synergistically Protects against Tumor Growth in a Murine Model of Ovarian Cancer. *PLoS One* **9,** e89350 (2014).

298. Omer, F. M. & Riley, E. M. Transforming growth factor beta production is inversely correlated with severity of murine malaria infection. *J. Exp. Med.* **188,** 39–48 (1998).

299. Maintaining the Immunological Balance in Parasitic Infections: A Role for TGF-β? *Parasitol. Today* **16,** 18–23 (2000).

300. Gorelik, L. & Flavell, R. A. TRANSFORMING GROWTH FACTOR-β IN T-CELL BIOLOGY. *Nat. Rev. Immunol.* **2,** 46–53 (2002).

Appendices